The XMM-Newton serendipitous survey. IV. Optical identification of the XMM-Newton medium sensitivity survey (XMS)

X. Barcons, F. J. Carrera, M. T. Ceballos, M. J. Page, J. Bussons-Gordo, A. Corral, J. Ebrero, S. Mateos, J. A. Tedds, M. G. Watson, et al.

A&A 476, 1191–1203 (2007)
DOI: 10.1051/0004-6361:20077606

Astronomy & Astrophysics

The *XMM-Newton* serendipitous survey

IV. Optical identification of the *XMM-Newton* medium sensitivity survey (XMS)⋆,⋆⋆

X. Barcons[1], F. J. Carrera[1], M. T. Ceballos[1], M. J. Page[2], J. Bussons-Gordo[1], A. Corral[1], J. Ebrero[1], S. Mateos[1,3], J. A. Tedds[3], M. G. Watson[3], D. Baskill[3], M. Birkinshaw[4], T. Boller[5], N. Borisov[6], M. Bremer[4], G. E. Bromage[7], H. Brunner[5], A. Caccianiga[8], C. S. Crawford[9], M. S. Cropper[2], R. Della Ceca[8], P. Derry[3], A. C. Fabian[9], P. Guillout[10], Y. Hashimoto[5], G. Hasinger[5], B. J. M. Hassall[7], G. Lamer[11], N. S. Loaring[2,12], T. Maccacaro[8], K. O. Mason[2], R. G. McMahon[9], L. Mirioni[10], J. P. D. Mittaz[2], C. Motch[10], I. Negueruela[10,13], J. P. Osborne[3], F. Panessa[1], I. Pérez-Fournon[14], J. P. Pye[3], T. P. Roberts[3,15], S. Rosen[2,3], N. Schartel[16], N. Schurch[3,15], A. Schwope[11], P. Severgnini[8], R. Sharp[9,17], G. C. Stewart[3], G. Szokoly[5], A. Ullán[1,18], M. J. Ward[3,15], R. S. Warwick[3], P. J. Wheatley[3,19], N. A. Webb[20], D. Worrall[4], W. Yuan[9,21], and H. Ziaeepour[2]

(Affiliations can be found after the references)

Received 4 April 2007 / Accepted 25 September 2007

ABSTRACT

Aims. X-ray sources at intermediate fluxes (a few $\times 10^{-14}$ erg cm^{-2} s^{-1}) with a sky density of $\sim$100 deg^{-2} are responsible for a significant fraction of the cosmic X-ray background at various energies below 10 keV. The aim of this paper is to provide an unbiased and quantitative description of the X-ray source population at these fluxes and in various X-ray energy bands.

Methods. We present the XMM-Newton Medium sensitivity Survey (XMS), including a total of 318 X-ray sources found among the serendipitous content of 25 XMM-Newton target fields. The XMS comprises four largely overlapping source samples selected at soft (0.5−2 keV), intermediate (0.5−4.5 keV), hard (2−10 keV) and ultra-hard (4.5−7.5 keV) bands, the first three of them being flux-limited.

Results. We report on the optical identification of the XMS samples, complete to 85−95%. At the flux levels sampled by the XMS we find that the X-ray sky is largely dominated by Active Galactic Nuclei. The fraction of stars in soft X-ray selected samples is below 10%, and only a few per cent for hard selected samples. We find that the fraction of optically obscured objects in the AGN population stays constant at around 15−20% for soft and intermediate band selected X-ray sources, over 2 decades of flux. The fraction of obscured objects amongst the AGN population is larger (∼35−45%) in the hard or ultra-hard selected samples, and constant across a similarly wide flux range. The distribution in X-ray-to-optical flux ratio is a strong function of the selection band, with a larger fraction of sources with high values in hard selected samples. Sources with X-ray-to-optical flux ratios in excess of 10 are dominated by obscured AGN, but with a significant contribution from unobscured AGN.

Key words. X-rays: general – X-rays: galaxies – X-rays: stars – galaxies: active

1. Introduction

Supermassive black holes (SMBHs, i.e., with masses $\sim 10^6$−10^9 $M_\odot$) have been detected in the centers of virtually all nearby galaxies (Merritt & Ferrarese 2001; Tremaine et al. 2002). In many of these galaxies -including our own- the SMBH is largely dormant, i.e., the luminosity is many orders of magnitude below the Eddington limit. Only ∼10% of today's galaxies (at most) host active galactic nuclei (AGN), and a very large fraction of them are in fact inconspicuous at most wavelengths because of obscuration (Fabian & Iwasawa 1999).

It is generally believed that the seeds of these SMBHs were the remnants of the first generation of massive stars in the history of the Universe. These early black holes may have had masses of tens of $M_\odot$ at most. The growth of these relic black holes to their current sizes is very likely dominated by accretion, with additional contributions by other phenomena like black hole mergers and tidal capture of stars (Marconi et al. 2004). According to current synthesis models, the integrated X-ray emission produced by the growth of SMBHs by accretion over the history of the Universe is recorded in the X-ray background (XRB). Thus the XRB can be used to constrain the epochs and environments in which SMBHs developed.

There are currently a number of existing or on-going surveys in various X-ray energy bands (see Brandt & Hasinger 2005, for a recent compilation). In the pre-*Chandra* and pre-*XMM-Newton* era the Einstein Extended Medium Sensitivity Survey (Maccacaro et al. 1982; Gioia et al. 1990; Stocke et al. 1991) pioneered the procedure of determining typical X-ray to

⋆ Based on observations obtained with *XMM-Newton*, an ESA science mission with instruments and contributions directly funded by ESA Member States and the USA (NASA). Based on observations made with the INT/WHT, TNG and NOT operated on the island of La Palma by the Isaac Newton Group, the Centro Galileo Galilei and the Nordic Optical Telescope Science Association respectively, in the Spanish Observatorio del Roque de los Muchachos. Based on observations collected at the Centro Astronómico Hispano Alemán (CAHA) at Calar Alto, operated jointly by the Max-Planck Institut für Astronomie and the Instituto de Astrofísica de Andalucía (CSIC). Based on observations collected at the European Southern Observatory, Paranal, Chile, as part of programme 75.A-0336.

⋆⋆ Tables 2 and 5 are only available in electronic form at `http://www.aanda.org`

optical flux ratios for different classes of X-ray sources to facilitate the identification processes and has set the standard for serendipitous X-ray surveys. *ROSAT* produced a number of surveys in the soft 0.5−2 keV X-ray band at various depths, e.g., the *ROSAT* Bright Survey (Schwope et al. 2000), the intermediate flux RIXOS survey (Mason et al. 2000) and the *ROSAT* deep surveys (McHardy et al. 1998; Georgantopoulos et al. 1996; Hasinger et al. 1998; Lehmann et al. 2001) among others. These surveys show that AGN dominate the high Galactic latitude soft X-ray sky at virtually all relevant fluxes. The majority of these AGN are of spectroscopic type 1, which means that we are witnessing the growth of SMBH through unobscured lines of sight. In a moderate fraction of the sources identified, however, there is evidence for obscuration as their optical spectra lack broad emission lines (type 2 AGN).

Ueda et al. (2003) discuss the results from a large area X-ray survey in the 2−10 keV band with ASCA and those from HEAO-1 and *Chandra*, where a larger fraction of the sources identified correspond to type 2 AGN.

With *Chandra* and *XMM-Newton* coming into operation X-ray surveys, particularly at energies above a few keV, have been significantly boosted. Thanks to the high sensitivity and large field of view of the EPIC cameras (Turner et al. 2001; Strüder et al. 2001) on board *XMM-Newton* (Jansen et al. 2001), X-ray surveys requiring large solid angles have been dominated by this instrument. The Bright Source Survey-BSS (Della Ceca et al. 2004) contains 400 sources brighter than $\sim 7 \times 10^{-14}$ erg cm^{-2} s^{-1} either in 0.5−4.5 keV or 4.5−7.5 keV. The BSS samples[1], which have been identified to ∼90% (Caccianiga et al. 2007), show an X-ray sky dominated by AGN, where the fraction of obscured objects varies with the selection band (sample selection at harder energies reveals a higher fraction of obscured objects, as expected).

Deep surveys have also been conducted by *XMM-Newton*, for example in the Lockman Hole down to $\sim 10^{-15}$ erg cm^{-2} s^{-1} (Hasinger et al. 2001; Mateos et al. 2005b). However, thanks to its much better angular resolution, the *Chandra* deep surveys are photon counting limited and far from confusion and are consequently much more competitive at fainter fluxes (Alexander et al. 2003; Tozzi et al. 2006). Optical identification of these deep surveys is largely incomplete, a fact that is driven by the intrinsic faintness and red colour of most of the counterparts to the faintest X-ray sources. In the intermediate flux regime, however, the identified fractions are large and nearing completion. Deep surveys start to find a population of galaxies not necessarily hosting active nuclei as an important ingredient. In addition, the AGN population is found to contain an important fraction of obscured objects.

The wide range of intermediate X-ray fluxes, between 10^{-15} erg cm^{-2} s^{-1} and 10^{-13} erg cm^{-2} s^{-1}, have also been the subject of a number of on-going surveys. Besides bridging the gap between wide and deep surveys, intermediate fluxes sample the region around the break in the X-ray source counts (Carrera et al. 2007), and therefore their sources are responsible for a large fraction of the X-ray background. Among these, we highlight the *XMM-Newton* survey in the well-studied (at many bands) COSMOS field, which covers 2 deg^2 to fluxes $\sim 10^{-15}$ erg cm^{-2} s^{-1} (Hasinger et al. 2007). The optical identification is still on-going, reaching 40% (Brusa et al. 2007). At fluxes around 10^{-14} erg cm^{-2} s^{-1}, the HELLAS2XMM survey (Baldi et al. 2002; Fiore et al. 2003), now extended to cover 1.4 deg^2, contains over 220 X-ray sources, optically identified to 70% completeness (Cocchia et al. 2007).

Other surveys in this flux range include the *XMM-Newton* survey in the Marano field (Krumpe et al. 2007), which is 65% identified over a modest solid angle of 0.28 deg^2. Also the XMM-2dF survey (Tedds et al., in preparation), which contains almost 1000 X-ray sources optically identified in the Southern Hemisphere, is an important contributor in this regime. *Chandra* has also triggered surveys at intermediate fluxes, most notably the *Chandra* Multiwavelength Survey (Kim et al. 2004a,b; Green et al. 2004), covering 1.7 deg^2 and identified to ∼40% completeness (Silverman et al. 2005).

In the realm of this variety of X-ray surveys that yield a qualitative picture of the X-ray sky, the *XMM-Newton* Medium sensitivity Survey (XMS) discussed in this paper finds its place in three important ways: a) it deals with very large samples, selected at various X-ray bands where *XMM-Newton* is sensitive, from 0.5 to 10 keV; b) the samples that we consider have been identified almost in full, from 85% to 95% completeness and c) three out of the four samples that we explore are strictly flux limited in three energy bands (0.5−2 keV, 0.5−4.5 keV and 2−10 keV). Armed with these unique features, the XMS is a very powerful tool to derive a *quantitative* characterization of the population of X-ray sources selected in various bands, and also to study and characterize minority populations, all at specific intermediate X-ray fluxes where a substantial fraction of the X-ray background below 10 keV is generated. The power of the XMS is enhanced by the fact that to some extent it is a representative sub-sample of the *XMM-Newton* X-ray source catalogue 2XMM[2], containing 200 000 entries.

Specific goals that have driven the construction of the XMS whose results are presented in this paper include to a) quantify the fraction of stars versus extragalactic sources at intermediate X-ray fluxes and at different X-ray energy bands; b) quantify the fraction of AGN that are classified as obscured by optical spectroscopy at intermediate X-ray fluxes and for samples selected in different energy bands; c) find the redshift distribution for the various classes of extragalactic sources and compare soft and hard X-ray selected samples; d) study the distribution of the X-ray-to-optical flux ratio for the various classes of X-ray sources, also as a function of X-ray selection band. The X-ray spectral properties of the sources of the XMS were discussed in Mateos et al. (2005a).

Further goals that we will achieve with the XMS in forthcoming papers include to e) determine the fraction of "red QSOs" at intermediate X-ray fluxes and as a function of X-ray selection band; f) relate X-ray spectral properties (like photoelectric absorption) to optical colours of the counterpart; g) quantify the fraction of radio-loud AGN in the samples selected at various X-ray energies; h) construct Spectral Energy Distributions for the various classes of sources in the XMS. Results of these further analyses will be presented in a forthcoming paper (Bussons-Gordo et al., in preparation).

The paper is organized as follows: in Sect. 2 we define the XMS along with the 4 samples that constitute it, including the X-ray source list; in Sect. 3 we discuss the multi-band optical imaging conducted on the *XMM-Newton* target fields and the process for selecting candidate counterparts; this is continued in Sect. 4 where we discuss the identification of the XMS sources in terms of optical spectroscopy, and list photometric and spectroscopic information on each XMS source. Section 5 presents the first scientific results from the XMS, specifically a description of

[1] `http://www.brera.mi.astro.it/~xmm/`

[2] Pre-release under `http://xmm.vilspa.esa.es/xsa`

the overall source populations, the fraction of stars in the various samples, the fraction of optically obscured AGN, and the X-ray to optical flux ratio of the different source populations. Section 6 summarizes our main results.

To clarify the terminology used in this paper, an AGN not displaying broad emission lines in its optical spectrum is termed as type 2 or obscured, and type 1 or unobscured otherwise. The property of being absorbed or unabsorbed refers only to the detection or not of photoelectric X-ray absorption. Throughout this paper, we used a single power law X-ray spectrum to convert from X-ray source count rate to flux in physical units, with a photon spectral index $\Gamma = 1.8$ for the XMS-S and XMS-X samples and $\Gamma = 1.7$ for the XMS-H and XMS-U samples. These are the average values obtained by Carrera et al. (2007), which -as opposed to what we do here- used the specific value of Γ for each individual source and energy range. When computing luminosities, we also use the above spectra for K-correction and the concordance cosmology parameter values: $H_0 = 70$ km s^{-1} Mpc^{-1}, $\Omega_{\rm m} = 0.3$ and $\Omega_\Lambda = 0.7$. All quoted uncertainties in parameter estimates are shown at a 90% confidence level for one interesting parameter.

2. The *XMM-Newton* medium sensitivity survey (XMS)

The XMS is a serendipitous X-ray source survey with intermediate X-ray fluxes, which has been built using the AXIS[3] sample described in Carrera et al. (2007). The XMS uses 25 target fields (see Table 1, areas around targets themselves are excluded), which cover a geometric sky area $\sim$3 deg^2. The details of the source searching, screening, masking out of problematic detector areas (CCD gaps, bright targets, bad pixels and columns and out of time events) are extensively discussed in Carrera et al. (2007).

The XMS itself is made of four largely overlapping samples. The XMS-S, XMS-H and XMS-X are flux limited in the 0.5−2 keV, 2−10 keV and 0.5−4.5 keV bands respectively, with flux limits, well above the sensitivity of the data, listed in Table 3. A fourth sample (XMS-U) selected in the "ultrahard" band 4.5−7.5 keV is not artificially limited in flux, and due to the scarcity of these sources it contains all the sources detected in the 25 fields. Table 2 lists the X-ray source positions and fluxes in the various bands.

The XMS-S and XMS-H were constructed to match the standard "soft" and "hard" X-ray bands that have been extensively used in previous and contemporary X-ray surveys with *XMM-Newton* and other X-ray observatories. The 0.5−4.5 keV selection band of the XMS-X sample was chosen to maximize the *XMM-Newton*/EPIC sensitivity and is the largest of the 4 samples. The total number of distinct X-ray sources in the XMS is 318, out of which 272 (86%) have been spectroscopically identified. The identification completeness of the various samples is also shown in Table 3, which exceeds 90% for the softer XMS-S and XMS-X samples, and is around 85% for the hard XMS-H and ultra-hard XMS-U samples. The XMS-X sample extends the size of the pilot study presented in Barcons et al. (2002) by an order of magnitude.

[3] AXIS (An *XMM-Newton* International Survey) was an International Time Programme of the Observatorio del Roque de Los Muchachos, which was granted observing time in 2000 and 2001. See `http://venus.ifca.unican.es/~xray/AXIS` for details.

Table 1. XMS target fields.

Target field	RA (J2000)	Dec (J2000)	b^{II}(deg)	Phot[a]
Cl 0016+1609	00:18:33	+16:26:18	–45.5	SDSS
G 133-69 pos2	01:04:00	–06:42:00	–69.3	CMC
G 133-69 pos1	01:04:24	–06:24:00	–68.7	CMC
SDS-1b	02:18:00	–05:00:00	–59.7	CMC
SDS-3	02:18:48	–04:39:00	–59.3	CMC
SDS-2	02:19:36	–05:00:00	–58.9	CMC
A 399	02:58:25	+13:18:00	–39.2	CMC
Mrk 3	06:15:36	+71:02:05	+22.7	WFC[b]
MS 0737.9+7441	07:44:04	+74:33:49	+29.6	WFC
S5 0836+71	08:41:24	+70:53:41	+34.4	WFC
Cl 0939+4713	09:43:00	+46:59:30	+48.9	SDSS
B2 1028+31	10:30:59	+31:02:56	+59.8	SDSS
B2 1128+31	11:31:09	+31:14:07	+72.0	SDSS
Mrk 205	12:21:44	+75:18:37	+41.7	WFC
MS 1229.2+6430	12:31:32	+64:14:21	+53.0	SDSS
HD 117555	13:30:47	+24:13:58	+80.7	SDSS
A 1837	14:01:35	–11:07:37	+47.6	CMC
UZ Lib	15:32:23	–08:32:05	+36.6	WFC[c]
PKS 2126-15	21:29:12	–15:38:41	–42.4	CMC
PKS 2135-14	21:37:45	–14:32:55	–43.8	CMC
PB 5062	22:05:10	–01:55:18	–43.3	CMC
LBQS 2212-1759	22:15:32	–17:44:05	–52.9	CMC
PHL 5200	22:28:30	–05:18:55	–50.0	CMC
IRAS 22491-1808	22:51:50	–17:52:23	–61.4	CMC
EQ Peg	23:31:50	+19:56:17	–39.1	CMC

[a] This column gives the ultimate photometric calibration used: WFC if our own data from a photometric night was used as the main resource, SDSS for the Sloan Digital Sky Survey, and CMC for the Carlsberg Meridian Catalogue survey.
[b] In this case the extinction curve calibration in our data gives some scatter which means that the magnitudes are not as accurate as for the sources in the other fields.
[c] This field was not imaged in g' and r'. In addition to i', it was imaged in the Johnson filters B, V and R at the ESO/MPG 2.2 m telescope with the WFI camera.

3. Imaging and selection of candidate counterparts

3.1. The data

Target fields were observed primarily with the Wide-Field Camera (WFC) on the 2.5 m INT telescope. The observations were obtained via the AXIS programme and other programmes devoted to image a large number of *XMM-Newton* target fields in the optical. The WFC covers virtually all the field of view of EPIC, if centered optimally. We used the Sloan Digital Sky Survey filters g', r' and i' to image all the XMS target fields. In addition many of the fields were also imaged bluewards and redwards using existing facility filters at the WFC (u and Z Gunn). These data are available for all fields, except for the G 133-69 pos 1 and PB 5062 fields, while for UZ Lib and B2 1128+31 the u-band data are missing. Since data from these two additional filters are not used in this paper, we do not discuss them any further.

Exposure times were adjusted to be deep enough for most of the X-ray sources to have an optical counterpart in the r' and i' filters, and therefore had to be significantly deeper than those in the Digitized Sky Surveys. They were chosen as 600 s, 600 s and 1200 s respectively in the g', r', i' filters for dark time. This produced images with limiting magnitude for point sources going down to $r' \sim 23-24$ for $\sim$1−1.5″ seeing, typical in our observing runs, which our experience with the first fields (Barcons et al. 2002) demonstrated to be appropriate. When

Table 3. Summary of identifications in the various samples.

Sample	Sel. band (keV)	Limiting flux[a]	Number sources	Number ident.	Fract. (%)
XMS-S	0.5–2.0	1.5	210	200	95
XMS-X	0.5–4.5	2.0	284	261	92
XMS-H	2.0–10	3.3	159	132	83
XMS-U	4.5–7.5	1.15	70	60	86

[a] In units of 10^{-14} erg cm^{-2} s^{-1} in the selection X-ray band.

observing with brighter moon conditions, we restricted ourselves to the reddest filters and doubled the exposure times.

The WFC images were reduced using standard techniques including de-bias, non-linearity correction, flat fielding and fringe correction (in i' and Z). Bias frames and twilight flats obtained during the same observing nights were used, but for the fringe correction, contemporaneous archival i' and Z fringe frames were utilised. Information on the WFC pipeline procedures, that perform all these steps can be found in the Cambridge Astronomy Survey Unit[4] (CASU) web pages.

3.2. Photometric calibration

The photometric calibration of the WFC images was conducted in the standard way. Photometric standard stars were observed during the same nights as the *XMM-Newton* target fields were imaged, at different air masses. Then an extinction curve was fitted for each optical band. In several cases where we suspected that photometric conditions were not achieved, we re-imaged the same field with one WFC filter (r') or alternatively a part of it with the ALFOSC instrument in imaging mode on the NOT telescope.

However, in a number of target fields and for some of the bands, the extinction curve showed significant scatter that was attributed to these observations being done under non-photometric conditions. In order to improve the photometric quality of the data, two steps were taken. First we concentrated on calibrating one band (typically r') and later we applied colour corrections to propagate the improved photometry to all bands.

In the first step we used two complementary photometrically calibrated data sets. The first of these is the Sloan Digital Sky Survey, Data Release 5[5]. We could use the SDSS data on 6 *XMM-Newton* fields. The sky density of SDSS is lower than our WFC images, but we typically found a large enough number (∼100) of matches in every image.

The second data set used to improve the photometric calibration is the Carlsberg Meridian Catalogue (CMC) astrometric survey in the r' band[6], which we could apply to 19 fields. This survey is much shallower than the SDSS ($r' < 17$). In addition we found very significant systematic differences between WFC magnitudes and CMC ones at magnitudes less than $r' \sim 16$–16.5 which we attributed to saturation in our data. That typically leaves a very narrow dynamic range for cross-calibrating WFC versus CMC magnitudes, that we adopted as $16.5 < r' < 17$. Prompted by this, we also restricted the WFC versus SDSS cross calibration to magnitudes brighter than $r' \sim 16$. As a safety test, we cross-calibrated CMC versus SDSS r' magnitudes in the 5 fields where we could do that, but in this case using the full magnitude range from $r' \sim 14$–18 and found tiny significant shifts, all of them well below 0.1 mag in all fields. Figure 1 illustrates the residuals of the cross-calibration in the case of one target field where we had all three WFC, SDSS and CMC data sets.

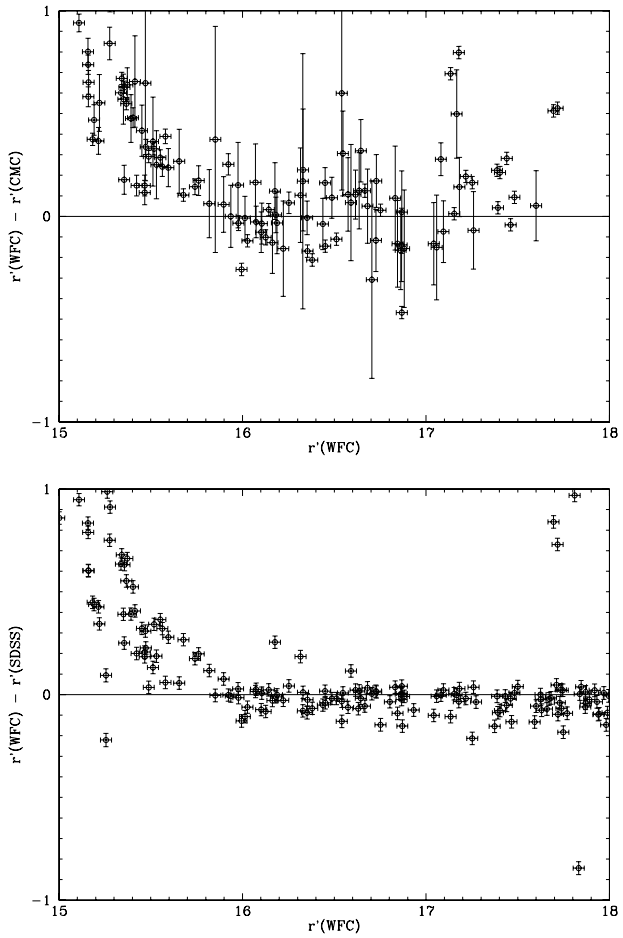

Fig. 1. Photometric cross-calibration in the B2 1128+31 field, where we have both coverage from the SDSS and CMC, along with our own WFC photometry.

In general, photometric shifts in fields where the quality of the WFC photometric calibration was thought to be good were found to be small (always $\Delta r' < 0.2$ mag) when calibrated against CMC or SDSS. In other cases where we had reason to suspect that our initial photometric calibration was not of high quality, we found photometric shifts as large as $\Delta r' \sim 0.5$ mag. This is why we applied these corrections to our photometry, with the SDSS one taking priority over CMC. Table 1 lists the photometric calibration data used in each field.

We then exported this refined calibration in r' into the g' and i' bands by constructing a $g'-r'$ vs. $r'-i'$ colour–colour diagram. We compared this to a calibrated colour–colour sequence pattern that was constructed using WFC observations of ELAIS fields. Shifts were applied to g' and i' WFC magnitudes as to match both. These shifts were propagated to all magnitudes listed in this paper.

We believe our photometry to be better than 0.1 mag in the majority of our fields and certainly better than 0.2 mag for all of them. In Sect. 5.5, where we analyze the X-ray-to-optical flux ratio, we use the quantity $\log f_{\rm opt}$, which has a maximum error due to these calibration uncertainties of well below 10%.

[4] `http://www.ast.cam.ac.uk/~wfcsur`

[5] `http://www.sdss.org`

[6] See `http://www.ast.cam.ac.uk/~dwe/SRF/camc.html` for details.

3.3. Astrometric calibration

Astrometric calibration of the WFC was performed using the Cambridge Astronomy Survey Unit (CASU) procedures. Typically, hundreds of matches per WFC image were obtained against the APM catalogue[7], which was used as the astrometric reference for the optical images. Specifically, a simple 6 parameter plate solution over the whole 4-CCD image was used, but accounting for a known and previously calibrated telescope distortion cubic radial term. The residuals from the plate solution were typically below 0.2 arcsec, which is good enough to identify candidate counterparts to the X-ray sources and for blind spectroscopic observations to identify these counterparts.

The astrometry of the *XMM-Newton* X-ray source position was registered against the USNO A2 (Monet et al. 1998) source catalogue (Carrera et al. 2007), but the optical astrometry refers to a different astrometric system. In order to ensure that this does not lead to artificial mismatches, we measured the USNO-APM shifts in each *XMM-Newton* field by cross-correlating both source catalogues in the corresponding region. The shifts were significant in most cases but small, typically <0.5 arcsec, which is less than the statistical accuracy in the X-ray source positions (0.6 arcsec averaged over the whole XMS sample). The positions of bright sources that were severely saturated in our WFC images were obtained from the USNO catalogue itself and therefore do not suffer from these small APM-USNO shifts. Given the small size of these shifts and in view of the much broader overall distribution of offsets between the position of the X-ray source and its optical counterpart (see Fig. 2) we conclude that the use of these two different astrometric reference frames does not affect in any noticeable way the results presented in this paper.

4. Identification of the XMS sources

In order to search for candidate counterparts of the X-ray sources, we normally used the r'-band WFC image. Optical source lists for these images were generated with the CASU procedures.

Counterparts for the X-ray sources were searched for in the optical image lists. Candidate counterparts had to be either within the 5 statistical errors (at 90% confidence) of the X-ray position or within 5 arcsec from the position of the X-ray source. This last criterion was used to accommodate any residual systematics in the astrometric calibration of the X-ray EPIC images.

As reported in Barcons et al. (2002) this resulted in the vast majority of the XMS sources having a single candidate counterpart. There are a few exceptions to this. In a few cases (15), the position of the X-ray source happened to fall in the gaps between CCDs in the WFC images. The strategy adopted to image in all optical filters with the same target point, which allowed us to obtain reliable optical colour information for the vast majority of the sources, also implied that for these few sources there is no optical image in any of the optical filters covering the region around these X-ray sources. In some of these sources (14 out of 15), the candidate counterpart was found by considering other optical imaging data, mostly the USNO A2 catalogue, or complementary imaging data.

Also, in a modest number of sources (78), there was more than one single candidate counterpart formally complying with our proximity criteria. But in 70 out of these 78 the optical source closest to the X-ray source position was also brightest and we adopted that as the likely counterpart. Given the brightness of the optical counterparts $r' < 22$ and the small region searched for around every X-ray source, we are confident that the number of spurious associations is insignificant in this sample.

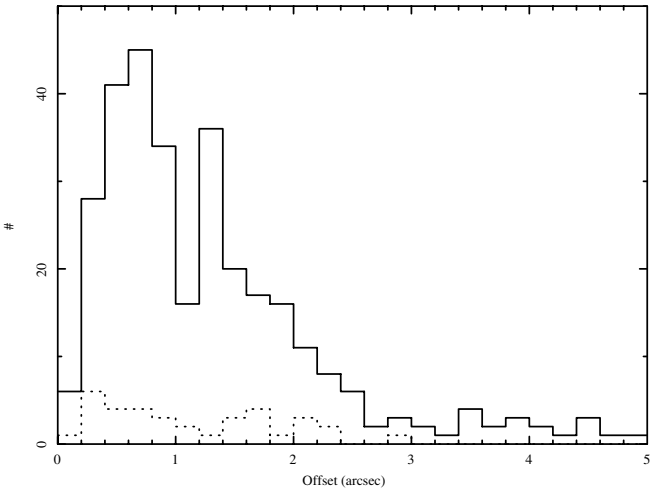

Fig. 2. Histogram of the distances from the optical source to the X-ray source centroid. The continuous line is for all sources with a counterpart and the dotted line for those with a likely counterpart without spectroscopic confirmation.

Figure 2 shows the histogram of the X-ray to optical angular separations for the sources spectroscopically identified and for those where a unique candidate counterpart is found but without a spectroscopic identification. The distribution peaks at small separations (~2″). Integrating this distribution outwards shows that in 68%, 90% and 95% of the cases the optical counterpart lies closer than 1.5″, 2.4″ and 3.6″ from the X-ray source respectively. Although the histogram of unidentified sources looks slightly more disperse than that of the identified ones, all candidate optical counterparts fall within 3″ of the position of the X-ray source.

There are a total of five sources that have no candidate counterpart in any of our optical images. For a further 3 sources, finding a candidate counterpart required a special strategy: in one case a counterpart was only found in the K-band (XMSJ 122143.6+752238), and in a further two cases the very faint optical counterparts were only detected via imaging with the VLT (XMSJ 225227.6-180223, in the I band) and Subaru (XMSJ 021705,4-045654, with $R = 25.60$) telescopes.

4.1. Optical spectroscopy

Searches for information on the XMS candidate counterparts in existing catalogues gave useful information (i.e., nature of the source and redshift) only for a handful of objects. Identifications for a few other X-ray sources were provided to us by the Subaru/*XMM-Newton* Deep Survey project (Akiyama, private communication) and by the *XMM-Newton* Bright Source Survey (Della Ceca et al. 2004). That means that the vast majority of the XMS sources were previously unidentified and required optical spectroscopy.

Optical spectroscopy was conducted in a number of ground-based optical facilities, following the strategy presented in Barcons et al. (2002). The low surface density in the sky of the XMS sources (~100 deg^{-2}) makes the use of multi-object slit-mask spectrographs not particularly efficient. Part of

[7] http://www.ast.cam.ac.uk/~mike/apmcat/

Table 4. List of spectroscopic setups relevant to this sample.

Telescope	Instrument	Spectral range (Å)	Slit width (arcsec)	Spectral resolution[a] (Å)	Comments
WHT/ORM	AUTOFIB2/WYFFOS	3900–7100	2.7[b]	7	Fibre
WHT/ORM	AUTOFIB2/WYFFOS	3900–7100	1.6[b]	6	Fibre
WHT/ORM	ISIS	3500–8500	1.2–2.0	3.0–3.3	Long slit
TNG/ORM	DOLORES	3500–8000	1.0–1.5	14–15	Long slit
NOT/ORM	ALFOSC	4000–9000	1.0–1.5	4	Long slit
3.5 m/CAHA	MOSCA	3300–10 000	1.0–1.7	24	Long slit
UT1/ESO	FORS2	4400–10 000	1.0	6–12	Long slit

[a] Measured from unsaturated arc lines. [b] Width of individual fibres.

the identifications were performed using a fibre spectrometer (AUTOFIB2/WYFFOS) which covers a much larger solid angle in the sky and therefore is better suited for the identification work.

The main limitation of the fibre spectrometers in obtaining the spectrum of faint sources resides in the subtraction of the sky which enters the fibres along with the light from the target objects. Wider fibres make this problem worse. This limits the ultimate sensitivity of the spectrometer, which for our exposure times and observing conditions was rarely good enough for magnitudes fainter than $r' \sim 20.5$.

Therefore, despite the larger solid angle covered by fibre spectrometers, the distribution of optical magnitudes in the XMS source candidate counterparts calls for the use of single object long-slit spectroscopy. A number of such spectrometers were used in a variety of ground-based telescopes, with apertures from 2.5 m to 8.2 m.

Table 4 lists the telescopes and observatories that were used, along with the specific spectrometers, with specification of the wavelength range, the slit width (or fibre width when applicable) along with the measured spectral resolution using unblended arc lines (or a sky line in the case of the fibre spectrometer). The spectral reduction process is standard and was described in Barcons et al. (2002). The final spectra will be available at `http://www.ifca.unican.es/~xray/AXIS` and in the long term in the *XMM-Newton* Science Archive[8] under the 2XMM catalogue.

These spectra are meant only to be reliable for *identification* purposes, i.e., the spectrophotometric calibration has only been performed at best in relative terms (i.e., up to an absolute normalisation factor). Even more, in the fibre spectra and in some of the long-slit spectra that were not taken with the slit aligned to the parallactic angle, differential refraction will cause the overall large-scale shape of the spectrum to be incorrect. None of these facts hamper the identification of the spectral features that we used in this paper, which is based on broad and/or narrow emission lines and on absorption bands, but not on broad-band features like the 4000 Å break. However we caution against the use of these spectra to measure line fluxes or line ratios because of the above limitations.

4.2. Classification of the sources

Based on the optical spectroscopy, we classify the counterparts to the XMS X-ray sources as in Barcons et al. (2002). Extragalactic sources exhibiting broad emission lines (velocity widths in excess of ~1500 km s^{-1}) are classified as BLAGN (Broad Line Active Galactic Nuclei); those exhibiting only narrow emission lines are termed NELG (Narrow Emission Line Galaxies); those with galaxy spectra without obvious emission lines are classified in principle as Absorption Line Galaxies (ALG). Of the latter, we distinguish two classes of exceptions: two of the sources with a galaxy spectrum without emission lines were previously catalogued as BL Lac objects and we classify them as such; if a qualitative inspection of the optical images show obvious evidence for a galaxy concentration we then classify the source as a cluster (Clus). Finally all X-ray sources with a stellar spectrum are labeled simply as "Star".

This classification is simple to perform, but in some cases it lacks a more detailed physical description of the source. This is particularly true in the case of the NELG, because no line diagnostics are performed to check whether the object hosts an AGN or not. The reason is that due to the rather wide redshift range spanned by these sources and the rather narrow wavelength coverage of the optical spectra (particularly for the fibre spectroscopy) the number of lines detected is small. Therefore it happens that typical diagnostic lines drift out of the spectrum with redshift. In addition, the quality of the spectra are in most cases not good enough to detect the weak lines necessary for these diagnostics. In fact the NELG are likely to be a mixture of type-2 AGN and star forming galaxies. In the discussion of the various samples we use the X-ray luminosity as an indicator of the presence of an AGN in these objects.

The second limitation of this simple classification is in the case of clusters. The very small number of X-ray sources identified as clusters (2) is not a real property of the X-ray sky at these flux levels, but an artifact of the detection and classification method. The detection method for X-ray sources is designed for point sources and might be missing a number of extended X-ray sources. In addition, in several optical images, the presence of a cluster of galaxies might not be obvious and the source might have been identified as a galaxy with or without emission lines.

The third and final limitation is in the stellar content. The stars that we identify have a varied range of spectral properties, but this is not explored in the present paper.

Redshifts have been measured by matching the most prominent features in emission or absorption to sliding wavelengths of these features. Templates for QSO and galaxies with a range of spectroscopic classes were used to assist in the generation of first guesses when necessary, especially when there were no prominent features.

Table 5 displays the full list of the 318 XMS sources, along with optical magnitudes of their counterparts, and the identifications.

[8] `http://xmm.vilspa.esa.es/xsa`

Table 6. Summary of the identifications of the various XMS samples.

Sample	Total	BLAGN	NELG	ALG	BL Lac	Clus	Star	Unid
XMS-S	210	150	26	6	2	1	15	10
XMS-X	284	192	38	7	2	2	20	23
XMS-X (South)	167	120	25	4	0	1	13	4
XMS-H	159	85	34	7	2	1	3	27
XMS-U	70	41	15	2	2	0	0	10

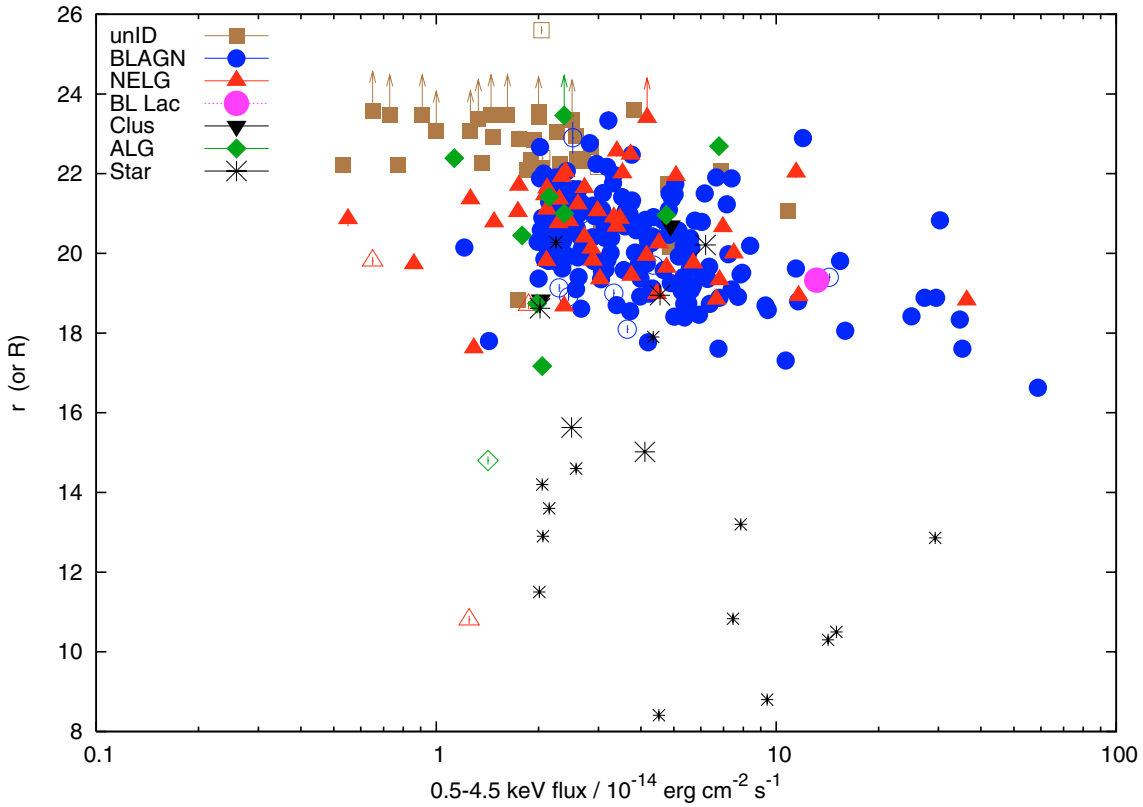

Fig. 3. Optical magnitude versus 0.5−4.5 keV flux for the XMS sources. The optical magnitude shown is r' (filled symbols) when available, and otherwise R (hollow symbols). Upward arrows denote lower limits in the magnitude derived from the lack of optical counterparts in the WFC r' band image, but several of these sources have counterparts in other optical bands.

5. The XMS X-ray source populations

5.1. General

The breakdown of the identifications in the 4 XMS samples is shown in Table 6. The completeness of these identifications is higher for the XMS-S (95%) and XMS-X (92%) than for the XMS-H (83%) and XMS-U (86%). There are several reasons for that, the most important one being that the XMS was originally conceived around the 0.5−4.5 keV band to optimise the *XMM-Newton* EPIC sensitivity and therefore the identification strategy has been especially successful in this band.

In particular, and as we will show later, the *Hard* and *Ultra-hard* samples contain a higher fraction of sources with a higher X-ray-to-optical flux ratio and therefore more sources have optically fainter counterparts. Given the limitations of the access to 8−10 m aperture class telescopes, in practice this means that the identification incompleteness is also biased. This implies that the fraction of unidentified sources is likely to be richer in potentially obscured objects than the average.

The results for the XMS-X are particularly robust and their robustness can be verified by using what we might call the "Southern" subset of the XMS-X. This is due to the fact that virtually all sources in this sample that are accessible from the VLT at ESO were observed in September 2005 during the 075.A-0336 run and the vast majority of them were identified. Table 6 also displays the numbers of identified targets in fields below a declination of +20° in the XMS-X sample. In this sample, at the price of reducing the size from the parent sample to ∼60%, we raise the identification fraction to over 98% (only 4 sources out of 167 remain unidentified).

A first glance at the overall source population that we are sampling, is given in Fig. 3, where we have plotted the optical magnitude (typically r', but R when r' is not available), as a function of 0.5−4.5 keV X-ray flux.

5.2. Stellar versus extragalactic content

Despite the high-galactic latitude selection of the *XMM-Newton* fields used in the XMS, a few of our X-ray sources have been identified as stars. A detailed study of the stellar content of the XMS is beyond the scope of this paper, but similarly to what is found in the *XMM-Newton* Galactic Plane Survey (Motch et al., in preparation) most of them will be active coronal stars.

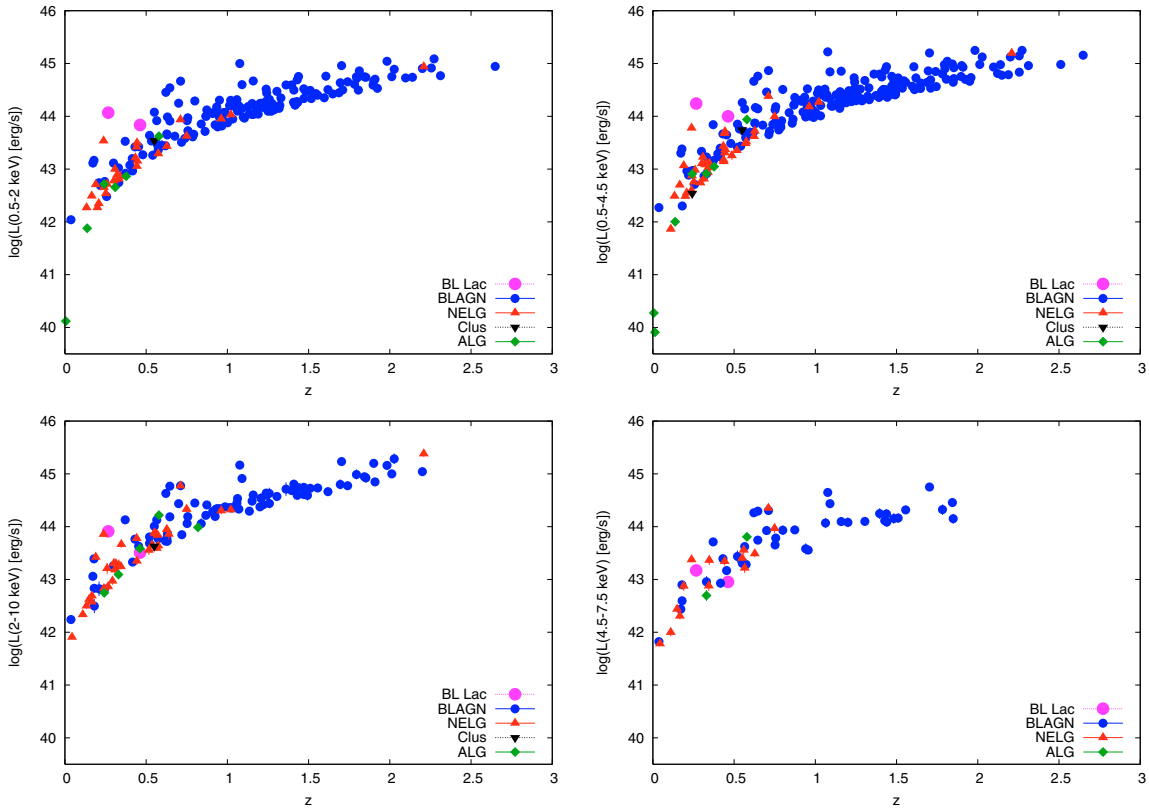

Fig. 4. X-ray luminosity in the selection band versus redshift for extragalactic sources in each of the XMS samples. *Top left* is for the XMS-S, *top right* for the XMS-X, *bottom left* for the XMS-H and *bottom right* for the XMS-U.

The current landscape of X-ray surveys indicates that the stellar content at high galactic latitudes decreases at faint fluxes. Since it is unlikely that any stellar X-ray source has escaped identification in the XMS survey, we are in a position to quantify this statement as well as to compare the stellar populations when selected at different energy bands.

The XMS-X sample contains a total of 20 stars, which represent 7^{+3}_{-2}% of the sample (henceforth errors on fractions are of 90% confidence and assuming a binomial distribution). If we split the XMS-X sample between bright (0.5−4.5 keV flux above 3.3×10^{-14} erg cm^{-2} s^{-1}) and faint (below the same flux) X-ray sources, the whole sample splits in two approximately equal halves (143 bright and 141 faint X-ray sources). The fraction of stars (8) in the faint sample is then $5.5^{+4.5}_{-2.5}$% and the fraction of stars (12) in the bright sample is $8.5^{+4.5}_{-3}$.

López-Santiago et al. (2007) have explored the stellar content of the BSS (Della Ceca et al. 2004), finding 58/389 (15 ± 3%) stars in the 0.5−4.5 keV sample. Combined with our own measurements on the XMS-X, this shows that there is a decrease in the stellar content when going to fainter X-ray fluxes.

It is also interesting to compare the fraction of stars in the various XMS samples. The soft XMS-S sample contains 15 stars, which represent 7^{+4}_{-2}% of the sample, similar to the XMS-X. The stellar content in the XMS-X and XMS-S samples is very similar.

Stars are much rarer in the XMS-H and XMS-U samples: the XMS-H contains only 3 stars ($2^{+2.5}_{-1}$%) and the XMS-U contains no stars whatsoever (<4% at 90% confidence). In this case we are totally confident that we are not missing any stars, as all unidentified sources in the XMS-H and XMS-U samples are optically extended. The low stellar content in these samples is not a surprise, as most of our stars are seen in X-rays because of their active coronae, which have X-ray spectra that are dominated by soft X-ray line emission and peak around 1 keV.

5.3. Luminosity and redshift distributions

The vast majority of XMS sources are extragalactic. We have computed the X-ray luminosities of the extragalactic sources (not corrected for absorption) and these are represented in Fig. 4 as a function of redshift for each of the XMS samples.

A visual inspection of these $L-z$ relations reveals that all but a few sources optically classified as NELGs have X-ray luminosities in the corresponding band in excess of 10^{42} erg s^{-1}, and are therefore most likely to host a hidden AGN. With very few exceptions, NELGs in our survey are therefore type 2 AGN. In fact, the 2−10 keV luminosity of 6 such objects exceeds 10^{44} erg s^{-1} and therefore qualify as type 2 QSOs by standard X-ray astronomy definitions.

The X-ray luminosity of a fraction of sources that we classified as ALG also exceeds 10^{42} erg s^{-1}. Specifically the number of ALG that exceed this luminosity threshold is 4 out of 7 in the most numerous and complete XMS-X. Such sources are often referred to as X-ray Bright Optically Normal Galaxies (XBONGS) and when studied in detail are invariably seen to host an AGN, which is either heavily obscured, or of low luminosity and outshone by the host galaxy, as shown by Severgnini et al. (2003), Rigby et al. (2006) and Caccianiga et al. (2007).

We also find a few X-ray sources classified as ALG with low X-ray luminosities (~10^{40} erg s^{-1}). In at least one case (XMSJ 084221.6+705758) the position of the X-ray source falls in the outskirts of the galaxy, and therefore is likely to be a

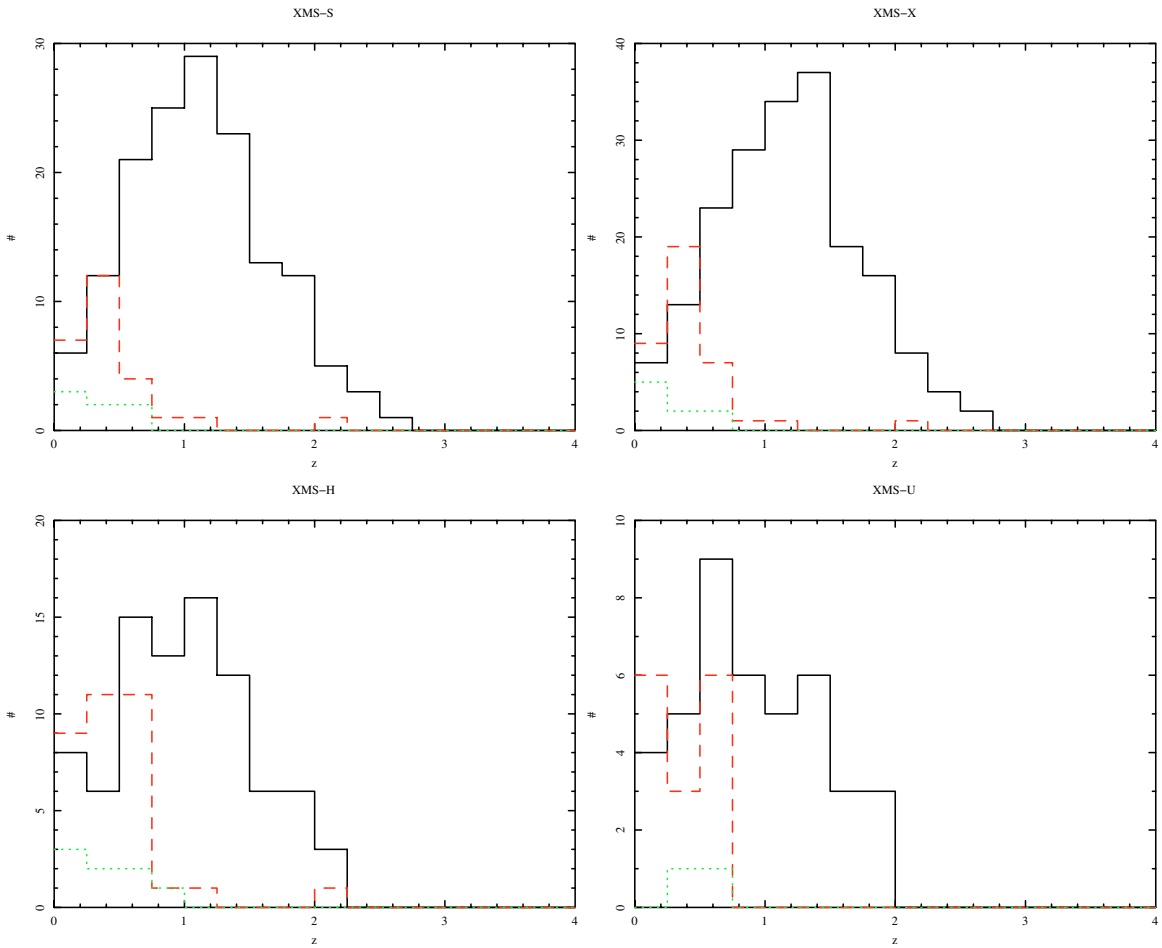

Fig. 5. Redshift histograms in each of the XMS samples. Solid line is for BLAGN, dashed line for NELG and dotted line for ALG. *Top left* is for the XMS-S, *top right* for the XMS-X, *bottom left* for the XMS-H and *bottom right* for the XMS-U.

candidate for an Ultra-luminous X-ray source. Watson et al. (2005) have discussed some of these sources in the context of the Subaru/*XMM-Newton* Deep Survey.

The overall luminosity distribution in all four samples is centered around 10^{44} erg s^{-1}, which means that the sample contains both Seyfert-like AGN and QSOs. This value is also where the AGN X-ray luminosity function exhibits a knee and therefore where most of the X-ray volume emissivity comes from.

The redshift distribution is displayed in Fig. 5 for the four samples. The peak of the BLAGN population in the XMS-S and XMS-X samples is around $z \sim 1.5$ which is not far from the one found in deeper surveys. However, the redshift cutoff at around $z \sim 3$ is due to the limited depth of the XMS that fails to find the higher redshift AGN revealed by deeper surveys.

The contribution from NELG and ALG, most of which are obscured AGN, peaks at low redshift, typically $z < 0.5$. This is lower than the peak revealed by deep surveys, due to the modest depth of the survey. Comparing the redshift distribution for the softer XMS-S sample to the hard XMS-H sample (which are drawn from different parent populations according to the Kolmogorov-Smirnov test which gives a probability of 10^{-13} for the null hypothesis) shows that with a similar sky density the hard sample misses an important fraction of unobscured AGN (BLAGN) at high redshift but includes virtually all the obscured objects. The redshift distribution is consequently shifted to lower values. We next discuss in more detail the relative fraction of obscured AGN.

5.4. Obscured versus unobscured AGN

The fraction of obscured AGN is known to have a strong dependence on the X-ray selection band and also on the depth of the survey. Typically soft X-ray selection misses a large fraction of obscured (and therefore likely absorbed in the X-ray band) AGN. Deeper X-ray surveys, even with soft X-ray sensitivity only, have also produced increasingly large fractions of obscured AGN.

The broad bandpass of *XMM-Newton* allows us to study the fraction of obscured AGN as a function of selection band and depth, at the intermediate fluxes sampled by the XMS. A detailed multi-wavelength study of the XMS survey, combining X-ray spectral information, optical colours and data at infrared and radio wavelengths is in preparation (Bussons-Gordo, in preparation).

For the current discussion, we now classify as an AGN any extragalactic X-ray source whose 2−10 keV X-ray luminosity exceeds 10^{42} erg s^{-1} and is not obviously associated with a cluster of galaxies. This stems from the observation that in the local Universe all sources more luminous than this are at the very least suspected to harbour an AGN. A potential limitation of our classification, and therefore of our estimates of the fraction of optically obscured sources among AGN, comes from the limited

quality of the optical spectra, in particular if weak broad emission lines are present. This is illustrated in the BSS (Caccianiga et al. 2007; Della Ceca et al., in preparation) where some of the sources originally classified as ALG or NELG turned out to have "elusive" broad emission lines. For this paper, an AGN that does not display an obvious dominant broad emission line is considered as an obscured AGN.

The sources that we have classified as BLAGN are unobscured AGN. A fraction of these (around 10 per cent) display X-ray photoelectric absorption (Mateos et al. 2005a,b), but whatever the nature of these absorbers, they do not contain enough dust to obscure the broad line regions of these AGN, and in this context we will not consider them to be obscured AGN.

Among the sources classified optically as NELG or ALG, a large fraction of them are AGN according to the above scheme, and we term these as obscured AGN, since their Broad Line Region is not seen. Obscured AGN are expected to follow the AGN unified model predictions in the sense that they host the same central engine as an unobscured AGN, but that due to the presence of dust the Broad Line Region is heavily reddened and therefore not seen. Photoelectric absorption is expected in their X-ray spectrum (and is seen in most cases), but in about half of AGN without broad emission lines X-ray absorption is undetected (Mateos et al. 2005a). There are a number of hypotheses that can explain this mismatch, some of them dealing with the structure of the AGN itself, and not with real obscuration of a standard AGN (Mateos et al. 2005b). However, this discussion is beyond the scope of this paper, and we stick to the standard interpretation that the lack of broad emission lines is equivalent to obscuration.

A potential problem in the study of the fraction of the obscured objects among the AGN population arises because the fraction of unidentified X-ray sources is higher for optically fainter sources and these are more likely to be obscured. There is an indication of this being true, as most of their optical counterparts appear extended and therefore dominated by host galaxy light rather than by the nucleus.

For the XMS-X, we find 42 optically obscured AGN out of a total sample of 236 identified AGN, which represents 18^{+4}_{-4}%. This fraction is rather robust as it remains virtually unchanged if we restrict its estimate to the "South" XMS-X sample complete sample (20^{+5}_{-5}%).

The fact that this fraction is much smaller than what is expected from local Universe studies, where obscured AGN outnumber unobscured ones by a factor of 3, is due to the fact that obscuration comes along with photoelectric X-ray absorption which suppresses X-rays, particularly in the soft band. This implies that at harder X-ray energies there should be a higher fraction of obscured AGN. Although this is what qualitatively emerges from existing X-ray surveys, the size and combination of various selection bands on the XMS can provide a quantitative measurement of these effects. There is also a qualitative impression that the fraction of obscured AGN increases substantially when going deeper in a given X-ray energy band. In what follows we attempt to test these statements.

If we divide again the XMS-X sample in two approximately equal halves of faint and bright X-ray sources (0.5–4.5 keV fluxes below and above 3.3×10^{-14} erg cm^{-2} s^{-1}), among the identified sources obscured AGN represent 17^{+6}_{-5}% of the faint AGN and 19^{+6}_{-5}% of the bright AGN. This lack of flux dependence is confirmed when we restrict it to the "South" XMS-X complete sample (20^{+9}_{-6}% and 19^{+9}_{-6}% of obscured AGN for faint and bright sources respectively). This is within the errors of what comes out if we assume that *all* unidentified sources in the XMS-X sample are obscured AGN, in which case the fraction of obscured AGN would be slightly higher (25^{+5}_{-4}%) and independent of flux. Comparison of this fraction to the ∼20% of obscured AGN in the South XMS-X sources shows that despite an important obscured AGN component being among the unidentified XMS-X sources, there might be some type 1 AGN among them. We will return to this point later when discussing X-ray-to-optical flux ratios.

In the XMS-S the fraction of obscured AGN is 17^{+5}_{-4}%, which is very marginally smaller than in the XMS-X sample. This fraction remains unchanged when we split the XMS-S in faint and bright sources.

Things change significantly when we deal with hard X-ray selected sources. The identified sources in the XMS-H sample contain 35 ± 7% obscured AGN which could be as high as 45 ± 7% if all unidentified sources are obscured AGN. None of these figures change between XMS-H bright and faint X-ray sources.

There are no dramatic changes when we use the XMS-U sample with respect to the XMS-H sample: obscured AGN represent 31^{+7}_{-6}% of the AGN population which might be slightly higher if all unidentified sources are obscured AGN (43^{+7}_{-6}%).

In summary, in soft X-ray selected samples at intermediate fluxes, about ∼20–25% of the AGN are obscured, and this applies to both 0.5–2 keV and 0.5–4.5 keV selection. The *XMM-Newton* BSS (Della Ceca et al. 2004), which is also selected in the 0.5–4.5 keV band but at brighter fluxes, finds a slightly smaller fraction of obscured AGN, in the range of 6 to 14%. In the opposite flux direction, the *ROSAT* ultra-deep survey (Lehmann et al. 2001), which contains 94 X-ray sources with a 0.5–2 keV flux down to 1.2×10^{-15} erg cm^{-2} s^{-1} and identified to 90% completeness, also found ∼20% of obscured objects among the AGN population (13 out of 70).

The fraction of obscured AGN goes up to ∼35–45% for hard X-ray selected samples at intermediate fluxes in the XMS. This applies equally to 2–10 keV selection and to 4.5–7.5 keV selection. This means that above 4.5 keV the sensitivity of *XMM-Newton* is not high enough, and our exposure times are not deep enough, to raise new heavily obscured X-ray sources that are not selected in the 2–10 keV band. These fractions do not appear to change with X-ray flux of the sources within the flux ranges sampled by our survey. In this case, comparison with the Hard Bright Source Survey (Caccianiga et al. 2004, 2007; Della Ceca et al., in preparation) selected in the 4.5–7.5 keV band shows no change in the fraction of obscured AGN, which these authors quantify as 31–33%. The *Chandra* Multi-wavelength Survey (Silverman et al. 2005) (which goes down to 2–10 keV fluxes beween 10^{-15} and 10^{-14} erg cm^{-2} s^{-1}), when restricted to optically bright sources, reports that 28% of the total source sample is obscured, but its identified fraction is only 77% and therefore this fraction is most likely a lower limit.

A final point to address is the dependence of the fraction of optically obscured AGN as a function of X-ray luminosity. This fraction is reported by Barger et al. (2005) and Gilli et al. (2007) among others to decrease towards high luminosities. From Fig. 4 we can see this effect clearly happening in the XMS. For the XMS-H the fraction of optically obscured extragalactic objects with 2–10 keV luminosity between 10^{42} and 10^{44} erg s^{-1} is 62% (34 out of 55 objects) and above 10^{44} erg s^{-1} is only 9% (6 out of 70 objects). These numbers are consistent, within errors, with those quoted by Barger et al. (2005) and Gilli et al. (2007). However, Fig. 4 shows the very restricted coverage of the luminosity-redshift plane of a single flux-limited survey. We believe that addressing this issue needs the combination of

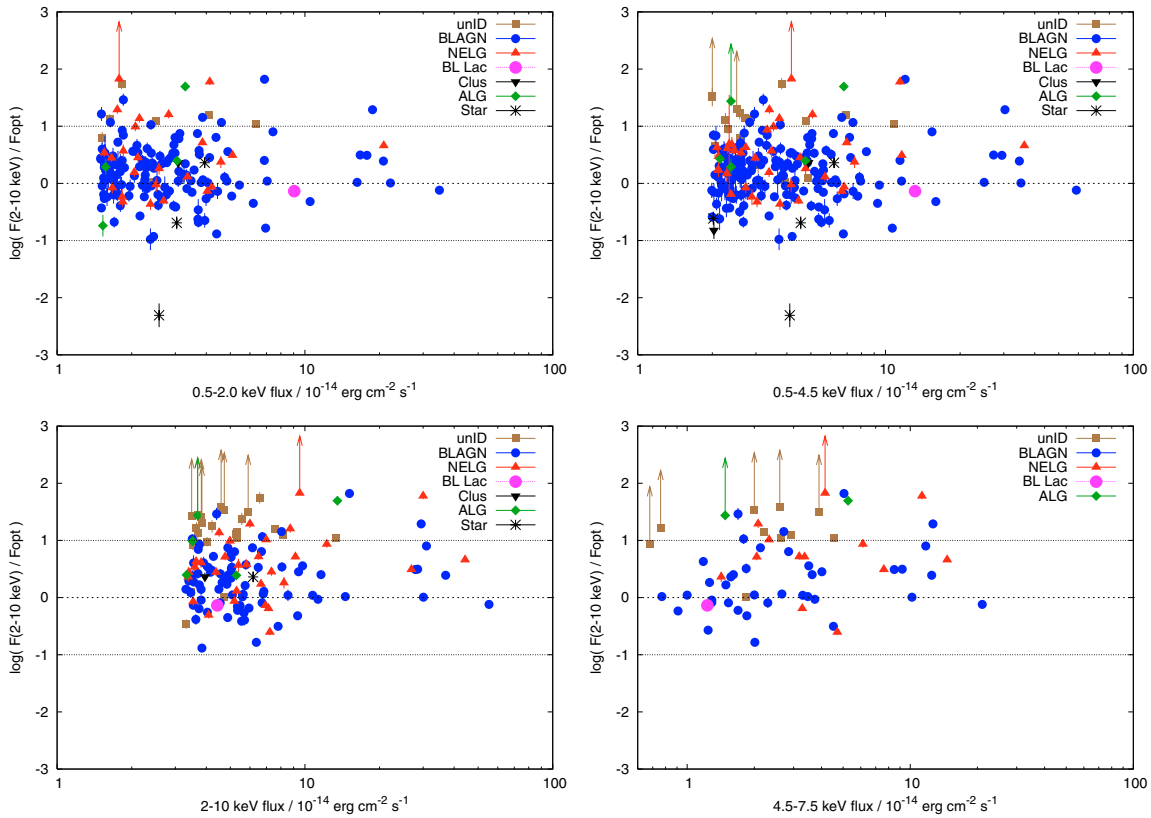

Fig. 6. X-ray to optical flux ratio as a function of X-ray flux in the corresponding X-ray band for all 4 XMS samples. Only those sources with known counterpart, which has a measured value (or a lower limit) of r' from our WFC imaging is included. In this way we miss a number of sources in each sample, but we avoid uncertain conversion factors between different bands. Top left is for the XMS-S, top right for the XMS-X, bottom left for the XMS-H and bottom right for the XMS-U. Symbols are as in Fig. 3.

multiple surveys covering different depths and solid angles in a way that evenly samples the luminosity-redshift plane.

5.5. X-ray to optical flux ratio

The X-ray to optical flux ratio has been used in various surveys as a proxy for obscuration. Similarly to other papers (Krumpe et al. 2007; Cocchia et al. 2007), we use as a proxy for optical flux that in the r' band and therefore compute $\log f_{\rm opt} = -0.4r' + \log(f_{r'0}\delta\lambda)$, where $f_{r'0} = 2.40 \times 10^{-9}$ erg cm^{-2} s^{-1} Å^{-1} is the zero-point for r' and $\delta\lambda = 1358$ Å is the FWHM of the r' filter. Note that this yields $X/O = \log(f_{\rm X}/f_{\rm opt}) = \log(f_{\rm X}) + 0.4r' + 5.49$, where $f_{\rm X}$ is the 2−10 keV flux in erg cm^{-2} s^{-1}, not corrected for Galactic absorption (the correction is insignificant at the XMS Galactic latitudes). Typically, unobscured type 1 AGN have $-1 < X/O < 1$, and therefore sources with X-ray to optical flux ratio in excess of 10 have been considered as likely obscured AGN.

We have excluded from this analysis those sources for which we have no reliable r' magnitudes, to avoid uncertainties. We attempted to calibrate the R versus r' relation, where the R magnitudes are mostly extracted from the literature and the USNO A2 catalogue. Specifically, Table 5 contains 105 BLAGN and 30 NELG for which we have both R and r'. Formally, $\log f_R$ versus $\log f_{r'}$ yields an offset of −0.30 for BLAGN and −0.49 for NELG, but in both cases the scatter is very large (0.25 dex). Therefore, by adding into this analysis those sources for which only R is available, we would be expanding considerably their uncertainties and therefore we ignore these sources.

We have studied the fraction of obscured AGN in the various XMS samples. This is best seen in Fig. 6, where we find that the vast majority of our objects lie in the "normal" type 1 AGN domain $-1 < X/O < 1$. However, a fraction of XMS sources have extreme values of X/O. Values below −1 are usually dominated by stars.

Far more important is the other extreme, $X/O > 1$, where obscured AGN are expected. Table 7 shows the numbers and fractions of obscured AGN in the various XMS samples and in 3 ranges of X/O. A difficulty is how we deal with lower limits to optical fluxes of various sources, where there is no detection in the WFC image, but only an upper limit in their magnitude from the sensitivity of the corresponding image. There are a number of uncertainties in this, including the likely possibility that the undetected counterpart is optically extended and therefore might be brighter (in integrated magnitude) than the quoted lower limit. For these sources (which are very few) we have used the lower limit in X/O as if it were a real detection.

The first result that becomes evident from Table 7 is the fact that the fraction of sources with $X/O > 1$, and therefore potentially obscured, varies substantially between samples. For the XMS-S, we find only 5 sources with $X/O > 1$ among a sample of 180 with measured X/O which represents only 3 ± 2%. This percentage grows to 7^{+4}_{-2}% (17/245) for XID-X and grows even further for the XMS-H to 17^{+7}_{-5}% (23/138) (for the XMS-U the numbers are too small to reach any conclusion). It is therefore clear that the fraction of sources with large X/O goes up from a small few per cent in the 0.5−2 keV selected XMS-S sample to 20% in the 2−10 keV selected XMS-H sample, with XMS-X in between. Note that these percentages have to be revised slightly

Table 7. Fraction of obscured AGN in the various XMS samples. ($f_{\rm obsc}$) is the fraction actually measured and ($f^*_{\rm obsc}$) the fraction that would result under the assumption that all unidentified sources are obscured AGN.

$\log(F(2-10\,{\rm keV})/F_{r'})$	$f_{\rm obsc}$	$f^*_{\rm obsc}$
XMS-S		
$-1.0:0.0$	17^{+8}_{-6}% (14/84)	18^{+8}_{-6}% (15/85)
$0.0:+1.0$	17^{+8}_{-6}% (14/81)	25^{+8}_{-7}% (22/89)
$>+1.0$	25^{+49}_{-15}% (1/4)	40^{+41}_{-21}% (2/5)
XMS-X		
$-1.0:0.0$	12^{+9}_{-5}% (8/65)	14^{+8}_{-6}% (9/66)
$0.0:+1.0$	20^{+6}_{-5}% (29/146)	25^{+6}_{-5}% (39/156)
$>+1.0$	36^{+29}_{-17}% (4/11)	59^{+19}_{-17}% (10/17)
XMS-H		
$-1.0:0.0$	21^{+16}_{-9}% (6/28)	24^{+16}_{-10}% (7/29)
$0.0:+1.0$	28^{+9}_{-7}% (22/78)	34^{+9}_{-8}% (29/85)
$>+1.0$	50^{+25}_{-18}% (6/12)	74^{+14}_{-14}% (17/23)
XMS-U		
$-1.0:0.0$	14^{+15}_{-7}% (4/29)	17^{+17}_{-8}% (5/30)
$0.0:+1.0$	39^{+22}_{-15}% (7/18)	50^{+19}_{-14}% (11/22)
$>+1.0$	50^{+40}_{-25}% (2/4)	50^{+40}_{-25}% (2/4)

downwards, as we are missing r' magnitudes for most of the stars (more abundant in the softer samples) which are saturated in our WFC images.

We see from Table 7 that the fraction of obscured AGN among the $X/O > 1$ sources is higher than in the whole sample, and this holds for all XMS samples. The second fact that can be seen by inspecting Table 7 is that in the XMS-H the fraction of obscured AGN amongst the $X/O > 1$ sources could be as high as 90% if all unidentified sources are obscured AGN, but this percentage is lower for the XMS-S and XMS-X.

But we can also look at this fact from a different point of view, which is that there are unobscured AGN with $X/O > 1$. There are at least 3/5, 7/17, 6/23 and 2/4 unobscured AGN with $X/O > 1$ in the XMS-S, XMS-X, XMS-H and XMS-U samples respectively, which represent somewhere between one fifth and one half of the corresponding sample with a selection cut at $X/O > 1$. The nature of these BLAGN with $X/O > 1$ will be investigated in future papers.

6. Conclusions

In this paper we have presented the *XMM-Newton* Medium sensitivity Survey XMS, and extracted a number of robust quantitative conclusions about the population of high Galactic latitude X-ray sources at intermediate flux levels. We have argued that given the completeness of our identifications and the relatively large size of the XMS samples, these conclusions can be safely exported to a much larger X-ray source catalogue like 2XMM.

Our conclusions can be summarized as follows:

1. The high galactic latitude X-ray sky at intermediate flux levels is dominated by AGN, which includes type-1 and type-2 AGN as well as the so-called XBONG which are likely to host a low luminosity or obscured nucleus (or both). The stellar content is less than 10% in soft X-ray selected samples, and drops to below 5% at around soft X-ray fluxes $\sim 10^{-14}$ erg cm s^{-1}. The stellar content in hard X-ray selected samples does not exceed a few per cent at most. Selection in 0.5−4.5 keV produces intermediate results.
2. Given the limited sensitivity of *XMM-Newton* above a few keV -which is due to the roll over of effective area- current surveys conducted in the so-called ultra-hard band (4.5−7.5 keV) do not bring any new source population or any significant difference with respect to 2−10 keV selected surveys. Much longer exposure times would be needed to reveal any new heavily obscured population with *XMM-Newton*.
3. Obscured AGN represent ∼20% of the soft X-ray selected population of AGN, from $\sim 10^{-13}$ erg cm^{-2} s^{-1} down to $\sim 10^{-15}$ erg cm^{-2} s^{-1}, with no compelling evidence for an increase of this fraction towards fainter fluxes within this range.
4. Obscured AGN represent ∼35% (45% if all unidentified sources are obscured AGN) of the hard X-ray selected population of AGN, with no hint of an increase down to a hard X-ray flux $\sim 10^{-14}$ erg cm^{-2} s^{-1}.
5. The fraction of X-ray sources with X-ray to optical flux ratio >10 (or $X/O > 1$ using the notation of this paper) is a mere 3% in soft X-ray selected samples, but grows to 20% in hard X-ray selected samples.
6. Those sources with $X/O > 1$ are mostly obscured AGN, but around 20% of them in the hard band are unobscured type-1 AGN. This means that $X/O > 1$ alone cannot be used as a proxy for obscured X-ray sources.

Acknowledgements. We are grateful to the International Scientific Committee of the Canary Islands' observatories for a generous allocation of observing time in 2000 and 2001, through the International Time Programme scheme. We are grateful to the Calar Alto Time Allocation Committee for continued support to the optical spectroscopic identification programme. Authors at the Instituto de Física de Cantabria (X.B., F.J.C., M.T.C., J.B.-G., A.C., J.E. and F.P.) acknowledge financial support by the Spanish Ministerio de Educación y Ciencia under projects ESP2003-00812 and ESP2006-13608-C02-01. We thank J. L. Muiños and D. W. Evans for help with the CMC survey. A.C., R.D.C., T.M. and P.S. acknowledge financial support from the Italian Space Agency (ASI), the Ministero dell'Universitat' e della Ricerca (MIUR) and Istituto Nazionale di Astrofisica (INAF) over the last few years. This work was supported by the German DLR under contract 50 OR 0201.

References

Alexander, D. M., Bauer, F. E., Brandt, W. N., et al. 2003, AJ, 125, 383
Barcons, X., Carrera, F. J., Watson, M. G., et al. 2002, A&A, 282, 522
Barger, A. J., Cowie, L. L., Muchotzky, R. F., et al. 2005, ApJ, 129, 578
Brandt, W. N., & Hasinger, G. 2005, ARA&A, 43, 827
Brusa, M., Zamorani, G., Comastri, A., et al. 2007, ApJ, in press [arXiv:astro-ph/0612358]
Baldi, A., Molendi, S., Comastri, A., et al. 2002, ApJ, 564, 190
Caccianiga, A., Severgnini, P., Braito, V., et al. 2004, A&A, 416, 201
Caccianiga, A., Severgnini, P., Della Ceca, R., et al. 2007, A&A, in press
Carrera, F. J., Ebrero, J., Mateos, S., et al. 2007, A&A, 469, 27
Cocchia, F., Fiore, F., Vignali, C., et al. 2007, A&A, 466, 31
Della Ceca, R., Maccacaro, T., Caccianiga, A., et al. 2004, A&A, 428, 383
Fabian, A. C., & Iwasawa, K. 1999, MNRAS, 303, L34
Fiore, F., Brusa, M., Cocchia, F., et al. 2003, A&A, 409, 79
Georgantopoulos, I., Stewart, G. C., Shanks, T., Boyle, B. J., & Griffiths, R. E. 1996, MNRAS, 280, 276
Gilli, R., Comastri, A., & Hasinger, G. 2007, A&A, 463, 79
Gioia, I. M., Maccacaro, T., Schild, R. E., et al. 1990, ApJS, 72, 567
Green, P. J., Silverman, J. D., Cameron, R. A., et al. 2004, ApJ, 150, 43
Hasinger, G., Burg, R., Giacconi, R., et al. 1998, A&A, 329, 482
Hasinger, G., Altieri, B., Arnaud, M., et al. 2001, A&A, 365, L45
Hasinger, G., Cappelluti, N., Brunner, H., et al. 2007, ApJ, in press [arXiv:astro-ph/0612311]
Kim, D.-W., et al. 2004a, ApJS, 150, 19
Kim, D.-W., Cameron, R. A., Drake, J. J., et al. 2004b, ApJS, 600, 59
Krumpe, M., Lamer, G., Schwope, A. D., et al. 2007, A&A, 466, 41
Lehmann, I., Hasinger, G., Schmidt, M., et al. 2001, A&A, 371, 833
López-Santiago, J., Micela, G., Sciortino, S., et al. 2007, A&A, 463, 165
Jansen, F. A., Lumb, D., Altieri, B., et al. 2001, A&A, 365, L1
Maccacaro, T., Gioia, I. M., Zamorani, G., et al. 1982, ApJ, 253, 504

Mainieri, V., Hasinger, G., Cappelluti, N., et al. 2007, ApJ, in press [arXiv:astro-ph/0612361]
Marconi, A., Risaliti, G., Gilli, R., et al. 2004, MNRAS, 351, 169
Mason, K. O., Carrera, F. J., Hasinger, G., et al. 2000, MNRAS, 311, 456
Mateos, S., Barcons, X., Carrera, F. J., et al. 2005, A&A, 433, 855
Mateos, S., Barcons, X., Carrera, F. J., et al. 2005, A&A, 444, 79
Mc Hardy, I. M., Jones, L. R., Merrifield, M. R., et al. 1998, MNRAS, 295, 641
Merritt, D., & Ferrarese, L. 2001, MNRAS, 320, L30
Monet, D., Canzian, B., Dahn, C., et al. 1998, A Catalog of Astrometric Standards, US Naval Observatory Flagstaff Station (USNOFFS) and Universities Space Research Association (USRA) stationed at USNOFFS
Rigby, J. R., Rieke, G. H., Donley, J. L., Alonso-Herrero, A., & Pérez-González, P. G. 2006, ApJ, 645, 115
Schwope, A. D., Hasinger, G., Lehmann, I., et al. 2000, Astron. Nachr., 321, 1
Severgnini, P., Caccianiga, A., Braito, V., et al. 2003, A&A, 406, 483
Silverman, J. D., Green, P. J., Barkhouse, W. A., et al. 2005, ApJ, 618, 123
Stocke, J. T., Morris, S. L., Gioia, I. M., et al. 1991, ApJS, 76, 813
Streblyanska, A., Hasinger, G., Finoguenov, A., et al. 2005, A&A, 432, 395
Strüder, L., Briel, U., Dennerl, R., et al. 2001, A&A, 365, L18
Tozzi, P., Gilli, R., Mainieri, V., et al. 2006, A&A, 451, 457
Tremaine, S., Gebhardt, K., Bender, R., et al. 2002, ApJ, 574, 740
Turner, M. J. L., Abbey, A., Arnaud, M., et al. 2001, A&A, 365, L27
Ueda, Y., Akiyama, M., Ohta, K., & Miyaji, T. 2003, ApJ, 598, 886
Watson, M. G., Roberts, T. P., Akiyama, M., & Ueda, Y. 2005, A&A, 437, 899

[1] Instituto de Física de Cantabria (CSIC-UC), 39005 Santander, Spain
e-mail: barcons@ifca.unican.es
[2] Mullard Space Science Laboratory, University College London, Holmbury St. Mary, Dorking, Surrey RH5 6NT, UK
[3] X-ray and Observational Astronomy Group, Department of Physics and Astronomy, Leicester University, Leicester LE1 7RH, UK
[4] H.H. Wills Physics Laboratory, University of Bristol, Tyndall Avenue, Bristol BS8 1TL, UK
[5] Max-Planck-Institut für Extraterrestrische Physik, Giessenbachstrasse, 85740 Garching, Germany
[6] Special Astrophysical Observatory, 369167 Nizhnij Arkhyz, Russia
[7] Centre for Astrophysics, University of Central Lancashire, Preston PRI 2HE, UK
[8] INAF - Osservatorio Astronomico di Brera, via Brera 28, 20121 Milano, Italy
[9] Institute of Astronomy, Madingley Road, Cambridge CB3 0HA, UK
[10] Observatoire Astronomique de Strasbourg, 11 rue de l'Université, 67000 Strasbourg, France
[11] Astrophysikalisches Institut Potsdam, An der Sternwarte 16, 144482, Potsdam, Germany
[12] South African Large Telescope, PO Box 9, Observatory, 7935, South Africa
[13] Departamento de Física, Ingeniería de Sistemas y Teoría de la Señal, Universidad de Alicante, 03080 Alicante, Spain
[14] Instituto de Astrofísica de Canarias, 38200 La Laguna, Spain
[15] Department of Physics, University of Durham, South Road, Durham DH1 3LE, UK
[16] European Space Astronomy Centre, Apartado 50727, 28080 Madrid, Spain
[17] Anglo-Australian Observatory, PO Box 296, Epping, NSW 1710, Australia
[18] Centro de Astrobiología (CSIC-INTA), PO Box 50727, 28080 Madrid, Spain
[19] Department of Physics, University of Warwick, Coventry CV4 7AL, UK
[20] Centre d'Étude Spatiale des Rayonnements, CNRS/UPS, 9 avenue du Colonel Roche, 31028 Toulouse Cedex 04, France
[21] National Astronomical Observatories of China/Yunnan Observatory, Phoenix Hill, PO Box 110, Kunming, Yunnan, PR China

Online Material

Table 2. XMS X-ray source list.

Source Name	RA (J2000)	Dec (J2000)	r_{90}^{a}	Sample	$S\,(0.5{-}2)^{b}$	$S\,(2{-}10)^{b}$	$S\,(0.5{-}4.5)^{b}$	$S\,(4.5{-}7.5)^{b}$	HR_2^{c}
XMSJ 001744.6+162815	00 : 17 : 44.6	+16 : 28 : 15.3	1.0	H	0.18 ± 0.05	3.54 ± 0.64	0.86 ± 0.16	1.17 ± 0.31	+0.44 ± 0.14
XMSJ 001800.9+163626	00 : 18 : 00.9	+16 : 36 : 26.2	0.7	HX	1.36 ± 0.17	3.70 ± 0.74	2.50 ± 0.28	1.10 ± 0.33	−0.45 ± 0.11
XMSJ 001802.7+161642	00 : 18 : 02.7	+16 : 16 : 42.2	0.3	S X	1.74 ± 0.18	1.95 ± 0.59	2.77 ± 0.27	0.54 ± 0.30	−0.68 ± 0.08
XMSJ 001817.3+161740	00 : 18 : 17.3	+16 : 17 : 40.1	0.5	SHX	3.08 ± 0.23	3.95 ± 0.67	4.89 ± 0.34	1.33 ± 0.44	−0.68 ± 0.05
XMSJ 001821.7+161943	00 : 18 : 21.7	+16 : 19 : 43.7	0.1	S X	1.62 ± 0.14	1.40 ± 0.29	2.53 ± 0.20	0.14 ± 0.06	−0.70 ± 0.05
XMSJ 001831.9+162926	00 : 18 : 31.9	+16 : 29 : 26.0	0.2	SHXU	10.50 ± 0.29	9.35 ± 0.63	15.96 ± 0.41	1.85 ± 0.34	−0.74 ± 0.02
XMSJ 001837.2+163446	00 : 18 : 37.2	+16 : 34 : 46.1	0.6	X	1.38 ± 0.13	1.62 ± 0.41	2.08 ± 0.20	0.63 ± 0.19	−0.76 ± 0.06
XMSJ 001838.3+162007	00 : 18 : 38.3	+16 : 20 : 07.1	0.4	S X	2.41 ± 0.15	2.96 ± 0.41	3.70 ± 0.22	1.21 ± 0.32	−0.74 ± 0.04
XMSJ 001841.8+162032	00 : 18 : 41.8	+16 : 20 : 32.9	0.2	SHXU	6.87 ± 0.25	15.13 ± 0.88	11.99 ± 0.39	5.05 ± 0.60	−0.52 ± 0.03
XMSJ 001845.7+163345	00 : 18 : 45.7	+16 : 33 : 45.2	0.5	X	1.49 ± 0.14	3.04 ± 0.57	2.73 ± 0.22	0.63 ± 0.26	−0.45 ± 0.07
XMSJ 001851.8+161621	00 : 18 : 51.8	+16 : 16 : 21.5	0.3	S X	1.63 ± 0.17	2.29 ± 0.48	2.62 ± 0.25	0.99 ± 0.38	−0.66 ± 0.07
XMSJ 001853.5+162751	00 : 18 : 53.5	+16 : 27 : 51.8	0.5	H	0.90 ± 0.09	3.52 ± 0.41	1.90 ± 0.16	1.08 ± 0.29	−0.24 ± 0.08
XMSJ 001901.9+161646	00 : 19 : 01.9	+16 : 16 : 46.5	0.5	S X	2.21 ± 0.19	1.66 ± 0.45	3.13 ± 0.27	0.67 ± 0.22	−0.89 ± 0.03
XMSJ 001911.8+161854	00 : 19 : 11.8	+16 : 18 : 54.0	0.4	S X	3.37 ± 0.24	0.22 ± 0.58	4.52 ± 0.33	–	−0.97 ± 0.02
XMSJ 001919.1+162015	00 : 19 : 19.1	+16 : 20 : 15.9	0.6	SHX	2.31 ± 0.21	3.90 ± 0.94	3.77 ± 0.32	0.40 ± 0.23	−0.63 ± 0.07
XMSJ 001928.0+163120	00 : 19 : 28.0	+16 : 31 : 20.2	0.6	S X	1.77 ± 0.20	0.36 ± 0.89	2.58 ± 0.30	–	−0.92 ± 0.06
XMSJ 010320.3-064159	01 : 03 : 20.3	−06 : 41 : 59.0	1.0	H	0.76 ± 0.14	4.17 ± 0.84	1.75 ± 0.27	1.24 ± 0.54	−0.18 ± 0.14
XMSJ 010324.6-065537	01 : 03 : 24.6	−06 : 55 : 37.6	1.1	S X	1.55 ± 0.27	2.17 ± 1.01	2.45 ± 0.43	0.69 ± 0.54	−0.76 ± 0.10
XMSJ 010327.3-064643	01 : 03 : 27.3	−06 : 46 : 43.8	0.3	SHXU	1.78 ± 0.22	9.53 ± 1.08	4.17 ± 0.39	4.15 ± 0.85	−0.17 ± 0.09
XMSJ 010333.9-064016	01 : 03 : 33.9	−06 : 40 : 16.4	0.6	SHX	1.55 ± 0.16	3.59 ± 0.53	2.61 ± 0.26	1.48 ± 0.36	−0.63 ± 0.08
XMSJ 010337.0-063337	01 : 03 : 37.0	−06 : 33 : 37.7	0.6	H	–	4.03 ± 0.72	0.77 ± 0.19	1.71 ± 0.41	+1.00 ± 0.18
XMSJ 010339.9-065225	01 : 03 : 39.9	−06 : 52 : 25.1	0.8	S X	2.43 ± 0.27	3.58 ± 0.86	4.03 ± 0.42	0.76 ± 0.40	−0.68 ± 0.08
XMSJ 010355.6-063711	01 : 03 : 55.6	−06 : 37 : 11.2	0.6	X	1.29 ± 0.14	2.01 ± 0.44	2.38 ± 0.23	0.01 ± 0.12	−0.49 ± 0.09
XMSJ 010358.0-062523	01 : 03 : 58.0	−06 : 25 : 23.0	0.6	SHX	1.66 ± 0.16	3.40 ± 0.57	2.98 ± 0.26	1.32 ± 0.42	−0.53 ± 0.07
XMSJ 010359.5-062655	01 : 03 : 59.5	−06 : 26 : 55.0	0.4	SHXU	3.86 ± 0.25	9.15 ± 0.85	6.97 ± 0.40	3.36 ± 0.61	−0.51 ± 0.05
XMSJ 010401.1-064948	01 : 04 : 01.1	−06 : 49 : 48.8	0.2	S X	1.80 ± 0.20	0.06 ± 0.43	2.50 ± 0.29	0.08 ± 0.20	−1.00 ± 0.04
XMSJ 010407.9-061736	01 : 04 : 07.9	−06 : 17 : 36.0	0.3	SHX	4.84 ± 0.28	5.60 ± 0.79	7.93 ± 0.43	0.92 ± 0.36	−0.67 ± 0.04
XMSJ 010410.6-063926	01 : 04 : 10.6	−06 : 39 : 26.9	0.4	SHX	2.84 ± 0.20	3.54 ± 0.47	4.67 ± 0.30	0.88 ± 0.19	−0.68 ± 0.05
XMSJ 010420.9-064701	01 : 04 : 20.9	−06 : 47 : 01.6	0.7	X	1.48 ± 0.17	2.39 ± 0.52	2.58 ± 0.27	0.54 ± 0.22	−0.58 ± 0.08
XMSJ 010421.5-061416	01 : 04 : 21.5	−06 : 14 : 16.4	0.4	SHXU	4.38 ± 0.31	6.68 ± 0.95	7.16 ± 0.47	2.85 ± 0.75	−0.69 ± 0.05
XMSJ 010428.2-061539	01 : 04 : 28.2	−06 : 15 : 39.5	0.8	H U	0.34 ± 0.08	7.79 ± 0.88	1.43 ± 0.20	4.52 ± 0.77	+0.37 ± 0.11
XMSJ 010430.2-064456	01 : 04 : 30.2	−06 : 44 : 56.4	0.4	SHX	3.01 ± 0.25	5.55 ± 0.82	5.38 ± 0.40	1.64 ± 0.52	−0.53 ± 0.06
XMSJ 010432.9-064452	01 : 04 : 32.9	−06 : 44 : 52.3	0.8	H	1.05 ± 0.16	4.22 ± 0.88	1.94 ± 0.26	2.14 ± 0.56	−0.48 ± 0.11
XMSJ 010437.5-064737	01 : 04 : 37.5	−06 : 47 : 37.7	0.9	X	1.36 ± 0.20	2.22 ± 0.73	2.32 ± 0.32	0.54 ± 0.32	−0.62 ± 0.11
XMSJ 010444.6-064832	01 : 04 : 44.6	−06 : 48 : 32.7	0.4	S X	2.53 ± 0.30	2.45 ± 1.05	4.31 ± 0.48	–	−0.65 ± 0.09
XMSJ 010449.5-062723	01 : 04 : 49.5	−06 : 27 : 23.0	0.6	HXU	0.76 ± 0.12	7.13 ± 0.71	2.38 ± 0.23	3.28 ± 0.54	+0.12 ± 0.10
XMSJ 010459.1-062845	01 : 04 : 59.1	−06 : 28 : 45.9	1.0	HX	0.53 ± 0.13	6.65 ± 0.89	2.11 ± 0.29	1.92 ± 0.40	+0.32 ± 0.13
XMSJ 010502.5-062124	01 : 05 : 02.5	−06 : 21 : 24.7	1.1	X	1.12 ± 0.16	1.88 ± 0.58	1.99 ± 0.26	0.48 ± 0.28	−0.56 ± 0.13
XMSJ 010506.6-061510	01 : 05 : 06.6	−06 : 15 : 10.6	0.7	X	0.96 ± 0.18	3.53 ± 1.38	2.07 ± 0.34	1.39 ± 0.50	−0.27 ± 0.15
XMSJ 021703.4-045533	02 : 17 : 03.4	−04 : 55 : 33.9	0.8	HX	0.96 ± 0.13	5.81 ± 0.81	2.46 ± 0.24	1.94 ± 0.50	−0.04 ± 0.10
XMSJ 021705.4-045654	02 : 17 : 05.4	−04 : 56 : 54.6	0.9	X	1.06 ± 0.14	2.72 ± 0.72	2.04 ± 0.23	–	−0.40 ± 0.10
XMSJ 021708.7-045741	02 : 17 : 08.7	−04 : 57 : 41.2	0.6	S X	1.65 ± 0.15	3.08 ± 0.59	2.83 ± 0.24	0.55 ± 0.29	−0.58 ± 0.07
XMSJ 021753.5-045541	02 : 17 : 53.5	−04 : 55 : 41.5	0.2	H U	0.40 ± 0.05	6.98 ± 0.47	1.75 ± 0.12	2.33 ± 0.32	+0.38 ± 0.06
XMSJ 021753.7-045748	02 : 17 : 53.7	−04 : 57 : 48.0	0.3	S XU	1.72 ± 0.09	3.18 ± 0.32	2.90 ± 0.14	1.29 ± 0.24	−0.58 ± 0.04

Table 2. continued.

Source Name	RA (J2000)	Dec (J2000)	r_{90}^{a}	Sample	$S\,(0.5{-}2)^{b}$	$S\,(2{-}10)^{b}$	$S\,(0.5{-}4.5)^{b}$	$S\,(4.5{-}7.5)^{b}$	HR_2^{c}
XMSJ 021808.3-045845	02 : 18 : 08.3	−04 : 58 : 45.6	0.1	SHXU	22.13 ± 0.32	30.03 ± 0.88	35.23 ± 0.47	10.17 ± 0.60	−0.68 ± 0.01
XMSJ 021815.4-045618	02 : 18 : 15.4	−04 : 56 : 18.7	0.3	XU	1.44 ± 0.09	3.19 ± 0.35	2.52 ± 0.15	1.18 ± 0.24	−0.53 ± 0.05
XMSJ 021817.2-050258	02 : 18 : 17.2	−05 : 02 : 58.6	0.3	X	1.49 ± 0.09	2.47 ± 0.33	2.52 ± 0.14	0.75 ± 0.21	−0.59 ± 0.05
XMSJ 021817.4-045112	02 : 18 : 17.4	−04 : 51 : 12.8	0.1	SHXU	17.80 ± 0.38	27.90 ± 1.19	29.49 ± 0.57	8.48 ± 0.79	−0.62 ± 0.02
XMSJ 021820.5-050426	02 : 18 : 20.5	−05 : 04 : 26.2	0.2	SHXU	4.89 ± 0.17	9.79 ± 0.63	8.38 ± 0.27	3.51 ± 0.44	−0.57 ± 0.03
XMSJ 021821.8-043449	02 : 18 : 21.8	−04 : 34 : 49.5	0.5	SHX	2.82 ± 0.23	8.72 ± 1.07	5.07 ± 0.37	2.45 ± 0.61	−0.49 ± 0.06
XMSJ 021822.1-050613	02 : 18 : 22.1	−05 : 06 : 13.5	0.4	H U	0.23 ± 0.06	17.92 ± 1.03	1.25 ± 0.13	13.47 ± 0.92	+0.50 ± 0.12
XMSJ 021827.2-045456	02 : 18 : 27.2	−04 : 54 : 56.8	0.3	SHX	2.63 ± 0.15	4.04 ± 0.47	4.33 ± 0.23	1.22 ± 0.31	−0.63 ± 0.04
XMSJ 021829.9-045514	02 : 18 : 29.9	−04 : 55 : 14.0	0.1	SHX	20.55 ± 0.39	6.28 ± 0.54	29.33 ± 0.55	0.53 ± 0.25	−0.89 ± 0.01
XMSJ 021830.5-045623	02 : 18 : 30.5	−04 : 56 : 23.1	0.2	SHX	4.40 ± 0.18	3.84 ± 0.49	6.76 ± 0.27	1.04 ± 0.29	−0.75 ± 0.03
XMSJ 021842.9-050437	02 : 18 : 42.9	−05 : 04 : 37.3	0.5	SHX	2.07 ± 0.15	4.98 ± 0.77	3.53 ± 0.24	1.77 ± 0.48	−0.58 ± 0.05
XMSJ 021855.1-044328	02 : 18 : 55.1	−04 : 43 : 28.1	0.7	H U	0.08 ± 0.05	4.59 ± 0.56	0.65 ± 0.13	2.60 ± 0.48	+0.66 ± 0.18
XMSJ 021902.6-044628	02 : 19 : 02.6	−04 : 46 : 28.2	0.5	SHX	2.55 ± 0.23	3.74 ± 0.62	3.99 ± 0.34	1.22 ± 0.33	−0.72 ± 0.05
XMSJ 021903.5-043935	02 : 19 : 03.5	−04 : 39 : 35.3	0.4	SHX	3.10 ± 0.21	5.74 ± 0.68	5.17 ± 0.32	1.64 ± 0.37	−0.61 ± 0.05
XMSJ 021905.7-051038	02 : 19 : 05.7	−05 : 10 : 38.8	0.5	S X	1.71 ± 0.16	1.99 ± 0.81	2.73 ± 0.25	0.74 ± 0.27	−0.71 ± 0.07
XMSJ 021908.3-045500	02 : 19 : 08.3	−04 : 55 : 00.5	0.4	SHXU	1.83 ± 0.12	4.93 ± 0.59	3.22 ± 0.19	1.61 ± 0.36	−0.52 ± 0.05
XMSJ 021921.7-043641	02 : 19 : 21.7	−04 : 36 : 41.8	0.6	S X	1.95 ± 0.21	2.86 ± 0.66	3.15 ± 0.32	0.87 ± 0.36	−0.67 ± 0.08
XMSJ 021922.6-044058	02 : 19 : 22.6	−04 : 40 : 58.1	0.6	SHX	1.73 ± 0.19	4.80 ± 0.87	3.14 ± 0.32	1.62 ± 0.55	−0.51 ± 0.09
XMSJ 021923.3-045148	02 : 19 : 23.3	−04 : 51 : 48.8	0.2	SHX	6.19 ± 0.22	4.88 ± 0.57	9.30 ± 0.31	1.47 ± 0.36	−0.79 ± 0.02
XMSJ 021931.0-044956	02 : 19 : 31.0	−04 : 49 : 56.1	0.8	HX	1.06 ± 0.11	3.64 ± 0.57	2.09 ± 0.19	1.32 ± 0.36	−0.35 ± 0.08
XMSJ 021934.3-050857	02 : 19 : 34.3	−05 : 08 : 57.3	0.5	S X	1.75 ± 0.13	2.23 ± 0.52	2.61 ± 0.20	0.91 ± 0.33	−0.80 ± 0.05
XMSJ 021934.6-044141	02 : 19 : 34.6	−04 : 41 : 41.0	0.9	X	1.36 ± 0.22	3.04 ± 0.92	2.13 ± 0.34	1.06 ± 0.45	−0.73 ± 0.13
XMSJ 021939.2-051132	02 : 19 : 39.2	−05 : 11 : 32.9	0.9	H U	0.35 ± 0.08	7.22 ± 0.84	1.29 ± 0.17	4.71 ± 0.75	+0.27 ± 0.13
XMSJ 021948.3-045128	02 : 19 : 48.3	−04 : 51 : 28.8	0.6	H	0.41 ± 0.07	3.52 ± 0.55	1.13 ± 0.13	0.85 ± 0.25	+0.06 ± 0.11
XMSJ 022002.1-050101	02 : 20 : 02.1	−05 : 01 : 01.6	0.3	S XU	2.16 ± 0.11	2.88 ± 0.39	3.39 ± 0.17	1.24 ± 0.28	−0.72 ± 0.04
XMSJ 022004.8-045514	02 : 20 : 04.8	−04 : 55 : 14.9	0.4	SHX	1.83 ± 0.12	3.75 ± 0.45	3.18 ± 0.20	1.30 ± 0.32	−0.55 ± 0.05
XMSJ 022013.0-045113	02 : 20 : 13.0	−04 : 51 : 13.2	0.4	SHX	1.76 ± 0.16	4.27 ± 0.66	3.09 ± 0.24	1.57 ± 0.44	−0.55 ± 0.06
XMSJ 022016.8-045646	02 : 20 : 16.8	−04 : 56 : 46.8	0.6	HX	1.23 ± 0.13	3.81 ± 0.75	2.30 ± 0.21	1.05 ± 0.36	−0.42 ± 0.08
XMSJ 025727.7+131504	02 : 57 : 27.7	+13 : 15 : 04.5	1.5	S X	1.76 ± 0.33	3.16 ± 1.52	2.92 ± 0.52	2.21 ± 0.71	−0.65 ± 0.17
XMSJ 025737.9+131623	02 : 57 : 37.9	+13 : 16 : 23.9	0.0	X	1.18 ± 0.22	1.61 ± 0.75	2.15 ± 0.38	–	−0.47 ± 0.17
XMSJ 025744.7+131538	02 : 57 : 44.7	+13 : 15 : 38.4	1.0	X	1.39 ± 0.24	2.37 ± 0.70	2.40 ± 0.37	1.01 ± 0.39	−0.54 ± 0.10
XMSJ 025748.3+131406	02 : 57 : 48.3	+13 : 14 : 06.0	0.8	X	1.41 ± 0.23	2.87 ± 0.58	2.47 ± 0.36	1.44 ± 0.39	−0.52 ± 0.09
XMSJ 025748.5+132317	02 : 57 : 48.5	+13 : 23 : 17.3	1.1	HX	1.26 ± 0.22	4.56 ± 0.91	2.53 ± 0.38	0.95 ± 0.36	−0.32 ± 0.14
XMSJ 025756.5+130836	02 : 57 : 56.5	+13 : 08 : 36.1	0.5	S X	2.26 ± 0.39	1.82 ± 1.20	3.67 ± 0.60	–	−0.65 ± 0.12
XMSJ 025808.4+132351	02 : 58 : 08.4	+13 : 23 : 51.0	0.6	S X	2.02 ± 0.23	3.25 ± 0.60	3.52 ± 0.37	0.25 ± 0.18	−0.52 ± 0.08
XMSJ 025808.8+132225	02 : 58 : 08.8	+13 : 22 : 25.9	0.4	SHX	1.74 ± 0.23	3.31 ± 0.47	2.77 ± 0.34	1.66 ± 0.33	−0.68 ± 0.09
XMSJ 025815.3+130938	02 : 58 : 15.3	+13 : 09 : 38.9	0.9	S X	1.57 ± 0.26	2.52 ± 0.79	2.38 ± 0.38	1.68 ± 0.71	−0.79 ± 0.11
XMSJ 025850.9+131809	02 : 58 : 50.9	+13 : 18 : 09.3	1.0	H	0.23 ± 0.11	5.26 ± 0.71	1.36 ± 0.25	1.63 ± 0.45	+0.53 ± 0.17
XMSJ 025855.3+132503	02 : 58 : 55.3	+13 : 25 : 03.7	1.2	HX	1.47 ± 0.32	5.63 ± 1.43	3.07 ± 0.52	3.15 ± 1.00	−0.27 ± 0.15
XMSJ 025906.3+131225	02 : 59 : 06.3	+13 : 12 : 25.9	1.3	S X	1.50 ± 0.26	2.07 ± 0.65	2.34 ± 0.40	0.85 ± 0.39	−0.76 ± 0.09
XMSJ 061316.7+710947	06 : 13 : 16.7	+71 : 09 : 47.2	0.7	HX	1.02 ± 0.15	3.40 ± 0.82	2.05 ± 0.24	1.06 ± 0.50	−0.29 ± 0.10
XMSJ 061322.5+705429	06 : 13 : 22.5	+70 : 54 : 29.5	0.7	HXU	1.10 ± 0.20	12.25 ± 1.72	3.33 ± 0.41	6.13 ± 1.25	+0.15 ± 0.12
XMSJ 061337.9+705001	06 : 13 : 37.9	+70 : 50 : 01.8	0.9	S X	1.56 ± 0.27	3.43 ± 1.18	2.66 ± 0.43	1.46 ± 0.94	−0.54 ± 0.14
XMSJ 061343.7+710727	06 : 13 : 43.7	+71 : 07 : 27.3	0.1	SHXU	54.90 ± 0.72	39.19 ± 1.35	82.03 ± 1.00	7.12 ± 0.73	−0.74 ± 0.01

Table 2. continued.

Source Name	RA (J2000)	Dec (J2000)	r^a_{90}	Sample	$S\,(0.5{-}2)^b$	$S\,(2{-}10)^b$	$S\,(0.5{-}4.5)^b$	$S\,(4.5{-}7.5)^b$	HR^c_2
XMSJ 061346.5+710347	06 : 13 : 46.5	+71 : 03 : 47.4	0.4	SHXU	2.43 ± 0.15	4.73 ± 0.59	3.94 ± 0.23	1.83 ± 0.38	−0.59 ± 0.05
XMSJ 061346.5+705025	06 : 13 : 46.5	+70 : 50 : 25.3	0.4	S X	2.05 ± 0.31	4.39 ± 1.26	3.87 ± 0.50	0.83 ± 0.52	−0.37 ± 0.12
XMSJ 061413.9+705236	06 : 14 : 13.9	+70 : 52 : 36.7	0.0	S X	1.67 ± 0.22	0.55 ± 0.29	2.15 ± 0.30	0.18 ± 0.27	−0.95 ± 0.02
XMSJ 061452.9+710505	06 : 14 : 52.9	+71 : 05 : 05.5	0.4	S X	1.87 ± 0.11	2.02 ± 0.29	2.89 ± 0.17	0.48 ± 0.17	−0.66 ± 0.05
XMSJ 061508.2+710702	06 : 15 : 08.2	+71 : 07 : 02.3	0.4	H U	0.66 ± 0.08	5.34 ± 0.44	1.85 ± 0.14	2.63 ± 0.35	+0.08 ± 0.08
XMSJ 061515.2+710204	06 : 15 : 15.2	+71 : 02 : 04.2	0.2	SHXU	3.86 ± 0.14	8.05 ± 0.46	6.66 ± 0.22	2.71 ± 0.32	−0.48 ± 0.03
XMSJ 061607.6+710638	06 : 16 : 07.6	+71 : 06 : 38.4	0.2	SHXU	5.44 ± 0.19	11.28 ± 0.61	9.44 ± 0.29	3.73 ± 0.41	−0.48 ± 0.03
XMSJ 061616.7+705605	06 : 16 : 16.7	+70 : 56 : 05.3	0.4	X	1.15 ± 0.10	2.03 ± 0.39	2.05 ± 0.16	0.35 ± 0.19	−0.44 ± 0.07
XMSJ 061728.7+710600	06 : 17 : 28.7	+71 : 06 : 00.5	0.3	SHX	3.57 ± 0.20	4.84 ± 0.71	5.62 ± 0.29	0.86 ± 0.36	−0.64 ± 0.04
XMSJ 061731.0+705955	06 : 17 : 31.0	+70 : 59 : 55.5	0.5	S X	1.67 ± 0.13	1.88 ± 0.43	2.73 ± 0.21	0.21 ± 0.26	−0.60 ± 0.07
XMSJ 074214.2+742319	07 : 42 : 14.2	+74 : 23 : 19.5	0.8	X	1.29 ± 0.22	3.69 ± 0.92	2.58 ± 0.36	0.02 ± 0.27	−0.34 ± 0.12
XMSJ 074214.6+744529	07 : 42 : 14.6	+74 : 45 : 29.5	0.2	S X	4.06 ± 0.36	4.57 ± 1.01	6.36 ± 0.54	2.16 ± 0.60	−0.73 ± 0.06
XMSJ 074243.9+743249	07 : 42 : 43.9	+74 : 32 : 49.3	0.5	S X	1.64 ± 0.16	3.00 ± 0.56	2.83 ± 0.24	0.36 ± 0.19	−0.56 ± 0.07
XMSJ 074248.7+742747	07 : 42 : 48.7	+74 : 27 : 47.5	0.2	S X	1.61 ± 0.17	1.26 ± 0.62	2.43 ± 0.25	0.34 ± 0.21	−0.76 ± 0.05
XMSJ 074350.8+743839	07 : 43 : 50.8	+74 : 38 : 39.9	0.3	SHXU	2.50 ± 0.18	8.16 ± 0.71	4.79 ± 0.29	2.93 ± 0.51	−0.39 ± 0.05
XMSJ 074352.9+744257	07 : 43 : 52.9	+74 : 42 : 57.0	0.3	SHXU	7.05 ± 0.35	10.74 ± 1.07	11.61 ± 0.54	3.29 ± 0.69	−0.62 ± 0.04
XMSJ 074400.4+744056	07 : 44 : 00.4	+74 : 40 : 56.4	0.3	S X	5.59 ± 0.29	1.21 ± 0.54	7.86 ± 0.40	0.29 ± 0.19	−0.93 ± 0.02
XMSJ 074435.6+744444	07 : 44 : 35.6	+74 : 44 : 44.0	0.3	S X	2.51 ± 0.25	3.26 ± 0.96	4.16 ± 0.38	0.67 ± 0.54	−0.62 ± 0.07
XMSJ 074457.9+742156	07 : 44 : 57.9	+74 : 21 : 56.9	0.7	SHX	1.82 ± 0.23	6.57 ± 1.07	3.81 ± 0.40	0.41 ± 0.39	−0.27 ± 0.10
XMSJ 074646.9+744500	07 : 46 : 46.9	+74 : 45 : 00.9	1.2	X	1.13 ± 0.23	3.99 ± 1.32	2.00 ± 0.38	–	−0.54 ± 0.17
XMSJ 074728.9+743804	07 : 47 : 28.9	+74 : 38 : 04.3	0.6	SHX	3.94 ± 0.38	6.18 ± 1.35	6.20 ± 0.57	2.79 ± 1.09	−0.71 ± 0.07
XMSJ 083859.0+705043	08 : 38 : 59.0	+70 : 50 : 43.1	0.7	SHX	1.85 ± 0.22	5.39 ± 1.43	3.47 ± 0.36	0.52 ± 0.63	−0.43 ± 0.10
XMSJ 084132.3+704757	08 : 41 : 32.3	+70 : 47 : 57.4	0.3	SHX	2.69 ± 0.18	4.09 ± 0.55	4.46 ± 0.27	1.09 ± 0.36	−0.60 ± 0.05
XMSJ 084144.2+704653	08 : 41 : 44.2	+70 : 46 : 53.2	0.6	X	1.49 ± 0.15	1.44 ± 0.51	2.03 ± 0.22	–	−0.91 ± 0.04
XMSJ 084150.4+705008	08 : 41 : 50.4	+70 : 50 : 08.8	0.3	SHX	3.50 ± 0.19	5.34 ± 0.60	5.61 ± 0.28	1.78 ± 0.42	−0.66 ± 0.04
XMSJ 084211.8+710146	08 : 42 : 11.8	+71 : 01 : 46.4	0.4	SHX	3.36 ± 0.22	5.30 ± 0.97	5.70 ± 0.35	–	−0.57 ± 0.05
XMSJ 084217.1+710009	08 : 42 : 17.1	+71 : 00 : 09.7	0.6	X	1.33 ± 0.14	1.54 ± 0.49	2.06 ± 0.22	0.57 ± 0.41	−0.73 ± 0.08
XMSJ 084221.6+705758	08 : 42 : 21.6	+70 : 57 : 58.2	0.4	X	1.35 ± 0.14	2.36 ± 0.43	2.15 ± 0.21	0.82 ± 0.23	−0.68 ± 0.08
XMSJ 084239.9+704431	08 : 42 : 39.9	+70 : 44 : 31.0	0.4	SHX	4.10 ± 0.27	7.58 ± 1.04	6.90 ± 0.42	2.37 ± 0.74	−0.60 ± 0.05
XMSJ 084310.1+705557	08 : 43 : 10.1	+70 : 55 : 57.2	0.4	SHX	3.74 ± 0.26	5.78 ± 1.18	5.76 ± 0.38	2.38 ± 0.69	−0.73 ± 0.05
XMSJ 084324.3+705235	08 : 43 : 24.3	+70 : 52 : 35.6	0.5	SHX	2.95 ± 0.24	5.70 ± 1.22	5.01 ± 0.38	1.42 ± 0.56	−0.59 ± 0.06
XMSJ 084334.6+704734	08 : 43 : 34.6	+70 : 47 : 34.2	0.9	X	1.33 ± 0.19	2.06 ± 0.89	2.05 ± 0.29	0.61 ± 0.37	−0.73 ± 0.10
XMSJ 094152.2+465116	09 : 41 : 52.2	+46 : 51 : 16.6	0.6	S X	1.50 ± 0.15	3.55 ± 0.92	2.61 ± 0.26	0.78 ± 0.39	−0.64 ± 0.09
XMSJ 094154.6+470637	09 : 41 : 54.6	+47 : 06 : 37.7	0.4	S X	2.58 ± 0.18	1.57 ± 0.75	4.11 ± 0.28	0.31 ± 0.23	−0.82 ± 0.05
XMSJ 094242.1+470618	09 : 42 : 42.1	+47 : 06 : 18.0	0.4	X	1.44 ± 0.10	1.88 ± 0.32	2.36 ± 0.16	0.59 ± 0.24	−0.72 ± 0.05
XMSJ 094251.5+464729	09 : 42 : 51.5	+46 : 47 : 29.6	0.6	X	1.47 ± 0.13	1.23 ± 0.45	2.28 ± 0.21	0.36 ± 0.19	−0.84 ± 0.07
XMSJ 094317.3+470040	09 : 43 : 17.3	+47 : 00 : 40.3	0.2	SHXU	2.77 ± 0.12	4.85 ± 0.39	4.84 ± 0.19	1.57 ± 0.28	−0.61 ± 0.03
XMSJ 094345.2+465155	09 : 43 : 45.2	+46 : 51 : 55.2	0.3	S X	2.45 ± 0.15	3.00 ± 0.46	4.20 ± 0.24	0.53 ± 0.19	−0.66 ± 0.05
XMSJ 094348.3+470155	09 : 43 : 48.3	+47 : 01 : 55.0	0.4	X	1.18 ± 0.10	2.99 ± 0.41	2.18 ± 0.17	1.33 ± 0.31	−0.52 ± 0.07
XMSJ 102950.8+310109	10 : 29 : 50.8	+31 : 01 : 09.7	0.5	S X	1.82 ± 0.23	3.63 ± 0.97	3.19 ± 0.37	1.26 ± 0.45	−0.56 ± 0.09
XMSJ 103007.0+311124	10 : 30 : 07.0	+31 : 11 : 24.4	0.8	S X	1.54 ± 0.20	1.35 ± 0.66	2.36 ± 0.30	0.30 ± 0.31	−0.76 ± 0.06
XMSJ 103015.5+310138	10 : 30 : 15.5	+31 : 01 : 38.9	0.8	HX	1.21 ± 0.14	3.67 ± 0.57	2.31 ± 0.23	0.54 ± 0.21	−0.41 ± 0.09
XMSJ 103020.7+305637	10 : 30 : 20.7	+30 : 56 : 37.2	0.5	SHXU	2.30 ± 0.19	6.72 ± 0.81	4.23 ± 0.31	2.30 ± 0.51	−0.46 ± 0.07
XMSJ 103028.4+305659	10 : 30 : 28.4	+30 : 56 : 59.4	0.3	SHX	3.33 ± 0.21	3.81 ± 0.63	5.34 ± 0.32	0.99 ± 0.24	−0.69 ± 0.04

Table 2. continued.

Source Name	RA (J2000)	Dec (J2000)	r_{90}^{a}	Sample	$S\,(0.5{-}2)^{b}$	$S\,(2{-}10)^{b}$	$S\,(0.5{-}4.5)^{b}$	$S\,(4.5{-}7.5)^{b}$	HR_2^{c}
XMSJ 103048.5+305702	10 : 30 : 48.5	+30 : 57 : 02.2	0.3	SHXU	3.75 ± 0.20	5.05 ± 0.58	6.04 ± 0.30	1.84 ± 0.43	−0.68 ± 0.04
XMSJ 103050.9+310538	10 : 30 : 50.9	+31 : 05 : 38.7	0.4	X	1.43 ± 0.12	2.08 ± 0.30	2.33 ± 0.17	0.68 ± 0.15	−0.65 ± 0.05
XMSJ 103101.8+305144	10 : 31 : 01.8	+30 : 51 : 44.0	0.4	S X	1.54 ± 0.19	0.16 ± 0.48	2.05 ± 0.27	0.21 ± 0.20	−1.00 ± 0.04
XMSJ 103104.7+305637	10 : 31 : 04.7	+30 : 56 : 37.5	0.8	H	0.56 ± 0.09	3.46 ± 0.51	1.21 ± 0.15	1.18 ± 0.31	−0.23 ± 0.12
XMSJ 103111.3+310332	10 : 31 : 11.3	+31 : 03 : 32.7	0.3	SHX	2.99 ± 0.17	4.06 ± 0.44	4.83 ± 0.25	1.00 ± 0.25	−0.66 ± 0.04
XMSJ 103123.0+310330	10 : 31 : 23.0	+31 : 03 : 30.5	1.0	H U	0.14 ± 0.05	3.38 ± 0.42	0.55 ± 0.11	1.42 ± 0.30	+0.33 ± 0.18
XMSJ 103150.6+310817	10 : 31 : 50.6	+31 : 08 : 17.5	1.0	H	0.74 ± 0.13	5.56 ± 0.86	1.75 ± 0.25	1.88 ± 0.46	−0.15 ± 0.13
XMSJ 103154.1+310731	10 : 31 : 54.1	+31 : 07 : 31.2	0.4	SHX	4.74 ± 0.32	6.83 ± 0.95	7.85 ± 0.48	1.70 ± 0.41	−0.64 ± 0.05
XMSJ 103157.0+310535	10 : 31 : 57.0	+31 : 05 : 35.3	0.6	SHX	2.64 ± 0.25	4.99 ± 0.88	4.41 ± 0.39	2.34 ± 0.71	−0.63 ± 0.06
XMSJ 113034.4+312422	11 : 30 : 34.4	+31 : 24 : 22.0	0.3	S X	3.71 ± 0.36	2.42 ± 1.04	5.68 ± 0.54	–	−0.79 ± 0.05
XMSJ 113042.5+311227	11 : 30 : 42.5	+31 : 12 : 27.3	0.1	S X	1.66 ± 0.18	2.54 ± 0.41	2.63 ± 0.27	1.11 ± 0.29	−0.69 ± 0.06
XMSJ 113049.2+311403	11 : 30 : 49.2	+31 : 14 : 03.8	0.7	X	1.26 ± 0.15	2.08 ± 0.48	2.18 ± 0.24	0.32 ± 0.20	−0.56 ± 0.09
XMSJ 113052.1+310940	11 : 30 : 52.1	+31 : 09 : 40.2	0.4	SHX	3.10 ± 0.24	5.03 ± 0.84	5.03 ± 0.36	1.02 ± 0.30	−0.66 ± 0.05
XMSJ 113102.9+311015	11 : 31 : 02.9	+31 : 10 : 15.4	0.5	S X	2.01 ± 0.20	1.37 ± 0.46	2.99 ± 0.29	0.52 ± 0.19	−0.83 ± 0.07
XMSJ 113117.0+310039	11 : 31 : 17.0	+31 : 00 : 39.2	0.4	S X	1.68 ± 0.28	3.63 ± 1.18	3.07 ± 0.47	1.29 ± 0.64	−0.51 ± 0.13
XMSJ 113118.4+310114	11 : 31 : 18.4	+31 : 01 : 14.7	0.3	S X	1.56 ± 0.27	2.21 ± 2.12	2.59 ± 0.43	0.84 ± 0.58	−0.66 ± 0.14
XMSJ 113121.8+310254	11 : 31 : 21.8	+31 : 02 : 54.7	0.4	SHXU	5.10 ± 0.39	26.91 ± 2.61	11.63 ± 0.70	7.61 ± 1.58	−0.18 ± 0.06
XMSJ 113126.6+311241	11 : 31 : 26.6	+31 : 12 : 41.1	0.4	SHX	3.81 ± 0.25	5.60 ± 0.71	6.05 ± 0.37	1.90 ± 0.47	−0.69 ± 0.05
XMSJ 113129.3+310945	11 : 31 : 29.3	+31 : 09 : 45.0	0.2	SHXU	16.71 ± 0.53	28.52 ± 1.75	27.31 ± 0.79	9.20 ± 1.13	−0.65 ± 0.02
XMSJ 113138.2+311230	11 : 31 : 38.2	+31 : 12 : 30.8	0.8	X	1.26 ± 0.19	2.52 ± 0.69	2.26 ± 0.30	–	−0.49 ± 0.11
XMSJ 113144.7+311340	11 : 31 : 44.7	+31 : 13 : 40.0	0.4	SHX	3.13 ± 0.26	4.89 ± 0.79	5.05 ± 0.39	1.64 ± 0.54	−0.68 ± 0.05
XMSJ 113151.6+312144	11 : 31 : 51.6	+31 : 21 : 44.0	1.1	X	1.47 ± 0.23	1.49 ± 0.78	2.06 ± 0.34	0.22 ± 0.36	−0.96 ± 0.08
XMSJ 113154.3+311137	11 : 31 : 54.3	+31 : 11 : 37.1	0.6	S X	2.76 ± 0.29	2.62 ± 0.95	4.16 ± 0.43	1.05 ± 0.40	−0.77 ± 0.04
XMSJ 113201.2+311211	11 : 32 : 01.2	+31 : 12 : 11.9	0.8	S X	1.59 ± 0.23	1.09 ± 1.13	2.48 ± 0.36	–	−0.75 ± 0.07
XMSJ 121819.5+751922	12 : 18 : 19.5	+75 : 19 : 22.7	1.0	S X	1.88 ± 0.25	1.94 ± 46.23	3.05 ± 0.38	0.24 ± 1.58	−0.67 ± 0.10
XMSJ 121828.3+752225	12 : 18 : 28.3	+75 : 22 : 25.6	1.2	X	1.07 ± 0.34	8.01 ± 2.44	2.69 ± 0.59	1.84 ± 1.36	−0.07 ± 0.23
XMSJ 121912.7+751441	12 : 19 : 12.7	+75 : 14 : 41.4	1.0	X	1.39 ± 0.20	2.70 ± 5.36	2.34 ± 0.32	1.38 ± 0.68	−0.61 ± 0.11
XMSJ 122004.0+752145	12 : 20 : 04.0	+75 : 21 : 45.8	0.7	S X	2.66 ± 0.31	2.37 ± 19.35	3.90 ± 0.43	0.91 ± 0.48	−0.81 ± 0.07
XMSJ 122004.9+752103	12 : 20 : 04.9	+75 : 21 : 03.6	0.6	SHX	2.21 ± 0.23	3.95 ± 5.27	3.84 ± 0.35	0.57 ± 0.40	−0.54 ± 0.07
XMSJ 122018.2+752215	12 : 20 : 18.2	+75 : 22 : 15.0	0.3	SHX	16.57 ± 0.61	5.78 ± 17.62	23.65 ± 0.84	0.87 ± 0.44	−0.88 ± 0.02
XMSJ 122048.3+751807	12 : 20 : 48.3	+75 : 18 : 07.4	0.5	S X	1.70 ± 0.16	2.47 ± 0.54	2.67 ± 0.24	1.11 ± 0.36	−0.69 ± 0.06
XMSJ 122051.4+750531	12 : 20 : 51.4	+75 : 05 : 31.9	0.3	SHXU	20.73 ± 0.80	36.98 ± 2.87	34.66 ± 1.22	12.47 ± 1.84	−0.61 ± 0.03
XMSJ 122051.8+752821	12 : 20 : 51.8	+75 : 28 : 21.8	0.7	HX	1.29 ± 0.18	3.55 ± 1.07	2.23 ± 0.29	1.29 ± 0.63	−0.55 ± 0.11
XMSJ 122110.8+751119	12 : 21 : 10.8	+75 : 11 : 19.2	0.5	SHX	2.56 ± 0.21	3.63 ± 0.77	3.98 ± 0.31	1.01 ± 0.45	−0.73 ± 0.05
XMSJ 122120.4+751618	12 : 21 : 20.4	+75 : 16 : 18.2	0.4	S X	1.95 ± 0.16	0.93 ± 10.02	2.86 ± 0.23	–	−0.81 ± 0.05
XMSJ 122135.0+750916	12 : 21 : 35.0	+75 : 09 : 16.4	0.5	SHXU	3.06 ± 0.25	4.83 ± 27.19	4.90 ± 0.38	2.69 ± 0.67	−0.67 ± 0.06
XMSJ 122135.2+752838	12 : 21 : 35.2	+75 : 28 : 38.0	1.5	H	0.12 ± 0.08	4.66 ± 1.06	0.65 ± 0.17	2.62 ± 0.69	+0.52 ± 0.27
XMSJ 122143.6+752238	12 : 21 : 43.6	+75 : 22 : 38.3	0.6	X	1.14 ± 0.14	2.52 ± 3.17	2.05 ± 0.22	0.55 ± 0.31	−0.49 ± 0.08
XMSJ 122206.7+752614	12 : 22 : 06.7	+75 : 26 : 14.7	0.2	SHXU	20.81 ± 0.59	44.29 ± 2.04	36.32 ± 0.91	14.64 ± 1.35	−0.53 ± 0.02
XMSJ 122226.8+752742	12 : 22 : 26.8	+75 : 27 : 42.5	1.1	H	0.59 ± 0.12	3.82 ± 1.01	1.33 ± 0.22	0.35 ± 0.54	−0.17 ± 0.14
XMSJ 122233.4+750303	12 : 22 : 33.4	+75 : 03 : 03.9	1.7	H	0.34 ± 0.17	8.48 ± 6.67	1.42 ± 0.34	4.88 ± 1.38	+0.38 ± 0.24
XMSJ 122344.7+751923	12 : 23 : 44.7	+75 : 19 : 23.9	0.5	S X	2.19 ± 0.22	1.91 ± 22.50	3.27 ± 0.32	0.42 ± 0.36	−0.77 ± 0.05
XMSJ 122351.0+752228	12 : 23 : 51.0	+75 : 22 : 28.3	0.3	SHXU	6.86 ± 0.37	11.61 ± 1.25	11.43 ± 0.56	3.63 ± 0.69	−0.61 ± 0.04
XMSJ 122435.0+750810	12 : 24 : 35.0	+75 : 08 : 10.8	1.0	X	1.40 ± 0.25	0.95 ± 55.45	2.19 ± 0.39	0.16 ± 3.66	−0.78 ± 0.16

Table 2. continued.

Source Name	RA (J2000)	Dec (J2000)	r_{90}^{a}	Sample	$S\,(0.5{-}2)^{b}$	$S\,(2{-}10)^{b}$	$S\,(0.5{-}4.5)^{b}$	$S\,(4.5{-}7.5)^{b}$	HR_2^{c}
XMSJ 122445.5+752225	12 : 24 : 45.5	+75 : 22 : 25.3	0.6	S X	2.67 ± 0.29	2.58 ± 7.60	4.09 ± 0.44	0.43 ± 0.57	−0.78 ± 0.07
XMSJ 123049.9+640848	12 : 30 : 49.9	+64 : 08 : 48.1	0.3	S X	3.72 ± 0.19	2.14 ± 0.44	5.51 ± 0.27	0.46 ± 0.17	−0.83 ± 0.03
XMSJ 123110.8+641849	12 : 31 : 10.8	+64 : 18 : 49.3	0.4	SHXU	2.40 ± 0.14	3.81 ± 0.42	3.94 ± 0.21	1.29 ± 0.30	−0.64 ± 0.04
XMSJ 123116.6+641113	12 : 31 : 16.6	+64 : 11 : 13.8	0.2	SHXU	3.68 ± 0.16	6.14 ± 0.49	6.16 ± 0.25	2.13 ± 0.36	−0.60 ± 0.03
XMSJ 123129.3+642215	12 : 31 : 29.3	+64 : 22 : 15.8	0.5	X	1.30 ± 0.12	3.17 ± 0.49	2.25 ± 0.19	0.84 ± 0.28	−0.56 ± 0.07
XMSJ 123139.9+641123	12 : 31 : 39.9	+64 : 11 : 23.9	0.5	X	1.21 ± 0.10	1.51 ± 0.27	2.00 ± 0.15	0.07 ± 0.11	−0.61 ± 0.06
XMSJ 123141.1+642132	12 : 31 : 41.1	+64 : 21 : 32.7	0.6	X	1.37 ± 0.13	2.39 ± 0.47	2.26 ± 0.20	1.01 ± 0.35	−0.63 ± 0.07
XMSJ 123214.1+640455	12 : 32 : 14.1	+64 : 04 : 55.6	0.6	X	1.45 ± 0.15	3.02 ± 0.56	2.51 ± 0.23	0.82 ± 0.25	−0.57 ± 0.08
XMSJ 123218.6+640309	12 : 32 : 18.6	+64 : 03 : 09.7	0.4	SHX	3.29 ± 0.23	5.04 ± 0.73	5.58 ± 0.36	0.99 ± 0.32	−0.59 ± 0.05
XMSJ 123325.9+641450	12 : 33 : 25.9	+64 : 14 : 50.0	0.9	S X	1.83 ± 0.19	2.22 ± 0.72	2.89 ± 0.29	0.77 ± 0.34	−0.73 ± 0.07
XMSJ 132943.5+241123	13 : 29 : 43.5	+24 : 11 : 23.9	0.8	S X	1.54 ± 0.19	3.59 ± 0.85	2.62 ± 0.30	1.00 ± 0.37	−0.62 ± 0.09
XMSJ 132958.6+242435	13 : 29 : 58.6	+24 : 24 : 35.3	0.3	SHXU	8.81 ± 0.40	14.23 ± 1.61	14.33 ± 0.61	4.45 ± 0.85	−0.68 ± 0.03
XMSJ 133009.5+241938	13 : 30 : 09.5	+24 : 19 : 38.6	0.5	X	1.18 ± 0.12	2.76 ± 0.44	2.11 ± 0.19	0.63 ± 0.21	−0.51 ± 0.07
XMSJ 133012.2+241921	13 : 30 : 12.2	+24 : 19 : 21.7	0.6	X	1.29 ± 0.12	1.31 ± 0.45	2.03 ± 0.18	0.31 ± 0.18	−0.71 ± 0.06
XMSJ 133012.4+241301	13 : 30 : 12.4	+24 : 13 : 01.5	0.5	X	1.41 ± 0.12	2.12 ± 0.46	2.32 ± 0.18	0.23 ± 0.14	−0.65 ± 0.07
XMSJ 133015.7+241015	13 : 30 : 15.7	+24 : 10 : 15.3	0.1	S X	2.76 ± 0.16	2.79 ± 0.38	4.36 ± 0.23	0.75 ± 0.17	−0.72 ± 0.04
XMSJ 133023.8+241708	13 : 30 : 23.8	+24 : 17 : 08.4	0.2	SHXU	5.06 ± 0.19	5.35 ± 0.52	7.72 ± 0.28	1.69 ± 0.35	−0.77 ± 0.03
XMSJ 133026.1+241357	13 : 30 : 26.1	+24 : 13 : 57.5	0.5	H U	0.64 ± 0.08	6.66 ± 0.51	1.87 ± 0.14	2.77 ± 0.39	+0.06 ± 0.07
XMSJ 133026.5+241521	13 : 30 : 26.5	+24 : 15 : 21.0	0.2	SHXU	9.06 ± 0.24	4.43 ± 0.43	13.16 ± 0.34	1.23 ± 0.27	−0.86 ± 0.01
XMSJ 133027.7+242430	13 : 30 : 27.7	+24 : 24 : 30.8	0.7	H	0.54 ± 0.10	4.38 ± 0.65	1.48 ± 0.18	1.96 ± 0.51	+0.01 ± 0.12
XMSJ 133038.1+240528	13 : 30 : 38.1	+24 : 05 : 28.9	0.5	SHX	1.63 ± 0.13	3.70 ± 0.62	2.85 ± 0.21	0.97 ± 0.30	−0.55 ± 0.06
XMSJ 133041.0+241120	13 : 30 : 41.0	+24 : 11 : 20.7	0.4	S XU	1.55 ± 0.10	1.93 ± 0.28	2.38 ± 0.15	1.00 ± 0.24	−0.75 ± 0.05
XMSJ 133108.8+240249	13 : 31 : 08.8	+24 : 02 : 49.8	0.6	S X	1.79 ± 0.19	3.19 ± 1.04	3.06 ± 0.29	1.18 ± 0.58	−0.59 ± 0.08
XMSJ 133109.5+242302	13 : 31 : 09.5	+24 : 23 : 02.1	0.3	SHX	3.16 ± 0.19	3.48 ± 0.51	4.88 ± 0.29	0.98 ± 0.25	−0.76 ± 0.04
XMSJ 133118.1+241405	13 : 31 : 18.1	+24 : 14 : 05.0	0.4	HXU	1.33 ± 0.11	5.32 ± 0.55	2.70 ± 0.18	2.20 ± 0.40	−0.32 ± 0.06
XMSJ 133120.4+242304	13 : 31 : 20.4	+24 : 23 : 04.1	0.3	SHXU	6.32 ± 0.28	13.39 ± 1.09	10.86 ± 0.44	4.56 ± 0.73	−0.58 ± 0.03
XMSJ 133122.4+241300	13 : 31 : 22.4	+24 : 13 : 00.2	0.5	S X	1.80 ± 0.13	1.19 ± 0.31	2.68 ± 0.19	0.19 ± 0.14	−0.82 ± 0.05
XMSJ 133127.4+242100	13 : 31 : 27.4	+24 : 21 : 00.8	0.6	S X	1.52 ± 0.15	2.28 ± 0.54	2.59 ± 0.23	0.26 ± 0.21	−0.60 ± 0.07
XMSJ 140044.0-110034	14 : 00 : 44.0	−11 : 00 : 34.8	0.4	SHX	2.60 ± 0.21	4.21 ± 0.92	4.36 ± 0.32	1.62 ± 0.59	−0.66 ± 0.05
XMSJ 140046.6-111216	14 : 00 : 46.6	−11 : 12 : 16.1	0.5	S X	2.38 ± 0.18	1.30 ± 0.57	3.72 ± 0.26	–	−0.78 ± 0.05
XMSJ 140049.5-110738	14 : 00 : 49.5	−11 : 07 : 38.5	0.3	S X	5.24 ± 0.24	0.58 ± 0.41	7.46 ± 0.34	0.34 ± 0.16	−0.97 ± 0.01
XMSJ 140050.6-111243	14 : 00 : 50.6	−11 : 12 : 43.1	0.7	H	0.56 ± 0.10	3.65 ± 0.69	1.47 ± 0.18	1.76 ± 0.41	−0.06 ± 0.12
XMSJ 140059.9-110941	14 : 00 : 59.9	−11 : 09 : 41.1	0.3	SHX	4.21 ± 0.19	5.19 ± 0.58	6.81 ± 0.28	0.85 ± 0.23	−0.71 ± 0.03
XMSJ 140100.5-110009	14 : 01 : 00.5	−11 : 00 : 09.3	0.4	S X	2.05 ± 0.15	2.72 ± 0.48	3.39 ± 0.23	1.01 ± 0.33	−0.69 ± 0.05
XMSJ 140101.8-111223	14 : 01 : 01.8	−11 : 12 : 23.1	0.1	SHXU	34.92 ± 0.52	55.33 ± 1.61	58.87 ± 0.81	21.04 ± 1.14	−0.64 ± 0.01
XMSJ 140105.7-110659	14 : 01 : 05.7	−11 : 06 : 59.0	0.3	SHXU	1.57 ± 0.11	3.75 ± 0.39	2.88 ± 0.18	1.49 ± 0.28	−0.50 ± 0.06
XMSJ 140215.6-110718	14 : 02 : 15.6	−11 : 07 : 18.1	0.4	S X	2.28 ± 0.15	2.35 ± 0.55	3.74 ± 0.24	0.56 ± 0.26	−0.69 ± 0.05
XMSJ 140219.5-110458	14 : 02 : 19.5	−11 : 04 : 58.7	0.2	S X	10.56 ± 0.41	2.27 ± 0.79	15.04 ± 0.58	0.34 ± 0.39	−0.97 ± 0.01
XMSJ 153134.0-083610	15 : 31 : 34.0	−08 : 36 : 10.3	0.7	S X	2.10 ± 0.25	2.98 ± 0.77	3.31 ± 0.38	1.22 ± 0.42	−0.65 ± 0.07
XMSJ 153142.0-082109	15 : 31 : 42.0	−08 : 21 : 09.4	0.3	S X	2.84 ± 0.33	2.21 ± 1.23	4.35 ± 0.50	0.55 ± 0.45	−0.73 ± 0.09
XMSJ 153156.5-082610	15 : 31 : 56.5	−08 : 26 : 10.1	0.2	S X	7.29 ± 0.35	–	9.40 ± 0.46	–	−1.00 ± 0.02
XMSJ 153205.6-084323	15 : 32 : 05.6	−08 : 43 : 23.7	0.4	SHX	4.60 ± 0.34	6.73 ± 1.17	7.39 ± 0.51	3.26 ± 0.80	−0.62 ± 0.06
XMSJ 153205.7-082951	15 : 32 : 05.7	−08 : 29 : 51.6	0.3	SHX	4.15 ± 0.23	5.95 ± 0.58	6.81 ± 0.34	1.33 ± 0.36	−0.57 ± 0.04
XMSJ 153206.0-083055	15 : 32 : 06.0	−08 : 30 : 55.2	0.5	X	1.42 ± 0.14	2.87 ± 0.42	2.45 ± 0.22	0.97 ± 0.30	−0.47 ± 0.07

Table 2. continued.

Source Name	RA (J2000)	Dec (J2000)	r_{90}^{a}	Sample	$S\,(0.5{-}2)^{b}$	$S\,(2{-}10)^{b}$	$S\,(0.5{-}4.5)^{b}$	$S\,(4.5{-}7.5)^{b}$	HR_2^{c}
XMSJ 153226.2-084250	15 : 32 : 26.2	−08 : 42 : 50.1	0.6	SHX	2.40 ± 0.25	5.07 ± 1.08	4.12 ± 0.37	2.38 ± 0.76	−0.50 ± 0.08
XMSJ 212847.5-153156	21 : 28 : 47.5	−15 : 31 : 56.3	0.7	S X	1.55 ± 0.21	2.95 ± 0.59	2.43 ± 0.31	1.33 ± 0.37	−0.72 ± 0.06
XMSJ 212904.5-154448	21 : 29 : 04.5	−15 : 44 : 48.9	0.4	SHXU	4.12 ± 0.28	9.42 ± 1.00	7.24 ± 0.45	4.02 ± 0.77	−0.56 ± 0.05
XMSJ 212909.7-153041	21 : 29 : 09.7	−15 : 30 : 41.0	0.7	S X	1.69 ± 0.21	1.16 ± 0.42	2.50 ± 0.30	0.31 ± 0.23	−0.81 ± 0.06
XMSJ 212913.9-154537	21 : 29 : 13.9	−15 : 45 : 37.1	0.5	SHX	2.99 ± 0.25	5.20 ± 0.82	4.85 ± 0.39	2.88 ± 0.76	−0.70 ± 0.06
XMSJ 212922.3-154123	21 : 29 : 22.3	−15 : 41 : 23.1	0.3	H	–	3.52 ± 0.65	0.53 ± 0.17	1.52 ± 0.45	+1.00 ± 0.42
XMSJ 212924.4-154824	21 : 29 : 24.4	−15 : 48 : 24.1	0.6	S X	3.94 ± 0.37	3.02 ± 0.87	5.93 ± 0.55	1.26 ± 0.63	−0.80 ± 0.05
XMSJ 212925.9-153807	21 : 29 : 25.9	−15 : 38 : 07.9	0.7	H	0.81 ± 0.13	5.29 ± 0.71	1.79 ± 0.23	2.07 ± 0.49	−0.23 ± 0.11
XMSJ 212930.1-153313	21 : 29 : 30.1	−15 : 33 : 13.0	0.3	X	1.39 ± 0.18	0.93 ± 0.42	2.14 ± 0.28	0.21 ± 0.24	−0.77 ± 0.07
XMSJ 212934.7-154428	21 : 29 : 34.7	−15 : 44 : 28.6	0.2	X	1.42 ± 0.19	0.69 ± 0.57	2.01 ± 0.28	–	−0.97 ± 0.05
XMSJ 212956.2-153850	21 : 29 : 56.2	−15 : 38 : 50.1	0.9	X	1.39 ± 0.22	2.40 ± 0.75	2.29 ± 0.34	1.13 ± 0.66	−0.68 ± 0.08
XMSJ 213000.8-154632	21 : 30 : 00.8	−15 : 46 : 32.0	1.2	S X	2.03 ± 0.50	3.51 ± 2.26	3.60 ± 0.81	1.39 ± 0.92	−0.57 ± 0.20
XMSJ 213712.6-142321	21 : 37 : 12.6	−14 : 23 : 21.4	0.3	S X	2.72 ± 0.25	2.19 ± 0.96	4.29 ± 0.38	–	−0.70 ± 0.07
XMSJ 213714.1-142619	21 : 37 : 14.1	−14 : 26 : 19.9	0.4	S X	2.38 ± 0.19	2.36 ± 0.54	3.75 ± 0.29	0.20 ± 0.21	−0.68 ± 0.06
XMSJ 213720.0-144458	21 : 37 : 20.0	−14 : 44 : 58.0	0.3	SHX	4.44 ± 0.34	5.47 ± 1.71	7.40 ± 0.52	0.74 ± 0.42	−0.61 ± 0.06
XMSJ 213739.7-143626	21 : 37 : 39.7	−14 : 36 : 26.2	0.7	H U	0.36 ± 0.08	4.76 ± 0.59	1.26 ± 0.16	2.05 ± 0.44	+0.25 ± 0.14
XMSJ 213744.0-143632	21 : 37 : 44.0	−14 : 36 : 32.4	0.6	X	1.44 ± 0.13	1.73 ± 0.36	2.30 ± 0.19	0.26 ± 0.23	−0.63 ± 0.07
XMSJ 213746.6-144223	21 : 37 : 46.6	−14 : 42 : 23.4	0.4	H	0.71 ± 0.13	3.32 ± 0.63	1.74 ± 0.23	0.39 ± 0.39	−0.07 ± 0.12
XMSJ 213747.7-144510	21 : 37 : 47.7	−14 : 45 : 10.5	0.7	S X	1.69 ± 0.20	4.39 ± 0.87	3.02 ± 0.32	1.97 ± 0.46	−0.50 ± 0.09
XMSJ 213755.8-142749	21 : 37 : 55.8	−14 : 27 : 49.1	0.4	SHX	2.15 ± 0.16	4.51 ± 0.53	3.73 ± 0.24	1.65 ± 0.38	−0.52 ± 0.05
XMSJ 213809.5-142917	21 : 38 : 09.5	−14 : 29 : 17.6	0.6	H U	0.56 ± 0.10	6.50 ± 0.75	1.74 ± 0.19	3.18 ± 0.58	+0.16 ± 0.10
XMSJ 213811.8-142619	21 : 38 : 11.8	−14 : 26 : 19.7	0.5	SHX	2.27 ± 0.19	4.50 ± 0.71	3.84 ± 0.29	1.31 ± 0.49	−0.57 ± 0.07
XMSJ 213813.1-143653	21 : 38 : 13.1	−14 : 36 : 53.1	0.3	X	1.38 ± 0.14	0.94 ± 0.45	2.05 ± 0.20	0.25 ± 0.30	−0.79 ± 0.07
XMSJ 213813.8-143852	21 : 38 : 13.8	−14 : 38 : 52.1	0.6	HX	1.28 ± 0.15	3.51 ± 0.79	2.37 ± 0.24	1.52 ± 0.46	−0.42 ± 0.10
XMSJ 213814.6-142618	21 : 38 : 14.6	−14 : 26 : 18.8	0.6	S X	1.63 ± 0.17	1.75 ± 0.69	2.67 ± 0.25	–	−0.61 ± 0.08
XMSJ 213820.2-142532	21 : 38 : 20.2	−14 : 25 : 32.9	0.2	SHXU	7.44 ± 0.35	30.92 ± 1.83	15.39 ± 0.59	11.74 ± 1.27	−0.28 ± 0.04
XMSJ 213824.5-143129	21 : 38 : 24.5	−14 : 31 : 29.5	0.7	X	1.49 ± 0.17	1.95 ± 0.60	2.12 ± 0.24	0.88 ± 0.46	−0.80 ± 0.08
XMSJ 213830.5-143639	21 : 38 : 30.5	−14 : 36 : 39.2	0.5	SHX	2.59 ± 0.23	5.54 ± 0.98	4.27 ± 0.35	2.33 ± 0.72	−0.62 ± 0.07
XMSJ 220421.3-020425	22 : 04 : 21.3	−02 : 04 : 25.5	0.7	SHX	2.12 ± 0.26	7.33 ± 1.13	4.52 ± 0.44	0.97 ± 0.45	−0.29 ± 0.09
XMSJ 220441.5-021007	22 : 04 : 41.5	−02 : 10 : 07.4	1.0	X	1.29 ± 0.19	2.04 ± 1.31	2.18 ± 0.32	1.18 ± 0.45	−0.67 ± 0.13
XMSJ 220449.6-015817	22 : 04 : 49.6	−01 : 58 : 17.0	0.5	X	1.18 ± 0.12	1.96 ± 0.36	2.02 ± 0.18	0.81 ± 0.30	−0.58 ± 0.07
XMSJ 220450.2-015342	22 : 04 : 50.2	−01 : 53 : 42.6	0.5	HXU	1.28 ± 0.12	3.69 ± 0.43	2.38 ± 0.19	1.48 ± 0.34	−0.46 ± 0.07
XMSJ 220508.0-020100	22 : 05 : 08.0	−02 : 01 : 00.9	0.4	SHX	2.29 ± 0.16	3.56 ± 0.43	3.88 ± 0.25	0.84 ± 0.18	−0.63 ± 0.06
XMSJ 220530.0-015739	22 : 05 : 30.0	−01 : 57 : 39.7	0.4	SHX	2.15 ± 0.15	3.40 ± 0.49	3.59 ± 0.23	1.02 ± 0.29	−0.63 ± 0.05
XMSJ 221453.1-174232	22 : 14 : 53.1	−17 : 42 : 32.9	0.3	S X	1.54 ± 0.08	1.92 ± 0.34	2.52 ± 0.12	0.44 ± 0.18	−0.65 ± 0.05
XMSJ 221456.7-175050	22 : 14 : 56.7	−17 : 50 : 50.9	0.3	SHXU	1.75 ± 0.09	6.00 ± 0.53	3.40 ± 0.15	2.08 ± 0.31	−0.38 ± 0.04
XMSJ 221515.2-173222	22 : 15 : 15.2	−17 : 32 : 22.0	0.1	SHXU	6.94 ± 0.19	6.37 ± 0.61	10.66 ± 0.28	2.01 ± 0.38	−0.77 ± 0.02
XMSJ 221518.8-174003	22 : 15 : 18.8	−17 : 40 : 03.6	0.5	U	0.55 ± 0.04	1.15 ± 0.18	0.91 ± 0.07	0.68 ± 0.15	−0.62 ± 0.05
XMSJ 221519.4-175109	22 : 15 : 19.4	−17 : 51 : 09.9	0.3	X	1.46 ± 0.07	1.61 ± 0.25	2.25 ± 0.11	0.63 ± 0.16	−0.75 ± 0.04
XMSJ 221523.6-174318	22 : 15 : 23.6	−17 : 43 : 18.8	0.2	S XU	2.25 ± 0.07	2.80 ± 0.21	3.56 ± 0.11	0.91 ± 0.14	−0.70 ± 0.02
XMSJ 221536.7-173355	22 : 15 : 36.7	−17 : 33 : 55.0	0.4	X	1.28 ± 0.08	2.27 ± 0.39	2.02 ± 0.12	0.93 ± 0.23	−0.70 ± 0.04
XMSJ 221537.6-173802	22 : 15 : 37.6	−17 : 38 : 02.9	0.6	U	0.26 ± 0.04	2.22 ± 0.25	0.73 ± 0.07	0.76 ± 0.17	+0.06 ± 0.08
XMSJ 221538.1-174631	22 : 15 : 38.1	−17 : 46 : 31.1	0.2	S X	1.51 ± 0.06	1.72 ± 0.19	2.35 ± 0.09	0.58 ± 0.14	−0.72 ± 0.03
XMSJ 221550.4-175207	22 : 15 : 50.4	−17 : 52 : 07.2	0.2	SHXU	3.34 ± 0.11	4.55 ± 0.40	5.34 ± 0.17	1.53 ± 0.25	−0.68 ± 0.02

Table 2. continued.

Source Name	RA (J2000)	Dec (J2000)	r_{90}^{a}	Sample	$S\,(0.5{-}2)^{b}$	$S\,(2{-}10)^{b}$	$S\,(0.5{-}4.5)^{b}$	$S\,(4.5{-}7.5)^{b}$	HR_2^{c}
XMSJ 221550.4-172947	22 : 15 : 50.4	−17 : 29 : 47.1	0.5	S X	2.21 ± 0.13	3.16 ± 0.66	3.61 ± 0.20	1.21 ± 0.38	−0.66 ± 0.04
XMSJ 221601.1-173721	22 : 16 : 01.1	−17 : 37 : 21.3	0.4	H	0.79 ± 0.06	3.49 ± 0.44	1.62 ± 0.11	0.86 ± 0.23	−0.31 ± 0.06
XMSJ 221603.1-174316	22 : 16 : 03.1	−17 : 43 : 16.9	0.3	XU	1.36 ± 0.07	1.84 ± 0.22	2.17 ± 0.10	0.77 ± 0.16	−0.68 ± 0.04
XMSJ 221604.6-175217	22 : 16 : 04.6	−17 : 52 : 17.7	0.3	S X	1.55 ± 0.09	1.87 ± 0.33	2.43 ± 0.14	0.68 ± 0.23	−0.71 ± 0.05
XMSJ 221623.2-174055	22 : 16 : 23.2	−17 : 40 : 55.9	0.6	H	0.58 ± 0.07	3.69 ± 0.58	1.45 ± 0.13	1.04 ± 0.30	−0.07 ± 0.08
XMSJ 221623.5-174316	22 : 16 : 23.5	−17 : 43 : 16.1	0.2	SHXU	3.47 ± 0.13	5.10 ± 0.58	5.57 ± 0.20	2.00 ± 0.36	−0.69 ± 0.03
XMSJ 221623.5-174723	22 : 16 : 23.5	−17 : 47 : 23.5	0.3	SHX	2.86 ± 0.13	4.16 ± 0.60	4.63 ± 0.20	1.18 ± 0.34	−0.67 ± 0.03
XMSJ 222729.1-051647	22 : 27 : 29.1	−05 : 16 : 47.5	1.4	X	1.34 ± 0.20	2.54 ± 1.09	2.25 ± 0.30	1.30 ± 0.44	−0.53 ± 0.11
XMSJ 222732.1-051643	22 : 27 : 32.1	−05 : 16 : 43.1	0.2	SHXU	18.73 ± 0.57	29.45 ± 1.76	30.31 ± 0.83	12.64 ± 1.27	−0.59 ± 0.02
XMSJ 222745.7-052539	22 : 27 : 45.7	−05 : 25 : 39.9	0.4	SHX	2.93 ± 0.22	6.48 ± 0.99	5.16 ± 0.34	2.08 ± 0.52	−0.45 ± 0.06
XMSJ 222812.3-052814	22 : 28 : 12.3	−05 : 28 : 14.0	0.7	X	1.13 ± 0.13	2.84 ± 0.70	2.02 ± 0.20	1.45 ± 0.45	−0.42 ± 0.09
XMSJ 222813.9-051623	22 : 28 : 13.9	−05 : 16 : 23.8	0.3	SHXU	2.46 ± 0.14	4.63 ± 0.41	4.21 ± 0.20	1.26 ± 0.25	−0.48 ± 0.04
XMSJ 222815.1-052417	22 : 28 : 15.1	−05 : 24 : 17.2	0.4	SHX	1.85 ± 0.13	3.71 ± 0.39	3.33 ± 0.20	0.84 ± 0.24	−0.41 ± 0.06
XMSJ 222822.1-052733	22 : 28 : 22.1	−05 : 27 : 33.4	0.7	HXU	0.84 ± 0.11	4.73 ± 0.52	2.00 ± 0.19	2.00 ± 0.40	−0.07 ± 0.09
XMSJ 222823.7-051306	22 : 28 : 23.7	−05 : 13 : 06.3	0.3	SHXU	3.87 ± 0.17	6.79 ± 0.52	6.28 ± 0.25	2.66 ± 0.37	−0.57 ± 0.03
XMSJ 222826.5-051820	22 : 28 : 26.5	−05 : 18 : 20.2	0.2	SHXU	4.13 ± 0.17	29.99 ± 0.84	11.44 ± 0.30	11.28 ± 0.60	+0.09 ± 0.03
XMSJ 222834.6-052151	22 : 28 : 34.6	−05 : 21 : 51.2	0.2	SHX	3.05 ± 0.15	3.33 ± 0.32	4.75 ± 0.21	0.59 ± 0.18	−0.64 ± 0.03
XMSJ 222845.6-052827	22 : 28 : 45.6	−05 : 28 : 27.4	0.6	X	1.27 ± 0.14	2.01 ± 0.50	2.12 ± 0.21	0.45 ± 0.17	−0.55 ± 0.09
XMSJ 222846.9-051146	22 : 28 : 46.9	−05 : 11 : 46.4	0.4	SHXU	2.39 ± 0.16	3.51 ± 0.50	3.76 ± 0.23	1.79 ± 0.37	−0.61 ± 0.05
XMSJ 222848.9-050934	22 : 28 : 48.9	−05 : 09 : 34.0	0.4	S X	3.70 ± 0.22	2.48 ± 0.57	5.37 ± 0.30	0.77 ± 0.19	−0.76 ± 0.04
XMSJ 222850.8-051658	22 : 28 : 50.8	−05 : 16 : 58.3	0.3	SHXU	1.85 ± 0.12	4.40 ± 0.44	3.21 ± 0.18	1.69 ± 0.29	−0.46 ± 0.04
XMSJ 222852.4-050913	22 : 28 : 52.4	−05 : 09 : 13.5	0.2	S X	10.94 ± 0.37	0.23 ± 0.53	14.20 ± 0.48	–	−0.99 ± 0.01
XMSJ 222905.1-051431	22 : 29 : 05.1	−05 : 14 : 31.3	0.3	SHXU	3.29 ± 0.21	13.52 ± 0.98	6.79 ± 0.33	5.26 ± 0.64	−0.23 ± 0.05
XMSJ 222914.2-052501	22 : 29 : 14.2	−05 : 25 : 01.5	0.4	SHX	2.79 ± 0.22	5.11 ± 0.91	4.83 ± 0.33	1.81 ± 0.50	−0.48 ± 0.06
XMSJ 222918.2-052217	22 : 29 : 18.2	−05 : 22 : 17.8	0.7	S X	1.59 ± 0.17	1.43 ± 0.49	2.36 ± 0.24	0.42 ± 0.33	−0.71 ± 0.07
XMSJ 225046.1-175424	22 : 50 : 46.1	−17 : 54 : 24.7	0.6	S X	1.91 ± 0.27	2.69 ± 1.10	3.33 ± 0.44	–	−0.56 ± 0.11
XMSJ 225110.4-180027	22 : 51 : 10.4	−18 : 00 : 27.5	0.8	S X	1.72 ± 0.22	1.72 ± 0.89	2.66 ± 0.32	0.62 ± 0.54	−0.73 ± 0.05
XMSJ 225115.6-175355	22 : 51 : 15.6	−17 : 53 : 55.6	0.5	S X	1.84 ± 0.17	2.80 ± 0.59	3.03 ± 0.26	1.11 ± 0.25	−0.63 ± 0.07
XMSJ 225118.1-175948	22 : 51 : 18.1	−17 : 59 : 48.3	0.2	SHXU	16.24 ± 0.56	14.55 ± 1.30	25.00 ± 0.82	3.47 ± 0.76	−0.76 ± 0.02
XMSJ 225130.4-174138	22 : 51 : 30.4	−17 : 41 : 38.4	0.8	S X	1.54 ± 0.20	2.24 ± 0.88	2.59 ± 0.30	0.50 ± 0.30	−0.60 ± 0.08
XMSJ 225153.8-174014	22 : 51 : 53.8	−17 : 40 : 14.6	0.7	H U	0.35 ± 0.12	5.90 ± 1.08	1.26 ± 0.24	3.90 ± 0.94	+0.25 ± 0.18
XMSJ 225155.6-175835	22 : 51 : 55.6	−17 : 58 : 35.3	0.9	H	0.23 ± 0.06	3.84 ± 0.49	1.00 ± 0.15	0.91 ± 0.22	+0.39 ± 0.14
XMSJ 225159.8-174216	22 : 51 : 59.8	−17 : 42 : 16.9	0.5	S X	3.04 ± 0.25	1.74 ± 0.45	4.55 ± 0.37	0.30 ± 0.25	−0.81 ± 0.05
XMSJ 225208.8-174121	22 : 52 : 08.8	−17 : 41 : 21.2	0.7	S X	1.97 ± 0.22	2.87 ± 0.79	3.26 ± 0.35	0.44 ± 0.35	−0.64 ± 0.09
XMSJ 225210.8-180127	22 : 52 : 10.8	−18 : 01 : 27.4	0.6	X	1.49 ± 0.18	1.65 ± 0.55	2.33 ± 0.28	0.63 ± 0.29	−0.76 ± 0.09
XMSJ 225211.6-174438	22 : 52 : 11.6	−17 : 44 : 38.4	0.6	S X	2.32 ± 0.21	3.08 ± 0.85	3.65 ± 0.31	1.62 ± 0.52	−0.72 ± 0.06
XMSJ 225219.5-174215	22 : 52 : 19.5	−17 : 42 : 15.2	0.9	S X	1.52 ± 0.22	3.54 ± 1.11	2.24 ± 0.32	1.28 ± 0.69	−0.82 ± 0.06
XMSJ 225227.6-180223	22 : 52 : 27.6	−18 : 02 : 23.8	1.0	X	1.17 ± 0.20	2.85 ± 0.89	1.99 ± 0.32	0.83 ± 0.40	−0.59 ± 0.12
XMSJ 225228.2-174917	22 : 52 : 28.2	−17 : 49 : 17.6	0.4	SHX	4.04 ± 0.29	6.93 ± 0.89	6.67 ± 0.44	2.49 ± 0.65	−0.63 ± 0.05
XMSJ 233049.5+200122	23 : 30 : 49.5	+20 : 01 : 22.6	0.9	S X	4.58 ± 0.56	7.70 ± 1.84	7.50 ± 0.87	1.82 ± 0.78	−0.60 ± 0.10
XMSJ 233113.8+200506	23 : 31 : 13.8	+20 : 05 : 06.7	0.7	SHX	2.58 ± 0.37	8.23 ± 1.92	4.76 ± 0.59	4.95 ± 1.34	−0.39 ± 0.11
XMSJ 233119.3+194512	23 : 31 : 19.3	+19 : 45 : 12.2	0.8	S X	3.25 ± 0.44	4.84 ± 1.84	5.49 ± 0.69	1.41 ± 0.73	−0.55 ± 0.10
XMSJ 233128.1+194605	23 : 31 : 28.1	+19 : 46 : 05.3	0.6	X	1.21 ± 0.24	2.17 ± 0.78	2.12 ± 0.39	0.49 ± 0.48	−0.44 ± 0.12
XMSJ 233156.2+195123	23 : 31 : 56.2	+19 : 51 : 23.5	0.7	S X	1.52 ± 0.20	1.95 ± 0.50	2.42 ± 0.31	0.63 ± 0.26	−0.61 ± 0.10

Table 2. continued.

Source Name	RA (J2000)	Dec (J2000)	r_{90}^{a}	Sample	$S\,(0.5{-}2)^{b}$	$S\,(2{-}10)^{b}$	$S\,(0.5{-}4.5)^{b}$	$S\,(4.5{-}7.5)^{b}$	HR_2^{c}
XMSJ 233158.7+194440	23 : 31 : 58.7	+19 : 44 : 40.9	1.3	S X	1.51 ± 0.27	6.75 ± 1.80	2.96 ± 0.47	1.79 ± 0.66	-0.30 ± 0.12
XMSJ 233201.5+200406	23 : 32 : 01.5	+20 : 04 : 06.6	0.8	S X	1.70 ± 0.24	2.92 ± 0.74	2.95 ± 0.39	0.68 ± 0.35	-0.48 ± 0.12
XMSJ 233203.2+200626	23 : 32 : 03.2	+20 : 06 : 26.8	0.9	SHX	2.12 ± 0.31	8.08 ± 1.48	4.19 ± 0.52	2.88 ± 1.12	-0.30 ± 0.12
XMSJ 233207.3+200529	23 : 32 : 07.3	+20 : 05 : 29.6	0.6	S X	1.80 ± 0.28	1.19 ± 0.84	2.62 ± 0.39	0.28 ± 0.35	-0.75 ± 0.08
XMSJ 233209.8+194517	23 : 32 : 09.8	+19 : 45 : 17.2	0.8	SHX	3.08 ± 0.38	8.54 ± 1.96	5.27 ± 0.61	3.36 ± 0.77	-0.53 ± 0.11
XMSJ 233212.2+200557	23 : 32 : 12.2	+20 : 05 : 57.9	0.2	S X	2.96 ± 0.40	4.33 ± 1.14	4.94 ± 0.60	1.19 ± 0.77	-0.54 ± 0.10
XMSJ 233226.5+195736	23 : 32 : 26.5	+19 : 57 : 36.5	0.8	HX	1.32 ± 0.24	5.03 ± 0.92	2.60 ± 0.39	1.47 ± 0.42	-0.29 ± 0.13
XMSJ 233228.2+195809	23 : 32 : 28.2	+19 : 58 : 09.9	1.4	S	1.53 ± 0.26	1.90 ± 0.83	1.98 ± 0.37	–	-0.95 ± 0.08
XMSJ 233232.0+195116	23 : 32 : 32.0	+19 : 51 : 16.9	0.8	X	1.42 ± 0.27	1.98 ± 0.91	2.25 ± 0.41	0.97 ± 0.44	-0.63 ± 0.10
XMSJ 233232.6+195809	23 : 32 : 32.6	+19 : 58 : 09.1	0.4	SHX	3.99 ± 0.42	5.68 ± 1.66	6.38 ± 0.62	–	-0.61 ± 0.08

[a] Statistical error radius at 90% confidence in the position of the X-ray source in arcsec.
[b] All fluxes are quoted in units of 10^{-14} erg cm^{-2} s^{-1} in the corresponding band.
[c] Hardness Ratio defined as $HR_2 = (H - S)/(H + S)$, where S and H are exposure-time corrected count rates in the 0.5−2 keV and 2−4.5 keV bands respectively.

Table 5. Optical identifications of the XMS.

X-ray source	RA_o (J2000)	Dec_o(J2000)	g'	r'	i'	R	Id[a]	Type	z
XMSJ 001744.6+162815	00 : 17 : 44.6	+16 : 28 : 18.1	20.98	19.73	19.16	18.76	Y	NELG	0.266
XMSJ 001800.9+163626	00 : 18 : 00.9	+16 : 36 : 25.4	21.57	20.91	20.65		Y	BLAGN	1.222
XMSJ 001802.7+161642	00 : 18 : 02.7	+16 : 16 : 42.7	20.58	20.16	20.02	19.30	Y	BLAGN	1.407
XMSJ 001817.3+161740	00 : 18 : 17.0	+16 : 17 : 40.0	22.61	20.70	19.22	19.85	Y	Clus	0.550
XMSJ 001821.7+161943	00 : 18 : 21.8	+16 : 19 : 43.6	22.14	21.61	21.26		Y	BLAGN	1.160
XMSJ 001831.9+162926	00 : 18 : 32.0	+16 : 29 : 26.5	18.28	18.06	17.80	18.40	Y	BLAGN	0.551
XMSJ 001837.2+163446	00 : 18 : 37.3	+16 : 34 : 46.8	20.25	19.86	19.48		Y	BLAGN	2.148
XMSJ 001838.3+162007	00 : 18 : 38.2	+16 : 20 : 07.5	21.83	20.98	21.06	19.40	Y	BLAGN	1.090
XMSJ 001841.8+162032	00 : 18 : 41.7	+16 : 20 : 33.4	24.51	22.89	22.22		Y	BLAGN	1.090
XMSJ 001845.7+163345	00 : 18 : 45.6	+16 : 33 : 46.6	22.61	21.64	20.62		Y	NELG	0.623
XMSJ 001851.8+161621	00 : 18 : 51.8	+16 : 16 : 21.4	21.61	21.23	20.64		Y	BLAGN	1.806
XMSJ 001853.5+162751	00 : 18 : 53.5	+16 : 27 : 53.6	<24.41	22.35	20.90		C	–	
XMSJ 001901.9+161646	00 : 19 : 01.8	+16 : 16 : 45.6	21.09	20.65	20.15	19.30	Y	BLAGN	0.572
XMSJ 001911.8+161854	00 : 19 : 11.9	+16 : 18 : 53.5				8.41	Y	Star	
XMSJ 001919.1+162015	00 : 19 : 19.0	+16 : 20 : 14.9	21.63	21.33	20.95		Y	BLAGN	0.839
XMSJ 001928.0+163120	00 : 19 : 27.9	+16 : 31 : 20.0				14.60	Y	Star	
XMSJ 010320.3-064159							E	–	
XMSJ 010324.6-065537	01 : 03 : 24.3	−06 : 55 : 34.5				18.91	Y	BLAGN	1.251
XMSJ 010327.3-064643	01 : 03 : 27.4	−06 : 46 : 43.7	<23.94	<23.40	22.00		Y	NELG	0.749
XMSJ 010333.9-064016	01 : 03 : 33.9	−06 : 40 : 16.3	22.89	21.23	19.98		Y	NELG	0.575
XMSJ 010337.0-063337	01 : 03 : 37.0	−06 : 33 : 39.8	<23.99	22.21	21.36		C	–	
XMSJ 010339.9-065225	01 : 03 : 39.9	−06 : 52 : 26.3	21.50	20.77	20.41		Y	BLAGN	1.128
XMSJ 010355.6-063711	01 : 03 : 55.6	−06 : 37 : 10.7	21.93	21.11	20.69		Y	BLAGN	0.315
XMSJ 010358.0-062523	01 : 03 : 58.0	−06 : 25 : 22.2	22.70	21.06	20.23	20.74	Y	NELG	0.443
XMSJ 010359.5-062655	01 : 03 : 59.5	−06 : 26 : 54.7	22.01	20.66	19.91	18.50	Y	NELG	0.442
XMSJ 010401.1-064948	01 : 04 : 01.1	−06 : 49 : 51.2	17.18	15.63		15.40	Y	Star	
XMSJ 010407.9-061736	01 : 04 : 07.8	−06 : 17 : 35.0	20.17	19.51	19.49	19.10	Y	BLAGN	0.951
XMSJ 010410.6-063926	01 : 04 : 10.5	−06 : 39 : 26.7	19.98	19.58	19.29	18.70	Y	BLAGN	0.630
XMSJ 010420.9-064701	01 : 04 : 21.0	−06 : 47 : 02.1	19.81	19.10	18.58	18.80	Y	BLAGN	1.536
XMSJ 010421.5-061416	01 : 04 : 21.6	−06 : 14 : 16.2	22.29	21.23	20.42		Y	BLAGN	0.520
XMSJ 010428.2-061539	01 : 04 : 28.2	−06 : 15 : 37.3	19.04	17.80	17.23	16.70	Y	BLAGN	0.180
XMSJ 010430.2-064456	01 : 04 : 30.1	−06 : 44 : 56.8	18.87	18.39	18.24	18.50	Y	BLAGN	0.910
XMSJ 010432.9-064452	01 : 04 : 33.0	−06 : 44 : 51.8	<23.87	22.84	22.28		C	–	
XMSJ 010437.5-064737	01 : 04 : 37.6	−06 : 47 : 37.5	21.30	20.82	20.42	19.30	Y	BLAGN	2.511
XMSJ 010444.6-064832	01 : 04 : 44.7	−06 : 48 : 33.6	20.62	20.43	20.14	20.76	Y	BLAGN	2.256
XMSJ 010449.5-062723	01 : 04 : 49.5	−06 : 27 : 23.2	19.79	18.67	18.05	17.90	Y	NELG	0.110
XMSJ 010459.1-062845	01 : 04 : 59.4	−06 : 28 : 45.5	21.33	19.81	19.09	19.40	Y	NELG	0.314
XMSJ 010502.5-062124	01 : 05 : 02.7	−06 : 21 : 25.5	20.51	20.29	19.61	19.40	Y	BLAGN	1.950
XMSJ 010506.6-061510	01 : 05 : 06.5	−06 : 15 : 09.5	23.09	22.00	21.52		Y	BLAGN	1.490
XMSJ 021703.4-045533	02 : 17 : 03.4	−04 : 55 : 33.3	23.07	20.81	20.00	20.52	Y	NELG	0.571
XMSJ 021705.4-045654	02 : 17 : 05.4	−04 : 56 : 54.4			25.10	25.60	C	–	
XMSJ 021708.7-045741	02 : 17 : 08.7	−04 : 57 : 42.0	22.33	21.05	21.06	20.52	Y	BLAGN	1.433
XMSJ 021753.5-045541	02 : 17 : 53.5	−04 : 55 : 41.1	24.05	21.70	20.81		Y	NELG	0.550
XMSJ 021753.7-045748	02 : 17 : 53.7	−04 : 57 : 47.3	20.43	19.81	19.63	18.90	Y	BLAGN	1.427

Table 5. continued.

X-ray source	RA_o (J2000)	Dec_o(J2000)	g'	r'	i'	R	Id[a]	Type	z
XMSJ 021808.3-045845	02 : 18 : 08.2	−04 : 58 : 45.1	17.82	17.61	17.63	16.80	Y	BLAGN	0.712
XMSJ 021815.4-045618	02 : 18 : 15.5	−04 : 56 : 18.1	22.57	21.60	21.46		Y	BLAGN	1.440
XMSJ 021817.2-050258	02 : 18 : 17.2	−05 : 02 : 58.5	21.57	20.67	20.53	20.60	Y	BLAGN	1.280
XMSJ 021817.4-045112	02 : 18 : 17.4	−04 : 51 : 12.4	19.65	18.89	18.80	18.20	Y	BLAGN	1.077
XMSJ 021820.5-050426	02 : 18 : 20.5	−05 : 04 : 26.1	20.42	20.19	19.65	19.00	Y	BLAGN	0.646
XMSJ 021821.8-043449	02 : 18 : 21.8	−04 : 34 : 49.8	23.37	21.94	22.51		Y	NELG	2.209
XMSJ 021822.1-050613	02 : 18 : 22.2	−05 : 06 : 14.6				10.80	Y	NELG	0.044
XMSJ 021827.2-045456	02 : 18 : 27.2	−04 : 54 : 56.6	19.61	19.12	18.91	18.50	Y	BLAGN	2.200
XMSJ 021829.9-045514	02 : 18 : 29.9	−04 : 55 : 13.6				12.86	Y	Star	
XMSJ 021830.5-045623	02 : 18 : 30.6	−04 : 56 : 22.7	18.27	17.61	17.49	16.90	Y	BLAGN	1.430
XMSJ 021842.9-050437	02 : 18 : 43.0	−05 : 04 : 37.2	24.44	22.01	21.54		Y	NELG	0.962
XMSJ 021855.1-044328	02 : 18 : 55.0	−04 : 43 : 28.1	<24.46	<23.57	22.03		C	–	
XMSJ 021902.6-044628	02 : 19 : 02.6	−04 : 46 : 28.1	20.04	19.37	19.16	19.00	Y	BLAGN	1.740
XMSJ 021903.5-043935	02 : 19 : 03.5	−04 : 39 : 34.8	20.42	19.92	19.64	19.68	Y	BLAGN	0.929
XMSJ 021905.7-051038	02 : 19 : 05.7	−05 : 10 : 39.1	21.24	20.29	20.50	20.43	Y	BLAGN	1.649
XMSJ 021908.3-045500	02 : 19 : 08.3	−04 : 55 : 01.1	21.27	20.55	20.54	20.73	Y	BLAGN	0.574
XMSJ 021921.7-043641	02 : 19 : 21.8	−04 : 36 : 42.1	20.25	19.60	19.55	19.44	Y	BLAGN	2.097
XMSJ 021922.6-044058	02 : 19 : 22.6	−04 : 40 : 57.5	21.17	20.39	20.56	20.83	Y	BLAGN	1.033
XMSJ 021923.3-045148	02 : 19 : 23.3	−04 : 51 : 48.6	19.49	18.69	19.00	18.60	Y	BLAGN	0.631
XMSJ 021931.0-044956	02 : 19 : 31.1	−04 : 49 : 57.1	23.09	21.46	21.49		Y	NELG	0.293
XMSJ 021934.3-050857	02 : 19 : 34.2	−05 : 08 : 59.2	20.96	19.90	20.26	20.26	Y	BLAGN	1.323
XMSJ 021934.6-044141	02 : 19 : 34.7	−04 : 41 : 40.9	21.21	20.84	20.63	20.24	Y	BLAGN	0.714
XMSJ 021939.2-051132	02 : 19 : 39.1	−05 : 11 : 33.5	19.14	17.62	17.62	16.50	Y	NELG	0.149
XMSJ 021948.3-045128	02 : 19 : 48.3	−04 : 51 : 30.6	<24.64	22.39	21.21		Y	ALG	0.819
XMSJ 022002.1-050101	02 : 20 : 02.1	−05 : 01 : 01.8	19.58	18.70	18.94	18.90	Y	BLAGN	1.783
XMSJ 022004.8-045514	02 : 20 : 04.9	−04 : 55 : 15.6	24.01	22.17	21.90		Y	BLAGN	1.470
XMSJ 022013.0-045113	02 : 20 : 13.1	−04 : 51 : 13.9	22.39	21.51	21.17	19.00	Y	BLAGN	0.925
XMSJ 022016.8-045646	02 : 20 : 16.9	−04 : 56 : 46.0	23.34	21.35	21.03		Y	NELG	0.517
XMSJ 025727.7+131504	02 : 57 : 27.8	+13 : 15 : 05.8	21.75	20.93	20.84		Y	BLAGN	0.983
XMSJ 025737.9+131623	02 : 57 : 37.9	+13 : 16 : 22.3	22.11	21.29	20.85		Y	BLAGN	0.775
XMSJ 025744.7+131538	02 : 57 : 44.6	+13 : 15 : 39.9	23.27	22.04	21.71		Y	NELG	0.238
XMSJ 025748.3+131406	02 : 57 : 48.3	+13 : 14 : 06.1			21.72		C	–	
XMSJ 025748.5+132317	02 : 57 : 48.6	+13 : 23 : 16.2	21.35	20.67	20.12		Y	BLAGN	1.852
XMSJ 025756.5+130836	02 : 57 : 56.5	+13 : 08 : 32.4	21.36	20.79	20.62		Y	BLAGN	0.677
XMSJ 025808.4+132351	02 : 58 : 08.3	+13 : 23 : 50.3	22.55	21.41	21.00		Y	BLAGN	1.545
XMSJ 025808.8+132225	02 : 58 : 08.8	+13 : 22 : 24.0	21.41	20.35	20.14	19.10	Y	BLAGN	1.135
XMSJ 025815.3+130938	02 : 58 : 15.4	+13 : 09 : 37.2	22.72	21.00	20.37		Y	ALG	0.377
XMSJ 025850.9+131809	02 : 58 : 50.9	+13 : 18 : 07.5	<24.73	22.27	21.06		C	–	
XMSJ 025855.3+132503	02 : 58 : 55.5	+13 : 25 : 01.1	20.84	19.55	19.39	19.30	Y	BLAGN	1.258
XMSJ 025906.3+131225	02 : 59 : 06.4	+13 : 12 : 26.0	22.72	21.60	21.51		Y	BLAGN	0.966
XMSJ 061316.7+710947	06 : 13 : 16.6	+71 : 09 : 46.7				22.39	C	–	
XMSJ 061322.5+705429	06 : 13 : 22.0	+70 : 54 : 28.6	22.47	20.90	20.05		Y	NELG	0.347
XMSJ 061337.9+705001	06 : 13 : 37.6	+70 : 49 : 60.0	21.54	21.28	21.01		Y	BLAGN	0.863
XMSJ 061343.7+710727	06 : 13 : 43.3	+71 : 07 : 27.0					Y	BLLac	0.267

Table 5. continued.

X-ray source	RA_o (J2000)	Dec_o(J2000)	g'	r'	i'	R	Id[a]	Type	z
XMSJ 061346.5+710347	06 : 13 : 46.3	+71 : 03 : 45.3	20.14	19.64	19.05		C	–	
XMSJ 061346.5+705025	06 : 13 : 46.8	+70 : 50 : 20.8	20.48	20.01	19.71		Y	BLAGN	1.276
XMSJ 061413.9+705236	06 : 14 : 13.8	+70 : 52 : 33.2				13.60	Y	Star	
XMSJ 061452.9+710505	06 : 14 : 52.4	+71 : 05 : 04.7	21.85	21.20	20.29		Y	BLAGN	1.710
XMSJ 061508.2+710702	06 : 15 : 07.9	+71 : 07 : 01.4	<24.46	22.09	20.56		C	–	
XMSJ 061515.2+710204	06 : 15 : 15.1	+71 : 02 : 03.7	22.07	21.91	21.36		Y	BLAGN	0.874
XMSJ 061607.6+710638	06 : 16 : 07.4	+71 : 06 : 36.9	19.05	18.58	18.00	18.00	Y	BLAGN	1.703
XMSJ 061616.7+705605	06 : 16 : 16.5	+70 : 56 : 03.6	21.11	20.89	20.27		Y	BLAGN	1.744
XMSJ 061728.7+710600	06 : 17 : 28.5	+71 : 05 : 59.5	21.00	20.15	19.45	19.30	Y	BLAGN	0.219
XMSJ 061731.0+705955	06 : 17 : 30.7	+70 : 59 : 53.2	21.27	20.40	19.72	19.27	Y	NELG	0.200
XMSJ 074214.2+742319	07 : 42 : 14.0	+74 : 23 : 19.1	24.15	22.95	21.45		C	–	
XMSJ 074214.6+744529	07 : 42 : 14.5	+74 : 45 : 28.0	20.53	19.66	19.37	19.20	Y	BLAGN	1.020
XMSJ 074243.9+743249	07 : 42 : 44.1	+74 : 32 : 49.6	23.71	22.76	22.05		Y	BLAGN	1.151
XMSJ 074248.7+742747	07 : 42 : 48.7	+74 : 27 : 46.9	21.99	21.36	20.73		Y	BLAGN	0.958
XMSJ 074350.8+743839	07 : 43 : 50.8	+74 : 38 : 40.5	23.23	21.75	20.85		C	–	
XMSJ 074352.9+744257	07 : 43 : 53.0	+74 : 42 : 57.8	19.21	18.80	18.73	19.70	Y	BLAGN	0.800
XMSJ 074400.4+744056	07 : 44 : 00.4	+74 : 40 : 56.6				13.20	Y	Star	
XMSJ 074435.6+744444	07 : 44 : 35.8	+74 : 44 : 43.9	21.19	19.94	19.24	18.70	Y	NELG	0.434
XMSJ 074457.9+742156	07 : 44 : 57.6	+74 : 21 : 54.2	24.23	23.60	22.29		C	–	
XMSJ 074646.9+744500	07 : 46 : 47.4	+74 : 45 : 00.1	<24.85	23.55	22.34		C	–	
XMSJ 074728.9+743804	07 : 47 : 29.2	+74 : 38 : 00.3	20.48	20.21	20.10	19.40	Y	Star	
XMSJ 083859.0+705043	08 : 38 : 58.7	+70 : 50 : 42.6	22.16	20.87	20.08		Y	NELG	0.332
XMSJ 084132.3+704757	08 : 41 : 32.4	+70 : 47 : 58.0	20.28	18.98	18.18	17.30	Y	NELG	0.240
XMSJ 084144.2+704653	08 : 41 : 44.1	+70 : 46 : 53.2	20.36	18.84	18.00	17.40	Y	Clus	0.242
XMSJ 084150.4+705008	08 : 41 : 50.4	+70 : 50 : 08.1	19.69	19.08	18.75	18.30	Y	BLAGN	1.242
XMSJ 084211.8+710146	08 : 42 : 11.8	+71 : 01 : 46.8	21.04	19.75	18.93	18.20	Y	NELG	0.308
XMSJ 084217.1+710009	08 : 42 : 16.1	+71 : 00 : 11.6				12.90	Y	Star	
XMSJ 084221.6+705758	08 : 42 : 22.5	+70 : 57 : 56.9	<24.71	21.42	<23.31		Y	ALG	0.013
XMSJ 084239.9+704431	08 : 42 : 39.7	+70 : 44 : 31.2	22.77	22.08	21.73		C	–	
XMSJ 084310.1+705557	08 : 43 : 10.0	+70 : 55 : 58.6	20.93	20.82	20.68	19.30	Y	BLAGN	0.935
XMSJ 084324.3+705235	08 : 43 : 24.3	+70 : 52 : 36.1	18.64	18.41	17.91	18.50	Y	BLAGN	1.795
XMSJ 084334.6+704734	08 : 43 : 34.7	+70 : 47 : 35.0	22.95	22.13	21.57		C	–	
XMSJ 094152.2+465116	09 : 41 : 52.2	+46 : 51 : 15.9	21.98	20.97	21.25		Y	BLAGN	1.270
XMSJ 094154.6+470637	09 : 41 : 54.6	+47 : 06 : 38.2	16.71	15.02		15.10	Y	Star	
XMSJ 094242.1+470618	09 : 42 : 42.2	+47 : 06 : 18.7	21.88	20.35	20.52	19.50	Y	BLAGN	1.003
XMSJ 094251.5+464729	09 : 42 : 51.4	+46 : 47 : 28.9	20.75	19.97	20.28	19.40	Y	BLAGN	1.287
XMSJ 094317.3+470040	09 : 43 : 17.3	+47 : 00 : 39.7	21.07	20.47	20.20	19.00	Y	BLAGN	1.844
XMSJ 094345.2+465155	09 : 43 : 45.2	+46 : 51 : 54.9	18.97	17.77	18.02	18.10	Y	BLAGN	1.240
XMSJ 094348.3+470155	09 : 43 : 48.4	+47 : 01 : 53.6	22.73	21.47	21.23		Y	BLAGN	1.648
XMSJ 102950.8+310109	10 : 29 : 50.7	+31 : 01 : 10.0	21.39	19.83	19.10	18.30	Y	BLAGN	0.373
XMSJ 103007.0+311124	10 : 30 : 07.0	+31 : 11 : 24.6				19.80	Y	BLAGN	1.288
XMSJ 103015.5+310138	10 : 30 : 14.9	+31 : 01 : 38.5		22.25			C	–	
XMSJ 103020.7+305637	10 : 30 : 20.6	+30 : 56 : 37.9	19.60	18.99	18.80	18.70	Y	BLAGN	1.063
XMSJ 103028.4+305659	10 : 30 : 28.3	+30 : 56 : 59.5	21.22	20.19	19.57	19.40	Y	BLAGN	0.245

Table 5. continued.

X-ray source	RA_o (J2000)	Dec_o(J2000)	g'	r'	i'	R	Id[a]	Type	z
XMSJ 103048.5+305702	10 : 30 : 48.4	+30 : 57 : 03.0	21.90	20.79	20.56		Y	BLAGN	1.396
XMSJ 103050.9+310538	10 : 30 : 50.8	+31 : 05 : 39.6	20.54	19.98	19.59	19.50	Y	BLAGN	1.958
XMSJ 103101.8+305144	10 : 31 : 01.8	+30 : 51 : 43.0	18.37	17.17	16.56	13.70	Y	ALG	0.137
XMSJ 103104.7+305637	10 : 31 : 04.8	+30 : 56 : 36.6	20.13	20.15	19.80	19.00	Y	BLAGN	0.720
XMSJ 103111.3+310332	10 : 31 : 11.3	+31 : 03 : 32.6	22.34	21.09	20.57		Y	BLAGN	0.627
XMSJ 103123.0+310330	10 : 31 : 22.9	+31 : 03 : 30.5	22.43	20.86	19.80	19.79	Y	NELG	0.565
XMSJ 103150.6+310817	10 : 31 : 50.6	+31 : 08 : 18.0	<24.68	22.87	21.59		C	–	
XMSJ 103154.1+310731	10 : 31 : 54.1	+31 : 07 : 31.4	20.13	19.47	18.86	17.80	Y	BLAGN	0.299
XMSJ 103157.0+310535	10 : 31 : 57.0	+31 : 05 : 36.4	20.52	20.38	20.34	19.00	Y	BLAGN	1.152
XMSJ 113034.4+312422	11 : 30 : 34.5	+31 : 24 : 23.2	19.54	19.17	18.49	18.90	Y	BLAGN	1.812
XMSJ 113042.5+311227	11 : 30 : 42.5	+31 : 12 : 27.8	20.89	20.45	20.34		Y	BLAGN	1.432
XMSJ 113049.2+311403	11 : 30 : 49.2	+31 : 14 : 03.9	22.66	21.86	21.67		Y	BLAGN	1.610
XMSJ 113052.1+310940	11 : 30 : 51.9	+31 : 09 : 40.5	22.02	21.48	20.78		Y	BLAGN	0.917
XMSJ 113102.9+311015	11 : 31 : 03.0	+31 : 10 : 15.3				22.17	C	–	
XMSJ 113117.0+310039	11 : 31 : 17.0	+31 : 00 : 38.6	21.40	21.09	20.56		Y	BLAGN	0.738
XMSJ 113118.4+310114	11 : 31 : 18.3	+31 : 01 : 13.3	21.78	21.45	20.96		Y	BLAGN	1.596
XMSJ 113121.8+310254	11 : 31 : 21.8	+31 : 02 : 54.7	19.82	18.93	18.10	17.90	Y	NELG	0.190
XMSJ 113126.6+311241	11 : 31 : 26.6	+31 : 12 : 41.6	19.83	19.45	19.36		Y	BLAGN	1.058
XMSJ 113129.3+310945	11 : 31 : 29.3	+31 : 09 : 45.1	19.90	18.89	18.06	17.90	Y	BLAGN	0.179
XMSJ 113138.2+311230	11 : 31 : 38.2	+31 : 12 : 33.0	23.37	23.05	22.42		C	–	
XMSJ 113144.7+311340	11 : 31 : 44.7	+31 : 13 : 40.2	22.38	21.74	21.45		Y	BLAGN	1.025
XMSJ 113151.6+312144	11 : 31 : 51.6	+31 : 21 : 44.9					Y	BLAGN	0.990
XMSJ 113154.3+311137	11 : 31 : 54.3	+31 : 11 : 38.3	19.91	19.74	19.10		Y	BLAGN	1.798
XMSJ 113201.2+311211	11 : 32 : 01.2	+31 : 12 : 09.8	22.04	21.52	21.03		Y	BLAGN	1.001
XMSJ 121819.5+751922	12 : 18 : 19.0	+75 : 19 : 22.2	19.97	19.35	19.08	18.90	Y	BLAGN	2.649
XMSJ 121828.3+752225	12 : 18 : 28.7	+75 : 22 : 26.5	21.92	21.23	20.71		Y	BLAGN	1.150
XMSJ 121912.7+751441	12 : 19 : 11.9	+75 : 14 : 42.6	22.74	21.92	21.79		Y	NELG	0.339
XMSJ 122004.0+752145	12 : 20 : 03.6	+75 : 21 : 45.7	20.03		19.34		Y	BLAGN	0.973
XMSJ 122004.9+752103	12 : 20 : 06.0	+75 : 21 : 04.3	22.52		19.65		Y	Star	
XMSJ 122018.2+752215	12 : 20 : 17.6	+75 : 22 : 15.2					Y	ALG	0.006
XMSJ 122048.3+751807	12 : 20 : 48.2	+75 : 18 : 07.3	18.89	18.61	18.05	18.40	Y	BLAGN	1.687
XMSJ 122051.4+750531	12 : 20 : 51.3	+75 : 05 : 31.5	18.45	18.34	17.79	17.70	Y	BLAGN	0.646
XMSJ 122051.8+752821	12 : 20 : 51.6	+75 : 28 : 22.8	22.24	21.43	21.00		Y	BLAGN	0.181
XMSJ 122110.8+751119	12 : 21 : 10.5	+75 : 11 : 19.3	19.91	18.92	18.75	18.70	Y	BLAGN	1.259
XMSJ 122120.4+751618	12 : 21 : 19.9	+75 : 16 : 18.0	21.03	20.12	19.56	19.30	Y	NELG	0.340
XMSJ 122135.0+750916	12 : 21 : 34.8	+75 : 09 : 16.0	21.08	19.25	18.57	18.30	Y	BLAGN	0.330
XMSJ 122135.2+752838	12 : 21 : 35.0	+75 : 28 : 37.2	22.85		20.01	19.81	Y	NELG	0.640
XMSJ 122143.6+752238	12 : 21 : 44.0	+75 : 22 : 38.3					C	–	
XMSJ 122206.7+752614	12 : 22 : 06.6	+75 : 26 : 15.4	20.23	18.82	18.06	16.70	Y	NELG	0.238
XMSJ 122226.8+752742			<24.93	<23.36	<23.18		E	–	
XMSJ 122233.4+750303	12 : 22 : 33.2	+75 : 03 : 02.5				14.80	Y	ALG	0.104
XMSJ 122344.7+751923	12 : 23 : 44.5	+75 : 19 : 21.9	20.55	20.39	20.03		Y	BLAGN	0.757
XMSJ 122351.0+752228	12 : 23 : 50.9	+75 : 22 : 28.7	19.54	19.62	18.66	19.20	Y	BLAGN	0.565
XMSJ 122435.0+750810	12 : 24 : 35.3	+75 : 08 : 09.8	21.29	20.47	20.48	19.42	Y	BLAGN	1.333

Table 5. continued.

X-ray source	RA_o (J2000)	Dec_o(J2000)	g'	r'	i'	R	Id[a]	Type	z
XMSJ 122445.5+752225	12 : 24 : 45.5	+75 : 22 : 25.0	19.84	19.96	19.26		Y	BLAGN	1.852
XMSJ 123049.9+640848	12 : 30 : 49.8	+64 : 08 : 48.5	19.65	18.75	18.88	18.90	Y	BLAGN	1.036
XMSJ 123110.8+641849	12 : 31 : 10.8	+64 : 18 : 49.8	19.98	19.73	19.46	18.70	Y	BLAGN	1.483
XMSJ 123116.6+641113	12 : 31 : 16.5	+64 : 11 : 14.4	21.70	21.50	20.70		Y	BLAGN	0.454
XMSJ 123129.3+642215	12 : 31 : 29.1	+64 : 22 : 12.2				20.27	Y	Star	
XMSJ 123139.9+641123	12 : 31 : 39.8	+64 : 11 : 24.7	20.03	19.37	19.34	18.80	Y	BLAGN	1.032
XMSJ 123141.1+642132	12 : 31 : 41.2	+64 : 21 : 35.1	20.74	21.07	20.31		Y	BLAGN	0.858
XMSJ 123214.1+640455	12 : 32 : 14.1	+64 : 04 : 55.4	22.87	<23.35	21.87		C	–	
XMSJ 123218.6+640309	12 : 32 : 18.8	+64 : 03 : 09.8	21.07	20.38	20.33		Y	BLAGN	1.013
XMSJ 123325.9+641450	12 : 33 : 26.1	+64 : 14 : 48.3	20.88	19.82	19.23	19.00	Y	NELG	0.208
XMSJ 132943.5+241123	13 : 29 : 43.5	+24 : 11 : 21.9	20.32	19.41	18.81	18.80	Y	BLAGN	0.257
XMSJ 132958.6+242435	13 : 29 : 58.7	+24 : 24 : 36.9				19.40	Y	BLAGN	0.700
XMSJ 133009.5+241938	13 : 30 : 09.4	+24 : 19 : 38.5	20.73	20.46	20.08	19.98	Y	BLAGN	2.256
XMSJ 133012.2+241921	13 : 30 : 12.2	+24 : 19 : 20.6	21.93	20.59	19.88	19.57	Y	BLAGN	1.443
XMSJ 133012.4+241301	13 : 30 : 12.3	+24 : 13 : 01.4	21.80	21.40	20.91		Y	BLAGN	0.787
XMSJ 133015.7+241015	13 : 30 : 15.6	+24 : 10 : 15.4				19.70	Y	BLAGN	0.560
XMSJ 133023.8+241708	13 : 30 : 23.8	+24 : 17 : 08.7	19.62	18.91	18.75	17.80	Y	BLAGN	1.438
XMSJ 133026.1+241357	13 : 30 : 26.1	+24 : 13 : 56.1	20.89			18.70	Y	NELG	0.166
XMSJ 133026.5+241521	13 : 30 : 26.5	+24 : 15 : 21.9	20.23	19.33	18.64	18.70	Y	BLLac	0.463
XMSJ 133027.7+242430	13 : 30 : 27.8	+24 : 24 : 31.3	22.45	20.78	19.91	20.00	Y	NELG	0.535
XMSJ 133038.1+240528	13 : 30 : 38.1	+24 : 05 : 28.6	23.76	22.67	22.38		C	–	
XMSJ 133041.0+241120	13 : 30 : 41.0	+24 : 11 : 21.5	21.16	20.68	20.42		Y	BLAGN	0.941
XMSJ 133108.8+240249	13 : 31 : 08.7	+24 : 02 : 49.0	22.35	20.82	20.05	19.92	C	–	
XMSJ 133109.5+242302	13 : 31 : 09.5	+24 : 23 : 02.5	20.89	20.16	19.81	18.50	C	–	
XMSJ 133118.1+241405	13 : 31 : 18.1	+24 : 14 : 04.9	23.63	22.33	21.81		C	–	
XMSJ 133120.4+242304	13 : 31 : 20.4	+24 : 23 : 04.4	21.61	21.06	20.41		C	–	
XMSJ 133122.4+241300	13 : 31 : 22.5	+24 : 13 : 01.0	20.74	20.12	20.01		Y	BLAGN	1.238
XMSJ 133127.4+242100	13 : 31 : 27.4	+24 : 21 : 00.6	23.33	22.37	22.82		C	–	
XMSJ 140044.0-110034	14 : 00 : 44.1	−11 : 00 : 34.1	21.36	20.91	20.52		Y	BLAGN	1.695
XMSJ 140046.6-111216	14 : 00 : 46.6	−11 : 12 : 16.6	19.09	18.55	18.27	18.30	Y	BLAGN	1.330
XMSJ 140049.5-110738	14 : 00 : 49.5	−11 : 07 : 37.6				10.83	Y	Star	
XMSJ 140050.6-111243	14 : 00 : 50.7	−11 : 12 : 44.5	23.50	22.91	22.29		C	–	
XMSJ 140059.9-110941	14 : 00 : 59.9	−11 : 09 : 40.7	20.31	19.33	18.76	18.80	Y	NELG	0.165
XMSJ 140100.5-110009	14 : 01 : 00.5	−11 : 00 : 09.2	21.55	20.67	20.24	19.30	Y	NELG	0.446
XMSJ 140101.8-111223	14 : 01 : 01.8	−11 : 12 : 22.7	17.53	16.63	16.17	12.70	Y	BLAGN	0.037
XMSJ 140105.7-110659	14 : 01 : 05.9	−11 : 06 : 59.4	21.90	20.40	19.30	19.86	Y	BLAGN	0.416
XMSJ 140215.6-110718	14 : 02 : 15.7	−11 : 07 : 17.7	21.98	21.28	20.68		Y	BLAGN	0.480
XMSJ 140219.5-110458	14 : 02 : 19.6	−11 : 04 : 56.7				10.50	Y	Star	
XMSJ 153134.0-083610	15 : 31 : 33.9	−08 : 36 : 09.8	22.24	21.76	21.02		Y	BLAGN	1.175
XMSJ 153142.0-082109	15 : 31 : 42.3	−08 : 21 : 10.6				17.90	Y	Star	
XMSJ 153156.5-082610	15 : 31 : 56.6	−08 : 26 : 09.1				8.80	Y	Star	
XMSJ 153205.6-084323	15 : 32 : 05.5	−08 : 43 : 23.5	22.47	21.88	20.78		Y	BLAGN	1.983
XMSJ 153205.7-082951	15 : 32 : 05.6	−08 : 29 : 50.6	19.40	18.89	18.64	18.70	Y	BLAGN	1.239
XMSJ 153206.0-083055	15 : 32 : 06.0	−08 : 30 : 54.5	21.65	20.91	20.65		Y	BLAGN	1.373

Table 5. continued.

X-ray source	RA_o (J2000)	Dec_o(J2000)	g'	r'	i'	R	Id[a]	Type	z
XMSJ 153226.2-084250	15 : 32 : 26.0	−08 : 42 : 48.8	21.43	20.84	20.34		Y	BLAGN	1.206
XMSJ 212847.5-153156	21 : 28 : 47.5	−15 : 31 : 57.1	21.45	20.81	20.52		Y	BLAGN	0.787
XMSJ 212904.5-154448	21 : 29 : 04.6	−15 : 44 : 49.0	21.30	19.98	19.39	19.35	Y	BLAGN	0.431
XMSJ 212909.7-153041	21 : 29 : 09.8	−15 : 30 : 40.6	21.49	20.62	20.08	19.00	Y	BLAGN	0.540
XMSJ 212913.9-154537	21 : 29 : 14.0	−15 : 45 : 36.5	22.09	21.50	21.01	20.52	Y	BLAGN	0.868
XMSJ 212922.3-154123	21 : 29 : 22.3	−15 : 41 : 23.9	<24.21	22.22	21.04		C	–	
XMSJ 212924.4-154824	21 : 29 : 24.4	−15 : 48 : 21.1	19.02	18.46	18.11	18.20	Y	BLAGN	1.606
XMSJ 212925.9-153807	21 : 29 : 25.9	−15 : 38 : 05.8	21.98	20.45	19.73	19.26	Y	ALG	0.462
XMSJ 212930.1-153313	21 : 29 : 30.1	−15 : 33 : 12.7	20.57	19.81	19.77	18.60	Y	BLAGN	1.150
XMSJ 212934.7-154428	21 : 29 : 34.7	−15 : 44 : 27.3				11.50	Y	Star	
XMSJ 212956.2-153850	21 : 29 : 56.3	−15 : 38 : 46.8	21.87	20.76	20.25	20.25	Y	NELG	0.435
XMSJ 213000.8-154632	21 : 30 : 00.8	−15 : 46 : 31.5					Y	BLAGN	0.597
XMSJ 213712.6-142321	21 : 37 : 12.7	−14 : 23 : 21.5	21.02	20.26	19.75	19.84	Y	BLAGN	0.414
XMSJ 213714.1-142619	21 : 37 : 14.0	−14 : 26 : 19.4	20.45	19.44	19.03	18.70	Y	NELG	0.321
XMSJ 213720.0-144458	21 : 37 : 20.0	−14 : 44 : 58.5	20.14	19.09	18.18	18.10	Y	BLAGN	0.210
XMSJ 213739.7-143626	21 : 37 : 39.7	−14 : 36 : 25.9	22.99	21.36	20.39	19.91	Y	NELG	0.344
XMSJ 213744.0-143632	21 : 37 : 43.9	−14 : 36 : 34.4				19.13	Y	BLAGN	2.122
XMSJ 213746.6-144223	21 : 37 : 46.7	−14 : 42 : 24.4	19.72	18.82	18.23	17.40	C	–	
XMSJ 213747.7-144510	21 : 37 : 47.8	−14 : 45 : 11.1	20.22	19.80	19.97	19.86	Y	BLAGN	0.793
XMSJ 213755.8-142749	21 : 37 : 55.8	−14 : 27 : 49.7	<23.88	22.48	21.65		Y	NELG	1.021
XMSJ 213809.5-142917	21 : 38 : 09.5	−14 : 29 : 18.0	23.02	21.04	19.92	19.99	Y	NELG	0.559
XMSJ 213811.8-142619	21 : 38 : 11.9	−14 : 26 : 19.9	20.46	20.02	19.65		Y	BLAGN	2.013
XMSJ 213813.1-143653	21 : 38 : 13.1	−14 : 36 : 53.7				14.20	Y	Star	
XMSJ 213813.8-143852	21 : 38 : 13.8	−14 : 38 : 53.4	21.57	20.87	20.48		Y	BLAGN	1.493
XMSJ 213814.6-142618	21 : 38 : 14.6	−14 : 26 : 18.5	21.94	21.22	21.02		Y	BLAGN	1.098
XMSJ 213820.2-142532	21 : 38 : 20.2	−14 : 25 : 32.6	21.13	19.81	19.20	18.70	Y	BLAGN	0.371
XMSJ 213824.5-143129	21 : 38 : 24.4	−14 : 31 : 31.2	20.71	20.14	19.74	19.30	Y	BLAGN	1.494
XMSJ 213830.5-143639	21 : 38 : 30.5	−14 : 36 : 39.5				20.68	Y	BLAGN	0.985
XMSJ 220421.3-020425	22 : 04 : 21.4	−02 : 04 : 25.7	21.78	20.25	19.08	19.10	Y	NELG	0.302
XMSJ 220441.5-021007	22 : 04 : 41.6	−02 : 10 : 06.1	20.69	20.42	19.79		Y	BLAGN	1.392
XMSJ 220449.6-015817	22 : 04 : 49.6	−01 : 58 : 15.7	22.67	22.67	22.11		Y	BLAGN	2.189
XMSJ 220450.2-015342	22 : 04 : 50.3	−01 : 53 : 41.6	<24.40	<23.46	22.98		Y	ALG	0.330
XMSJ 220508.0-020100	22 : 05 : 08.0	−02 : 00 : 59.7	20.80	20.58	19.86	20.91	Y	BLAGN	1.909
XMSJ 220530.0-015739	22 : 05 : 29.9	−01 : 57 : 38.1	20.86	20.68	20.07		Y	BLAGN	1.619
XMSJ 221453.1-174232	22 : 14 : 53.2	−17 : 42 : 33.7				22.90	Y	BLAGN	1.190
XMSJ 221456.7-175050	22 : 14 : 56.7	−17 : 50 : 50.8	<23.99	22.56	22.43		Y	NELG	0.627
XMSJ 221515.2-173222	22 : 15 : 15.2	−17 : 32 : 21.9	18.18	17.31	17.33	17.30	Y	BLAGN	1.159
XMSJ 221518.8-174003			<24.10	<23.48	<23.31		E	–	
XMSJ 221519.4-175109	22 : 15 : 19.5	−17 : 51 : 10.8	23.43	21.91	22.67		Y	BLAGN	1.464
XMSJ 221523.6-174318	22 : 15 : 23.7	−17 : 43 : 18.4	20.30	19.58	19.92	20.41	Y	BLAGN	0.956
XMSJ 221536.7-173355	22 : 15 : 36.7	−17 : 33 : 54.2	22.34	21.88	21.48	18.00	Y	BLAGN	1.710
XMSJ 221537.6-173802			<24.10	<23.48	<23.31		E	–	
XMSJ 221538.1-174631	22 : 15 : 38.2	−17 : 46 : 32.3	20.22	19.62	19.84	18.00	Y	BLAGN	1.416
XMSJ 221550.4-175207	22 : 15 : 50.3	−17 : 52 : 07.4	20.23	19.41	19.77	18.10	Y	BLAGN	1.305

Table 5. continued.

X-ray source	RA_o (J2000)	Dec_o(J2000)	g'	r'	i'	R	Id[a]	Type	z
XMSJ 221550.4-172947	22 : 15 : 50.5	−17 : 29 : 46.7	22.69	21.05	20.57	20.90	Y	BLAGN	0.400
XMSJ 221601.1-173721	22 : 16 : 01.2	−17 : 37 : 23.0	<24.10	<23.48	22.29		C	–	
XMSJ 221603.1-174316	22 : 16 : 03.1	−17 : 43 : 17.0	21.24	20.67	20.47	15.60	Y	BLAGN	1.849
XMSJ 221604.6-175217	22 : 16 : 04.7	−17 : 52 : 18.1	20.69	19.94	20.04	15.60	Y	BLAGN	1.319
XMSJ 221623.2-174055	22 : 16 : 23.3	−17 : 40 : 56.2	<24.10	<23.48	22.64		C	–	
XMSJ 221623.5-174316	22 : 16 : 23.5	−17 : 43 : 16.1	20.70	19.63	19.71	16.00	Y	BLAGN	0.752
XMSJ 221623.5-174723	22 : 16 : 23.6	−17 : 47 : 25.6	22.36	20.84	20.89		Y	BLAGN	1.070
XMSJ 222729.1-051647	22 : 27 : 29.1	−05 : 16 : 46.3	22.89	21.54	21.17	21.41	Y	BLAGN	1.620
XMSJ 222732.1-051643	22 : 27 : 32.1	−05 : 16 : 42.3	21.36	20.83	20.32	20.48	Y	BLAGN	0.622
XMSJ 222745.7-052539	22 : 27 : 45.6	−05 : 25 : 39.6	22.66	20.57	20.40	20.38	Y	BLAGN	1.409
XMSJ 222812.3-052814	22 : 28 : 12.5	−05 : 28 : 10.4	20.32	18.62	17.46	18.67	Y	Star	
XMSJ 222813.9-051623	22 : 28 : 13.9	−05 : 16 : 23.4	21.29	20.27	19.98	20.15	Y	BLAGN	1.510
XMSJ 222815.1-052417	22 : 28 : 15.0	−05 : 24 : 18.2	23.16	21.97	21.00		Y	BLAGN	0.619
XMSJ 222822.1-052733	22 : 28 : 22.0	−05 : 27 : 35.4	<24.32	<23.43	22.69		C	–	
XMSJ 222823.7-051306	22 : 28 : 23.7	−05 : 13 : 05.9	20.46	19.36	18.87	19.98	Y	BLAGN	0.756
XMSJ 222826.5-051820	22 : 28 : 26.4	−05 : 18 : 19.8	23.92	22.03	20.71	21.21	Y	NELG	0.711
XMSJ 222834.6-052151	22 : 28 : 34.6	−05 : 21 : 52.4	22.76	20.96	20.02	21.25	Y	ALG	0.242
XMSJ 222845.6-052827	22 : 28 : 45.6	−05 : 28 : 29.5	22.98	21.10	20.36	20.99	Y	NELG	0.436
XMSJ 222846.9-051146	22 : 28 : 47.0	−05 : 11 : 46.6	23.49	22.48	21.82		Y	BLAGN	1.200
XMSJ 222848.9-050934	22 : 28 : 48.9	−05 : 09 : 34.2	19.43	18.73	18.53	18.30	Y	BLAGN	2.272
XMSJ 222850.8-051658	22 : 28 : 50.7	−05 : 16 : 58.5	24.00	23.33	23.01		Y	BLAGN	1.556
XMSJ 222852.4-050913	22 : 28 : 52.4	−05 : 09 : 12.9				10.30	Y	Star	
XMSJ 222905.1-051431	22 : 29 : 05.2	−05 : 14 : 32.7	<24.37	22.69	21.81		Y	ALG	0.579
XMSJ 222914.2-052501	22 : 29 : 14.2	−05 : 25 : 02.0	21.79	20.51	20.19	20.63	Y	BLAGN	1.470
XMSJ 222918.2-052217	22 : 29 : 18.2	−05 : 22 : 17.6	21.70	20.30	19.89		Y	BLAGN	0.332
XMSJ 225046.1-175424	22 : 50 : 46.1	−17 : 54 : 25.4				19.00	Y	BLAGN	2.139
XMSJ 225110.4-180027	22 : 51 : 10.3	−18 : 00 : 26.6	20.93			20.97	Y	BLAGN	2.312
XMSJ 225115.6-175355	22 : 51 : 15.5	−17 : 53 : 55.9	20.70	19.35	18.93	17.90	Y	NELG	0.252
XMSJ 225118.1-175948	22 : 51 : 18.0	−17 : 59 : 49.0	19.17	18.42	17.94	17.80	Y	BLAGN	0.172
XMSJ 225130.4-174138	22 : 51 : 30.3	−17 : 41 : 38.6	21.29	20.64	20.56		Y	BLAGN	1.105
XMSJ 225153.8-174014			<24.28	<23.08	<23.26		E	–	
XMSJ 225155.6-175835	22 : 51 : 55.6	−17 : 58 : 34.7	<24.34	<23.07	21.88		C	–	
XMSJ 225159.8-174216	22 : 51 : 59.8	−17 : 42 : 16.6	20.75	18.95	17.35	18.10	Y	Star	
XMSJ 225208.8-174121	22 : 52 : 09.1	−17 : 41 : 21.0	20.92	20.01	19.80	18.00	Y	BLAGN	1.217
XMSJ 225210.8-180127	22 : 52 : 10.8	−18 : 01 : 27.0	23.04	21.40	21.41		Y	BLAGN	1.410
XMSJ 225211.6-174438	22 : 52 : 11.7	−17 : 44 : 38.1				18.10	Y	BLAGN	0.950
XMSJ 225219.5-174215	22 : 52 : 19.6	−17 : 42 : 16.0	20.00	19.80	19.44	18.10	Y	BLAGN	1.923
XMSJ 225227.6-180223	22 : 52 : 27.6	−18 : 02 : 23.6					C	–	
XMSJ 225228.2-174917	22 : 52 : 28.2	−17 : 49 : 16.5	19.75	18.84	18.32	17.60	Y	NELG	0.133
XMSJ 233049.5+200122	23 : 30 : 49.3	+20 : 01 : 24.3	22.04	20.00	19.22	18.08	Y	NELG	0.444
XMSJ 233113.8+200506	23 : 31 : 13.7	+20 : 05 : 08.3	21.47	19.64	18.85	18.80	Y	NELG	0.260
XMSJ 233119.3+194512	23 : 31 : 19.2	+19 : 45 : 12.9	20.54	19.96	19.49		Y	BLAGN	0.532
XMSJ 233128.1+194605	23 : 31 : 28.2	+19 : 46 : 02.7	23.46	21.63	21.01		Y	NELG	0.486
XMSJ 233156.2+195123	23 : 31 : 56.2	+19 : 51 : 22.6	22.98	22.06	21.15		Y	BLAGN	0.718

Table 5. continued.

X-ray source	RA_o (J2000)	Dec_o(J2000)	g'	r'	i'	R	Id[a]	Type	z
XMSJ 233158.7+194440	23 : 31 : 58.8	+19 : 44 : 39.2	23.47	22.24	21.21		Y	BLAGN	1.418
XMSJ 233201.5+200406	23 : 32 : 01.5	+20 : 04 : 06.4					Y	BLAGN	1.517
XMSJ 233203.2+200626	23 : 32 : 03.2	+20 : 06 : 27.7	21.07	20.36	20.12	19.30	Y	BLAGN	1.901
XMSJ 233207.3+200529	23 : 32 : 07.4	+20 : 05 : 29.1	22.26	21.61	21.48		Y	BLAGN	1.897
XMSJ 233209.8+194517	23 : 32 : 09.8	+19 : 45 : 17.4	20.26	19.05	18.37	19.30	Y	BLAGN	2.027
XMSJ 233212.2+200557	23 : 32 : 12.2	+20 : 05 : 58.7		21.38	20.55		Y	BLAGN	0.870
XMSJ 233226.5+195736	23 : 32 : 26.5	+19 : 57 : 40.7	23.20	21.29	20.67		Y	BLAGN	0.521
XMSJ 233228.2+195809	23 : 32 : 28.2	+19 : 58 : 08.5	20.67	18.74	18.08	17.40	Y	ALG	0.309
XMSJ 233232.0+195116	23 : 32 : 31.9	+19 : 51 : 18.9	21.12	20.30	20.11	19.90	Y	BLAGN	1.473
XMSJ 233232.6+195809	23 : 32 : 32.6	+19 : 58 : 09.2	19.65	18.73	18.82	18.70	Y	BLAGN	1.361

[a] This flag means: Y if the source has been positively identified via optical spectroscopy; C if there is a single clear optical candidate counterpart from in optical images; E if there is no candidate counterpart down to our imaging sensitivity.